UREP

UNCONVENTIONAL RESERVOIR ENGINEERING PROJECT

Advisory Board Meeting

May 4, 2016

Agenda

Wednesday, May 4, 2016

08:00 am – 08:30 am *Continental Breakfast*

08:30 am – 08:40 am *Opening Remarks* – *E. Ozkan*

08:40 am – 11:45 am *Presentations*

- 08:40 am – 09:00 am *Anomalous Diffusion Models for Unconventional Reservoirs* – *A. Albinali*
- 09:00 am – 09:25 am *Production Data Analysis Based on Anomalous Diffusion* – *R. Holy*
- 09:25 am – 09:40 am *Numerical Modeling of 1D Anomalous Diffusion* – *R. Holy*
- 09:40 am – 10:00 am *Gas Flow Inside Nano-Fluidic Chips* – *E. Parsa*

10:00 am – 10:15 am *Coffee Break*

- 10:15 am – 10:40 am *Impact of Confinement on Flow: Black Oil Simulation* – *T. Calisgan*
- 10:40 am – 11:05 am *Potential of Thermal Methods to Enhanced Recovery in Unconventional Oil Reservoirs* – *J. Huseynova*
- 11:05 am – 11:20 am *Experimental Study of the Membrane Properties of Nanoporous Reservoirs* – *Z. Zhu*
- 11:20 am – 11: 30 am *Slip Flow of Gas in Nanoporous Media using Lattice Boltzmann and DSMC*– *Z. Zhu*
- 11:30 am – 11:45 am *Pseudotransient Linear Flow in Unconventional Reservoirs* – *W. Assiri*

11:45 am – 12:00 pm *Discussions*

12:00 pm – Adjourn

Boxed lunch will be available for the guests attending the meeting

Address
Colorado School of Mines
Petroleum Engineering. Dept.
Marquez Hall
1600 Arapaho Street
Golden, Colorado 80401

Meeting Room
Marquez Hall (MZ) 106

Contact Person
Ms. Denise Winn-Bower
Research Administrator
Phone: 303-273-3945
Fax: 303-273-3189
E-mail: dwinnbow@mines.edu

Driving Directions
From Denver Int. Airport:
Take Peña Blvd and drive 11.4 miles to merge onto I-70W; in 18.1 miles take exit 265 to merge onto CO-58Wtoward Golden /Central City; drive 4.6 miles and take Washington St exit; turn left to Washington St and drive 0.7 miles; turn right to 16th street; Marquez Hall is on the left at the corner of the 16th St and Arapaho.
From Downtown Denver:
Take US-6W/6th Ave; drive 10 miles and turn right to 19th St; in 0.3 miles turn left to Illinois St and in 0.2 miles turn right to 16th St. Marquez Hall is on your right at the corner of the 16th St and Arapaho.

Parking Instructions
Parking on campus during operational hours (Monday-Friday 7 a.m.-5 p.m.) requires a metered parking permit. Park in the General (blue), street parking (blue) or Commuter (yellow) lots (http://www.mines.edu/MapsDirectionsParkingInfo). All visitor parking areas have a pay and display parking meter. Please visit the pay stations to receive a parking permit. Pay station meter rates for General (blue) parking are $1.50 per hour or $8 daily; rates for Commuter lots are $1.25 per hour or $6 daily. Metered parking permits must be displayed on your dashboard.

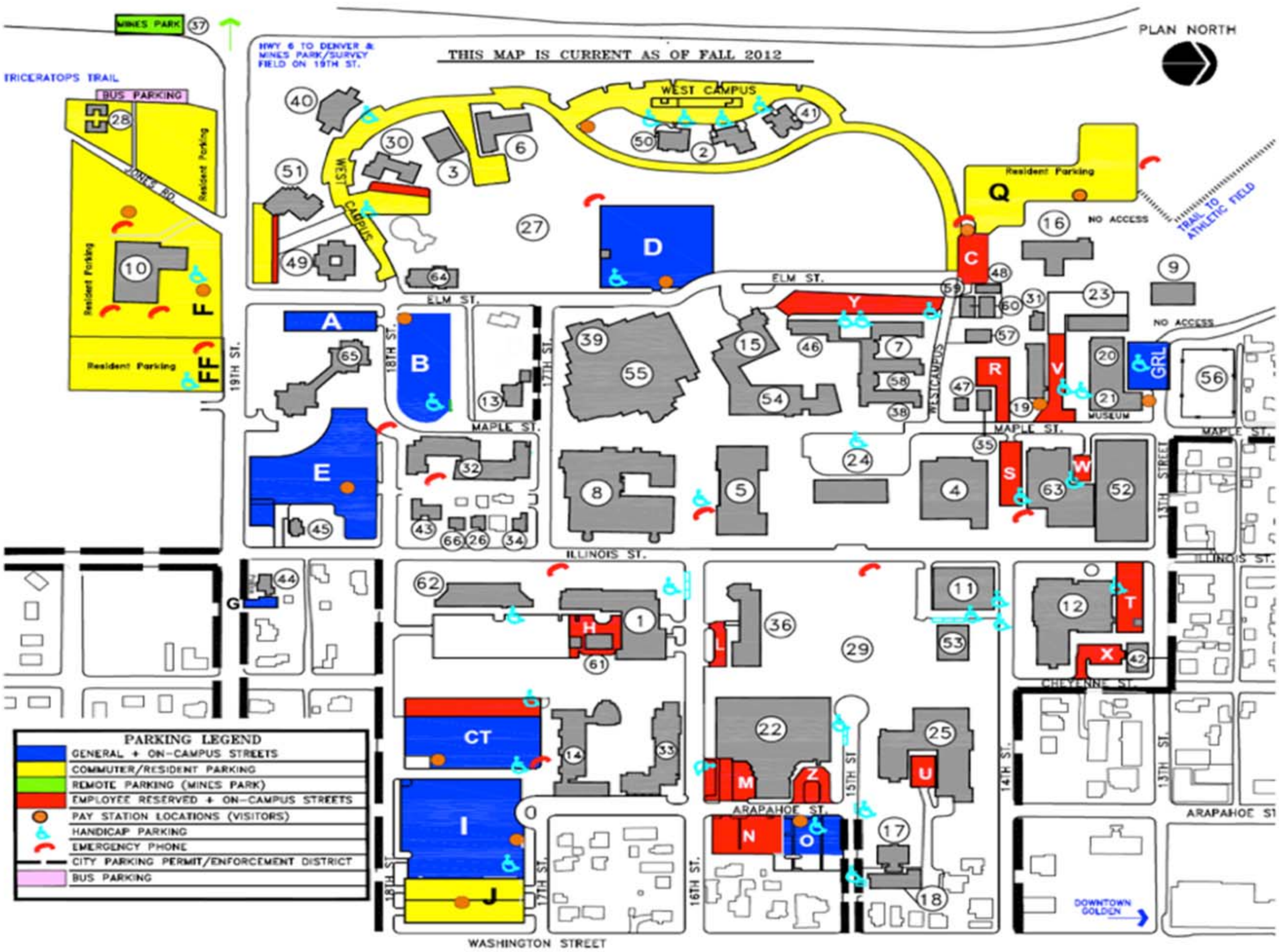

COLORADO SCHOOL OF MINES

KEY TO FACILITIES

1. ALDERSON HALL (AH)
2. ALPHA PHI SORORITY (Z4)
3. ALPHA TAU OMEGA FRATERNITY
4. ARTHUR LAKES LIBRARY (LB)
5. BERTHOUD HALL (BE)
6. BETA THETA PI FRATERNITY
7. BRADFORD HALL (BR)
8. BROWN HALL (BB)
9. CARPENTER SHOP (1S)
10. CENTRAL RECEIVING/RECYCLING AND MUSIC PROGRAM (CR)
11. CHAUVENET HALL (CH)
12. COOLBAUGH HALL (CO)
13. COOLBAUGH HOUSE (ZO)
14. CTLM (CT)
15. DINING HALL (SC)
16. EMI DRILLING LABORATORY (EM)
17. ENGINEERING HALL (EH)
18. ENGINEERING HALL ANNEX (EA)
19. FACILITIES MANAGEMENT, PARKING & CAPITAL PLANNING & CONSTRUCTIONS (FM)
20. GENERAL RESEARCH LAB (RL)
21. GEOLOGY MUSUEM (RL)
22. GREEN CENTER (GC)
23. GROUNDS/TRUCK SHOP (2S)
24. GUGGENHEIM HALL (GH)
25. HILL HALL (HH)
26. INTERNATIONAL PROGRAM (ZH)
27. INTRAMURAL FIELD (IM)
28. JONES APARTMENTS (ZQ & ZR)
29. KAFADAR COMMONS
30. KAPPA SIGMA FRATERNITY
31. LOCK SHOP (S3)
32. MAPLE HALL (RH)
33. MARQUEZ HALL (MZ)
34. MCBRIDE HONORS (ZS)
35. MEP (ZL)
36. MEYER HALL (MH)
37. MINES PARK COMMUNITY CENTER
38. MORGAN HALL (MO)
39. OUTDOOR RECREATION (RC)
40. PHI GAMMA DELTA FRATERNITY (Z1)
41. PI PHI SORORITY (Z3)
42. POWER PLANT (HP)
43. PRESIDENT'S HOME
44. PUBLIC SAFETY ANNEX (ZG)
45. PUBLIC SAFETY (ZJ)
46. RANDALL HALL (RA)
47. ROTC (ZK)
48. ROTC (5S)
49. SIGMA ALPHA EPSILON FRATERNITY
50. SIGMA KAPPA SORORITY (Z5)
51. SIGMA PHI EPSILON FRATERNITY
52. STEINHAUER FIELD HOUSE (FH)
53. STRATTON HALL (SH)
54. STUDENT CENTER (SC)
55. STUDENT RECREATION CENTER (RC)
56. TENNIS COURTS
57. THE PINES–FOUNDATION (6S)
58. THOMAS HALL (TH)
59. TIMBERLINE #1–UNIVERSITY ADVANCEMENT (7S)
60. TIMBERLINE #2–UNIVERSITY ADVANCEMENT (8S)
61. UNIT OPERATIONS LAB (UO)
62. U.S.G.S. OFFICES AND LAB (GS)
63. VOLK GYMNASIUM (GY)
64. W. LLOYD WRIGHT STUDENT WELLNESS CENTER (WC)
65. WEAVER TOWER (WT)
66. WISEM (ZV)

Suggested Hotels

The following hotels are located in Downtown Golden and within walking distance of Campus. Mention that you are attending a CSM function.

Table Mountain Inn
1310 Washington Avenue
Golden, Colorado 80401
(303) 277-9898
(800) 762-9898 (http://www.tablemountaininn.com/)

The Golden Hotel
800 11th Street
Golden, CO 80401
(303) 279 0100
(800) 233 7214 (http://www.golden-hotel.com/)

UREP

CSM

Research Summary

Anomalous Diffusion Models for Unconventional Reservoirs

Ali Albinali, Colorado School of Mines

Status of Research

- Mathematical equations derived.
- Fortran F90 computer code built.
- Solution verified and sensitivity analysis conducted.
- Solution applied to field data.

Scope of Research

- Unconventional reservoirs:
    - Different levels of heterogeneities.
    - Abrupt variations.
    - Conventional fluid flow models.
- Using anomalous diffusion to model fluid flow in unconventional naturally fractured reservoirs.
- Derive an analytical solution for multi-fractured horizontal wells.

Approach

- Modifying Darcy's law following Fomin et al. 2011, Raghavan 2011, Chen and Raghavan, 2015:

$$v_x = \frac{k_\alpha}{\mu} \frac{\partial^{1-\alpha}}{\partial t^{1-\alpha}} \left(\frac{\partial p}{\partial x} \right)$$

- Tri-linear (TLM) flow scheme by Ozkan et al. (2009).
- Describe flow in matrix and natural fractures independently (α_m and α_f).
- Tri-linear anomalous diffusion and dual-porosity solution (TADDP).

Results/Sensitivity Analysis

- Diffusion Exponents α_f and α_m.

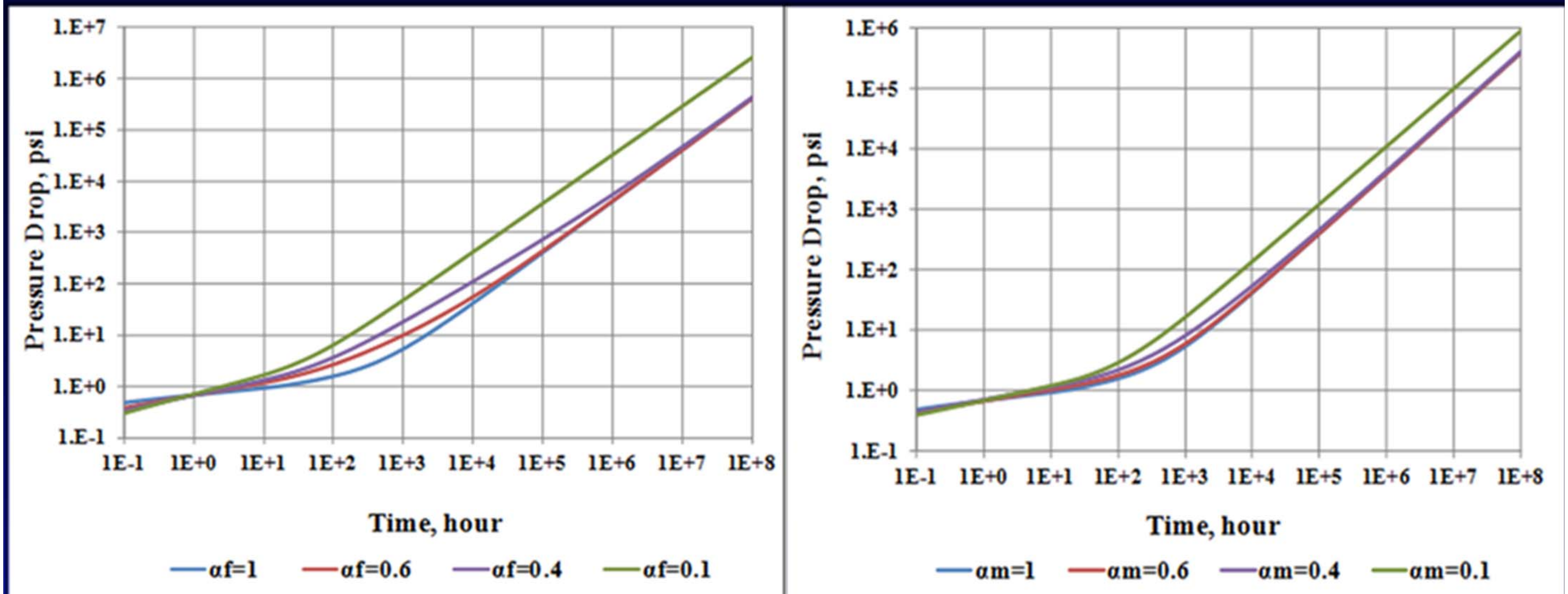

Figure 1: Sensitivity Analysis-Diffusion Exponent

Results/Sensitivity Analysis

- Diffusion Exponents and Regional Impact.

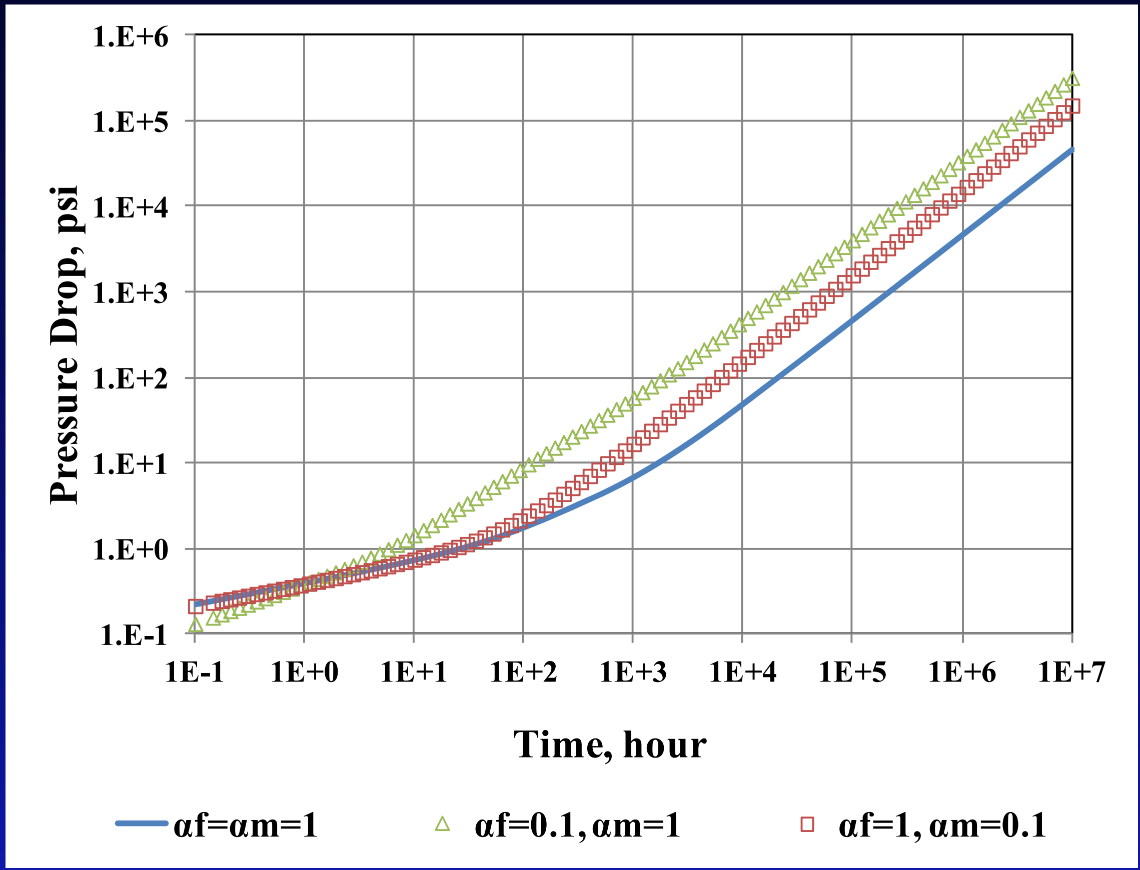

Figure 2: Sensitivity Analysis-Regional Impact

Results/Sensitivity Analysis

- Flow Capacity: $k_f^{\alpha_f} h_f$ and $k_m^{\alpha_m} h_m$.

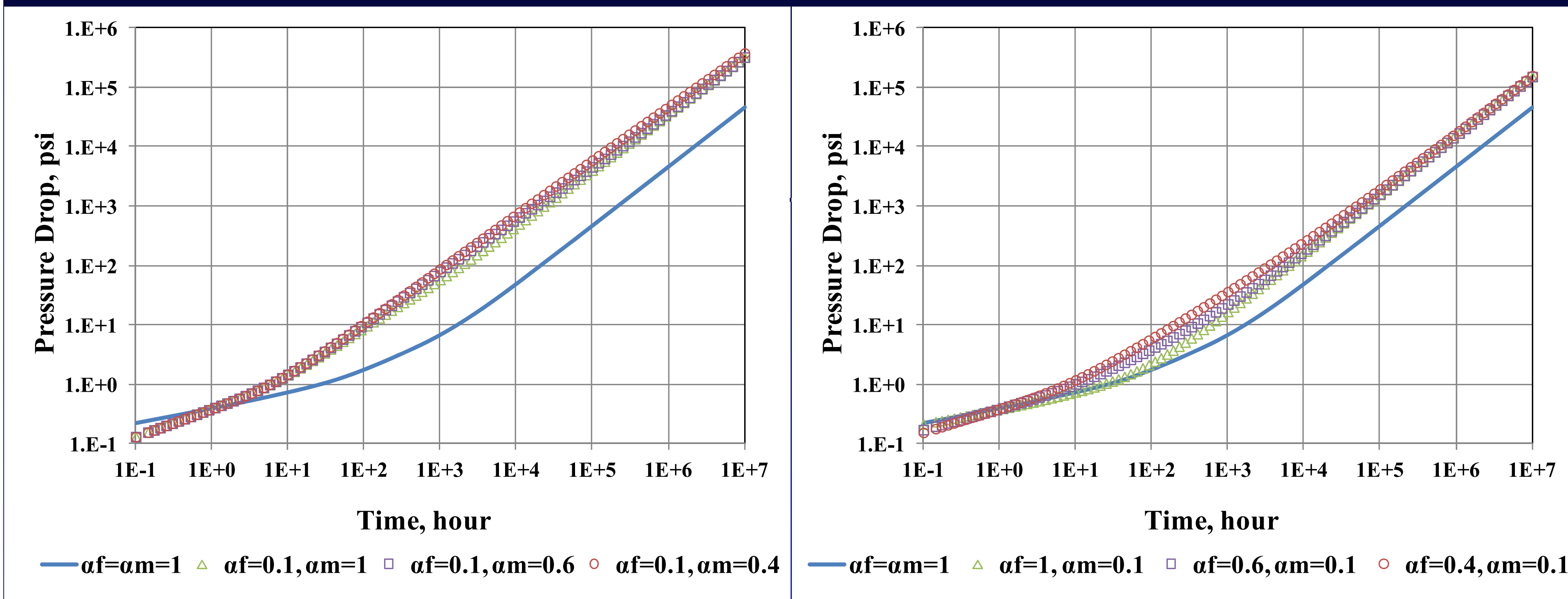

Figure 3: Sensitivity Analysis-Flow Capacity

Field Application

- Eagle Ford Shale formation.
- Single pad with 3 laterals (RRC Texas):
  - Each lateral make up 33% of the total production.
  - Similar simulation programs → hydraulic fractures are of uniform properties → equal contribution.
  - Monthly rates were converted to daily rates assuming full month production.
- Initialized with DPDK CMG model by Curnow (2015).

Field Application

- Match Results.

Table 1: TADDP Match Parameters

Distance to boundary parallel to well (1/2 well spacing), x_e, ft	625
Distance to boundary perpendicular to well, y_e, ft	170
Viscosity, μ, cp	0.5
Radius of Spherical matrix, r_m,ft	3
Matrix permeability, k_m, md	1E-4
Matrix porosity, ϕ_m	0.1
Matrix total compressibility, c_{tm}, psi^{-1}	1E-6
Matrix diffusion exponent, α_m	1.0
Natural fracture permeability, k_f, md·day$^{1-\alpha f}$	1E-1
Natural fracture porosity, ϕ_f	0.001
Natural fracture total compressibility, c_{tf}, psi^{-1}	1E-6
Natural fracture thickness, h_f, ft	3E-3
Density of natural fractures, ρ_f, n_f/ft	1
Natural fracture diffusion exponent, α_f	0.2
Hydraulic fracture porosity, ϕ_F	0.38
Hydraulic fracture permeability, k_F, md	5E+4
Hydraulic fracture total compressibility, c_{tF}, psi^{-1}	1E-6
Hydraulic fracture half-length, x_F, ft	550
Hydraulic fracture width, w_F, ft	0.01

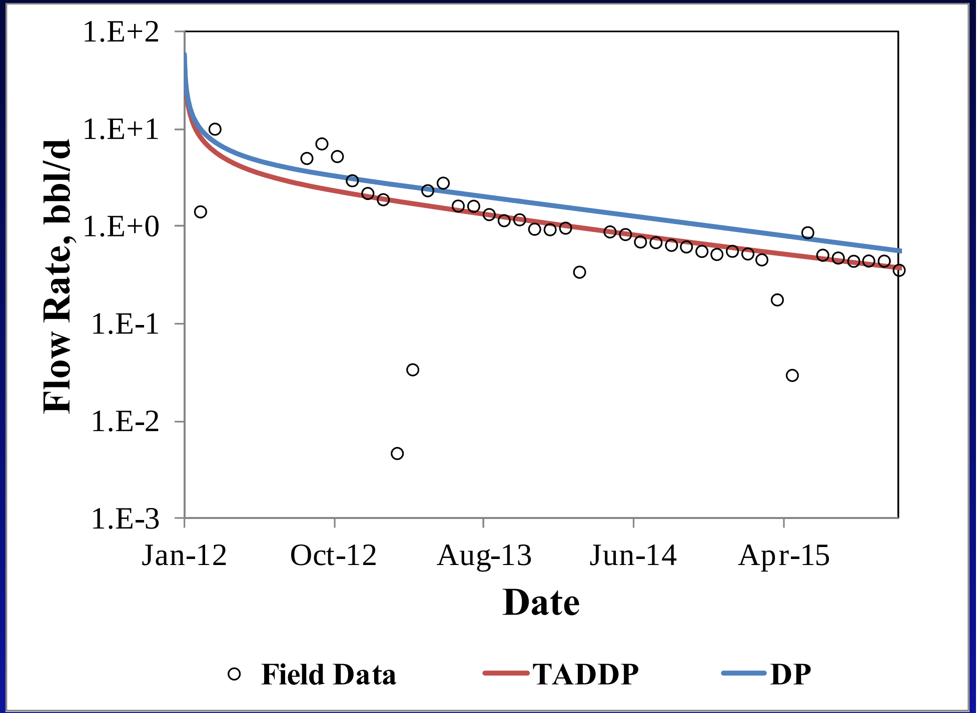

Figure 4: Field Application

Future Work

- Field application.
- Characterization of nano-porous reservoirs (Fractals).
- Elucidation about time-dependent transport.

UNCONVENTIONAL RESERVOIR ENGINEERING PROJECT
Colorado School of Mines

Production Data Analysis Based on Anomalous Diffusion

Ralf Holy
Colorado School of Mines

Outline

- Motivation
- Background - Anomalous Diffusion
- Single-Phase Flow Model
  - Constant terminal pressure solution
  - Production characteristics under anomalous diffusion
- Production Data Analysis Procedure
- Application to Barnett Shale Gas Wells
- Conclusions

Motivation

- Decline-curve analysis approaches are empirical
  - Empirical approaches are only justified for the conditions they are developed for
  - Decline-curve analysis assumes that the last flow regime observed on data is the terminal flow behavior. Otherwise, they have to make assumptions about the terminal flow behavior
  - Parameters obtained from decline-curve analysis cannot be used to construct analytical or numerical flow models
- Current modeling approaches may be inadequate or impractical
  - Dual- or (multi-) porosity idealization requires continuum of the media involved in the model
  - Discrete fracture network models are financially and computationally costly
  - Upscaling petrophysical heterogeneity characterized at pore level is usually not very successful and does not necessarily lead to an accurate flow model

Background-Anomalous Diffusion

- Anomalous diffusion – heterogeneous/disordered media
  - Sub-diffusion – flux hindrance $$\frac{\partial^2 C(x,t)}{\partial x^2} = D_\alpha \frac{\partial^\alpha C(x,t)}{\partial t^\alpha} \quad 0 < \alpha < 1$$
    - Particles can get trapped
    - Mean square displacement growth slower
    - Severity increases with decreasing exponent α
  - Super-diffusion – flux facilitation $$\frac{\partial^{1+\beta} C(x,t)}{\partial x^{1+\beta}} = D_\beta \frac{\partial C(x,t)}{\partial t} \quad 0 < \beta < 1$$
    - Particles can travel further
    - Mean square displacement growth faster
    - Severity increases with decreasing exponent β

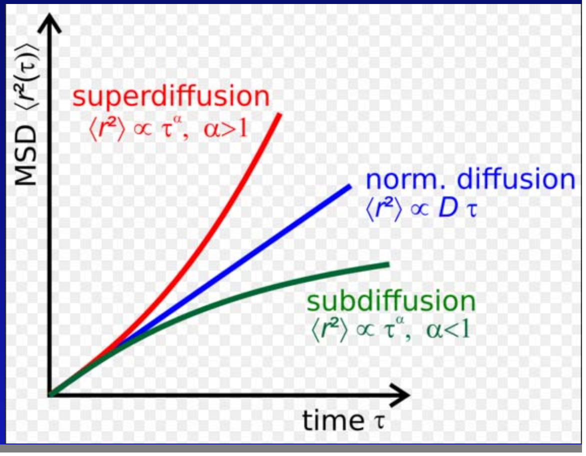

➔ Complexity of the heterogeneous media and flow mechanisms captured in α, β, $D_{\alpha,\beta}$

Anomalous Diffusion, Production Characteristics

- Analytical transient linear flow solution for constant pressure production: Chen and Raghavan (2015)

$$log(q_f(t)) = log\left(\frac{1}{2\pi\Gamma\left(\frac{\alpha}{\beta+1}\right)}\frac{p_i - p_f}{141.2\mu B}\left(\frac{\phi\mu c_t}{0.006328}\right)^{1-\frac{1}{\beta+1}} x_f h k_{\alpha,\beta}{}^{\frac{1}{\beta+1}}\right) - \left(1 - \frac{\alpha}{\beta+1}\right) log(t)$$

➔ Log-log straight line: $log(q_f(t)) = log(a) - mlog(t)$

- Case 1: pure sub-diffusion ($\beta = 1$)

slope: $0.5 < \mathrm{m} = 1 - \frac{\alpha}{2} < 1 \qquad for \quad 0 < \alpha < 1$

- Case 2: pure super-diffusion ($\alpha = 1$)

slope: $0 < \mathrm{m} = 1 - \frac{1}{\beta+1} < 0.5 \qquad for \quad 0 < \beta < 1$

Anomalous Diffusion, Production Characteristics

Constant pressure production – sensitivity on time fractional order α , (β =1)

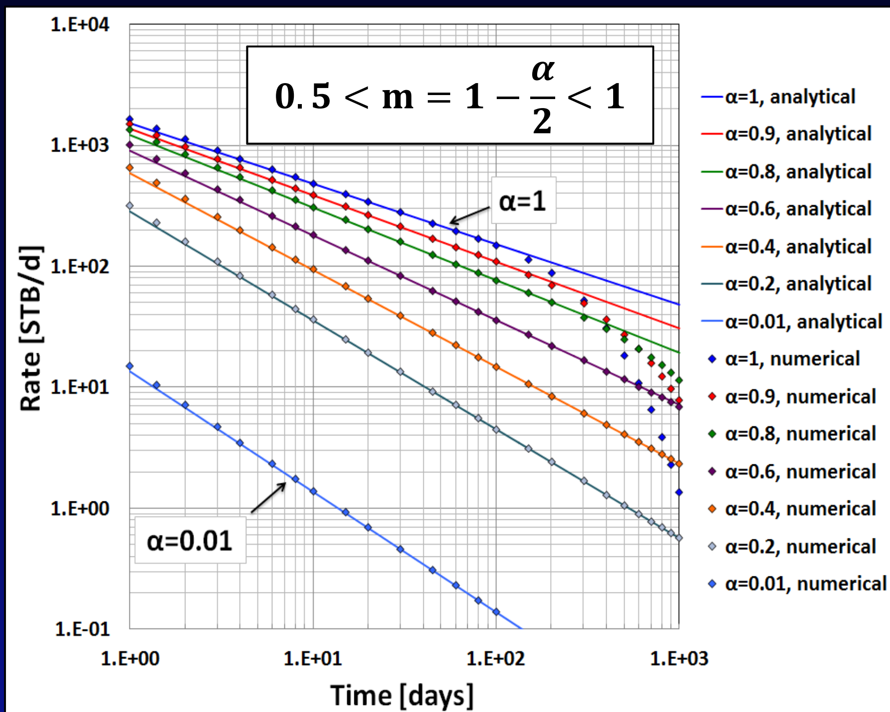

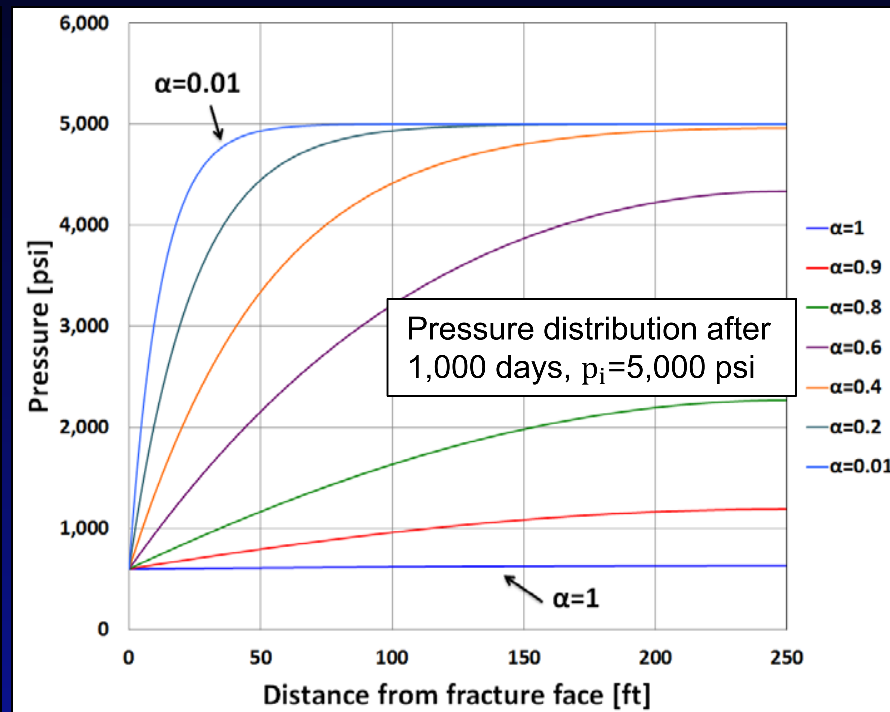

Sub-diffusion (α<1):

- Steeper transient slopes, boundary felt later
- Smaller areas drained in same amount of time

Anomalous Diffusion, Production Characteristics

Constant pressure production – sensitivity on time fractional order α , (β =1)

- Boundary dominated flow period: late time responses follow power-law decline

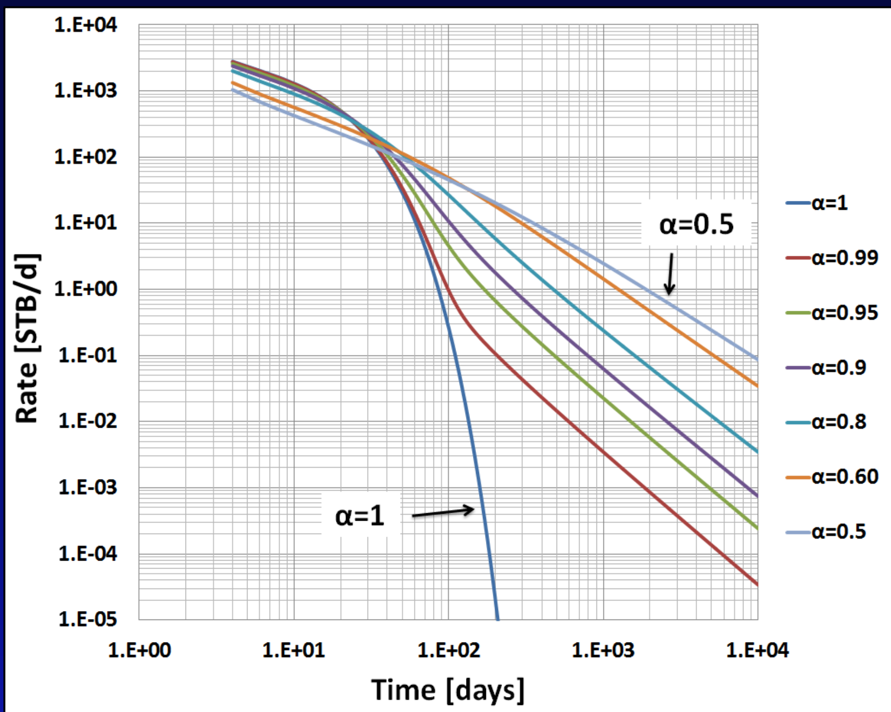

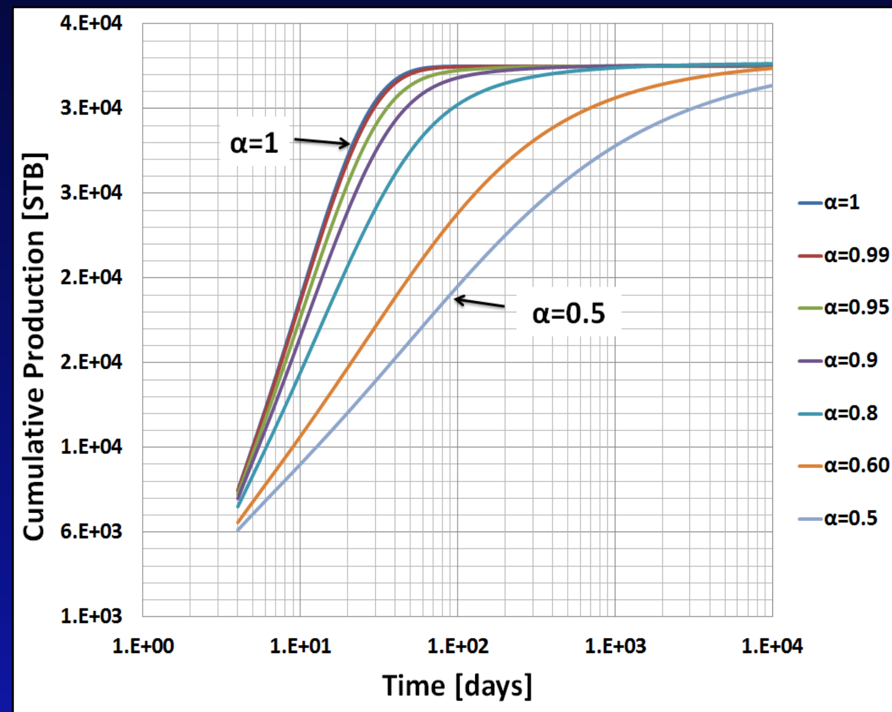

Anomalous Diffusion, Production Characteristics

Constant pressure production – sensitivity on space fractional order *β, (α* =1)

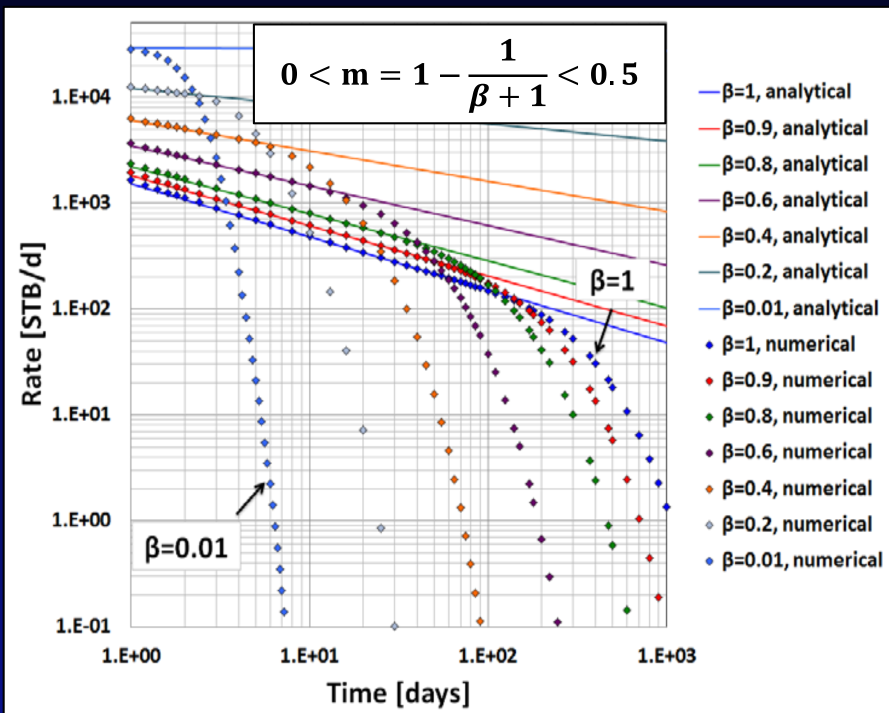

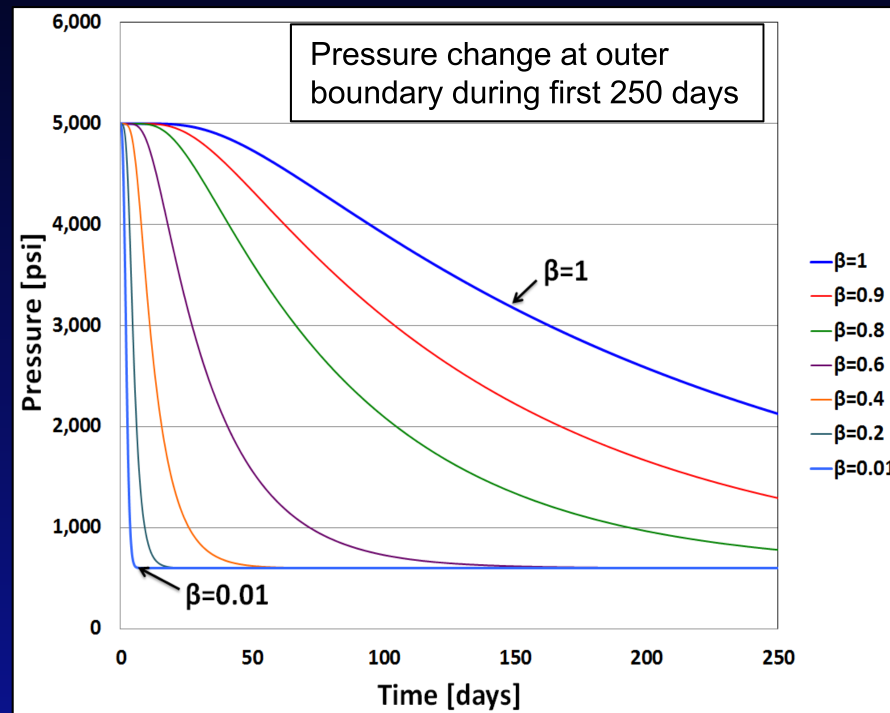

Superdiffusion (*β* <1):

- Gentler transient flow slopes, boundary felt earlier
- Rapid drainage of system

Anomalous Diffusion, Production Characteristics

Constant pressure production – sensitivity on space fractional order *β*, (*α* =1)

- Boundary dominated flow period: late time responses follow exponential decline

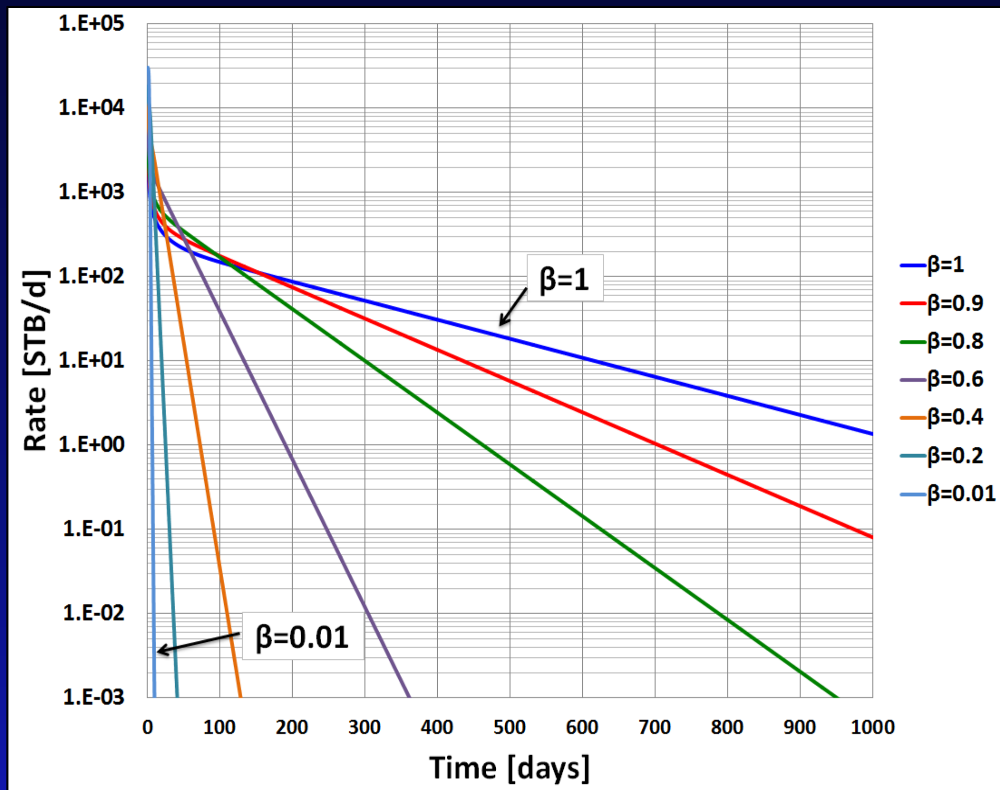

Production Data Analysis Procedure

4-Step Approach:

1. Identify straight-line slope from log-log plot of rate vs. time

$$\log(q) = \log(a) - m\log(t) \quad , \qquad m = \left(1 - \frac{\alpha}{\beta+1}\right)$$

2. Identify sub-or super-diffusive state of flow and solve for α and β

$$0.5 < m < 1 \quad \Rightarrow \text{sub-diffusion} \quad \Rightarrow \beta = 1\,, \qquad \alpha = 2(1-m)$$

$$0 < m < 0.5 \quad \Rightarrow \text{super-diffusion} \Rightarrow \alpha = 1\,, \qquad \beta = \frac{1}{1-m} - 1$$

3. Solve for phenomenological coefficient $k_{\alpha,\beta}$

   - Analytically $$a = \frac{1}{2\pi\Gamma\left(\frac{\alpha}{\beta+1}\right)} \frac{p_i - p_f}{141.2\mu B}\left(\frac{\phi\mu c_t}{0.006328}\right)^{1-\frac{1}{\beta+1}} x_f h k_{\alpha,\beta}{}^{\frac{1}{\beta+1}}$$
   - Numerically: history-match production data used for straight line

4. Forecast production using α , β and $k_{\alpha,\beta}$

Field Application –Barnett Shale Gas Wells

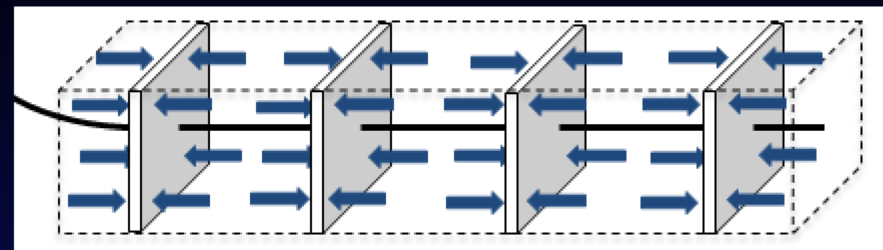

Assumptions

- Hydraulic fractures
  - Identical, equally spaced, infinite conductivity
  - Well chocking effects neglected.
  - Produced at same pressure $p_f = p_{bh}$
- Reservoir
  - Initially in equilibrium with uniform pressure p_i
  - Flow restricted to SRV, linear and perpendicular to fractures
  - SRV extends 1 fracture half-spacing beyond the first/last fracture
  - No-flow boundary between hydraulic fractures
- Reservoir Fluid
  - Single-phase gas
  - Conventional PVT correlations apply

Application – Barnett Shale Gas Well 1

API 42-497-36312

- Prod. start: June ’08
- Status: active as of January 2016
- 91 months of reported production

- First 27 month of data used for match

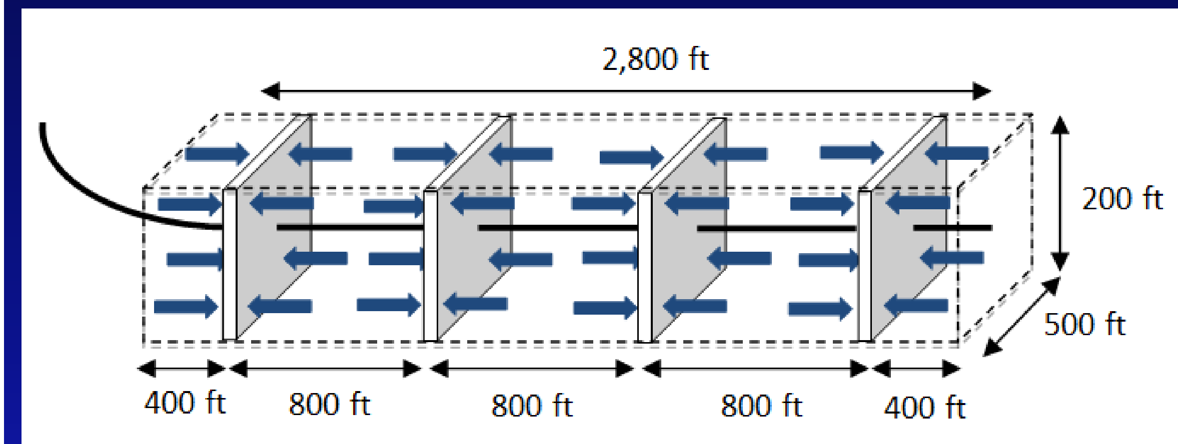

WELL PROPERTIES	
Well Depth, ft	7,700
Horizontal well length, ft	2,800
Number of Hydraulic fractures	4
Average fracture spacing, ft	800
RESERVOIR PROPERTIES	
Temperature, F	200
Porosity, fraction	0.05
Pressure gradient, psi.ft^{-1}	0.52
FLUID PROPERTIES	
Gas specific gravity, fraction	0.7
ASSUMED PROPERTIES	
Initial pressure, psi	4,004
Bottomhole flowing pressure, psi	800
Hydraulic fracture half-length, ft	250
Hydraulic fracture drainage length, ft	400
Hydraulic fracture height, ft	200

Application – Barnett Shale Gas Well 1

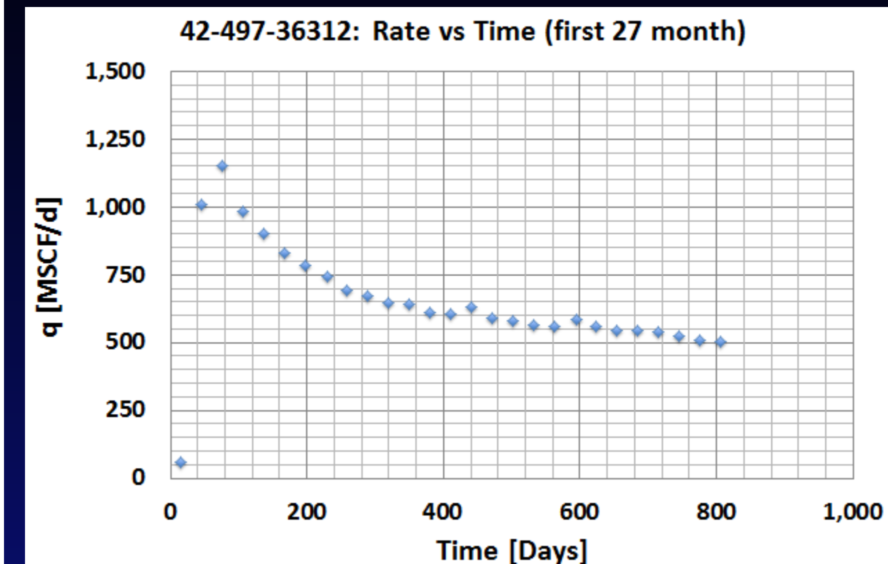

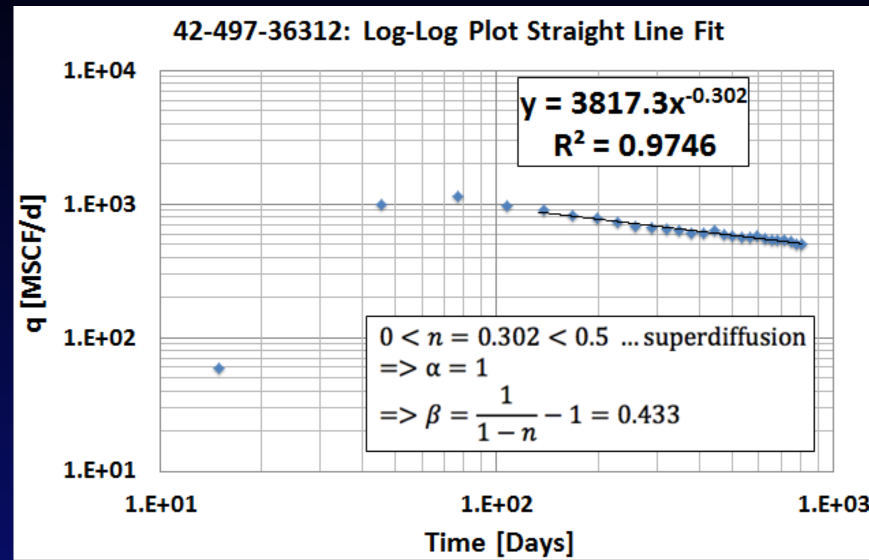

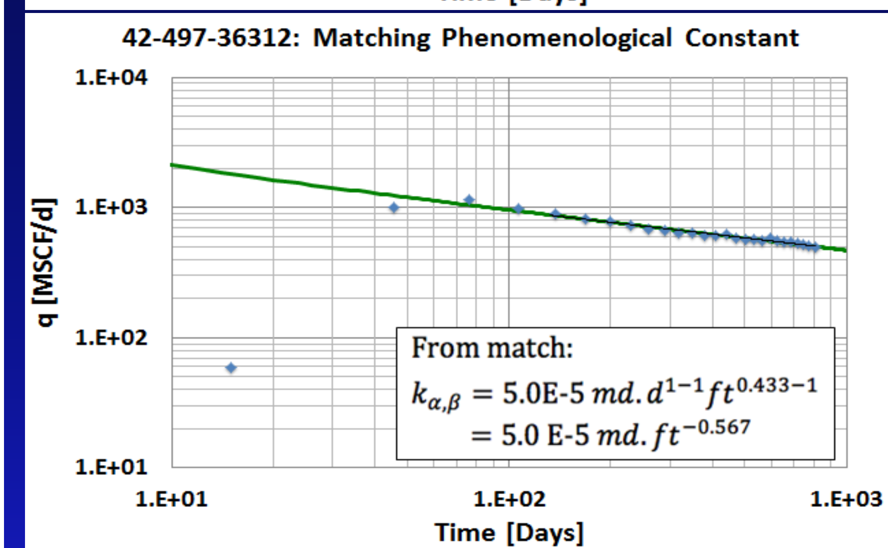

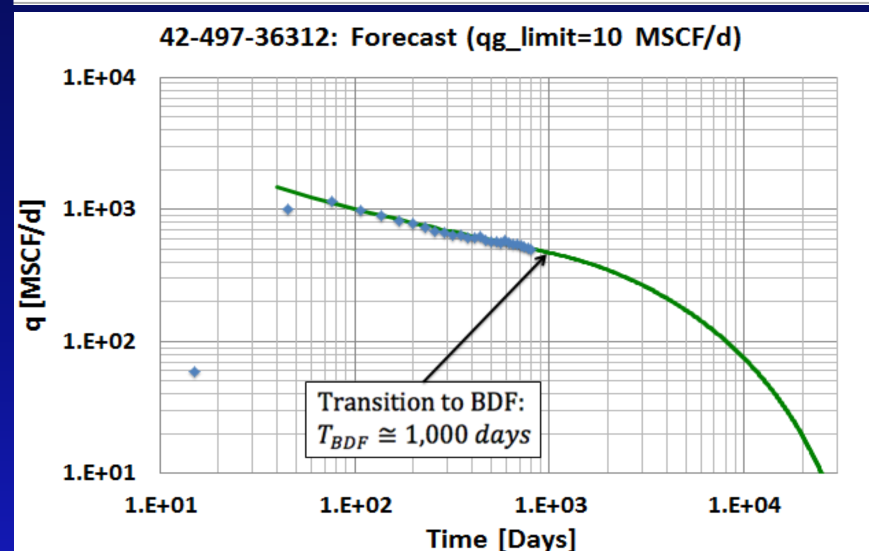

Application – Barnett Shale Gas Well 1

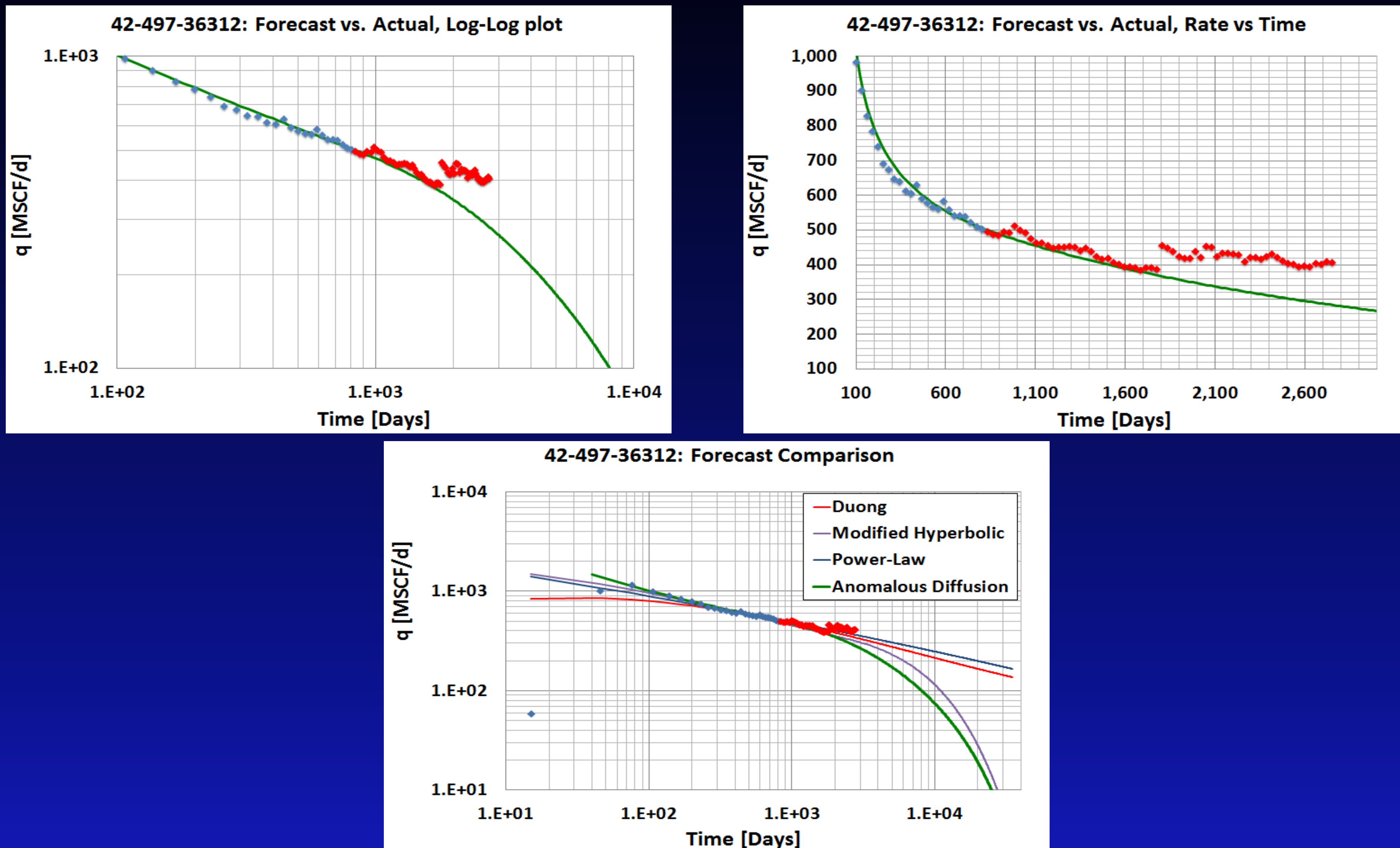

Application – Barnett Shale Gas Well 2

API 42-439-33141

- Prod. start: June '08
- Status: Active as of January 2016
- 3 month shut-in 2014
- 88 months of reported production

- First 23 month of data used for match

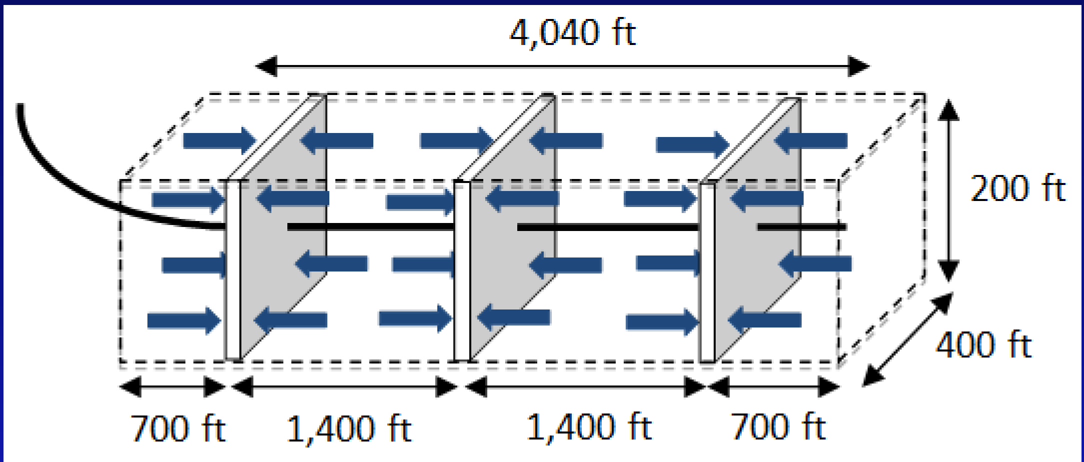

WELL PROPERTIES	
Well Depth, ft	6,900
Horizontal well length, ft	4,040
Number of Hydraulic fractures	3
Average fracture spacing, ft	1,400
RESERVOIR PROPERTIES	
Temperature, F	279
Porosity, fraction	0.05
Pressure gradient, psi.ft^{-1}	0.52
FLUID PROPERTIES	
Gas specific gravity, fraction	0.594
ASSUMED PROPERTIES	
Initial pressure, psi	3,588
Bottomhole flowing pressure, psi	700
Hydraulic fracture half-length, ft	200
Hydraulic fracture drainage length, ft	700
Hydraulic fracture height, ft	200

Application – Barnett Shale Gas Well 2

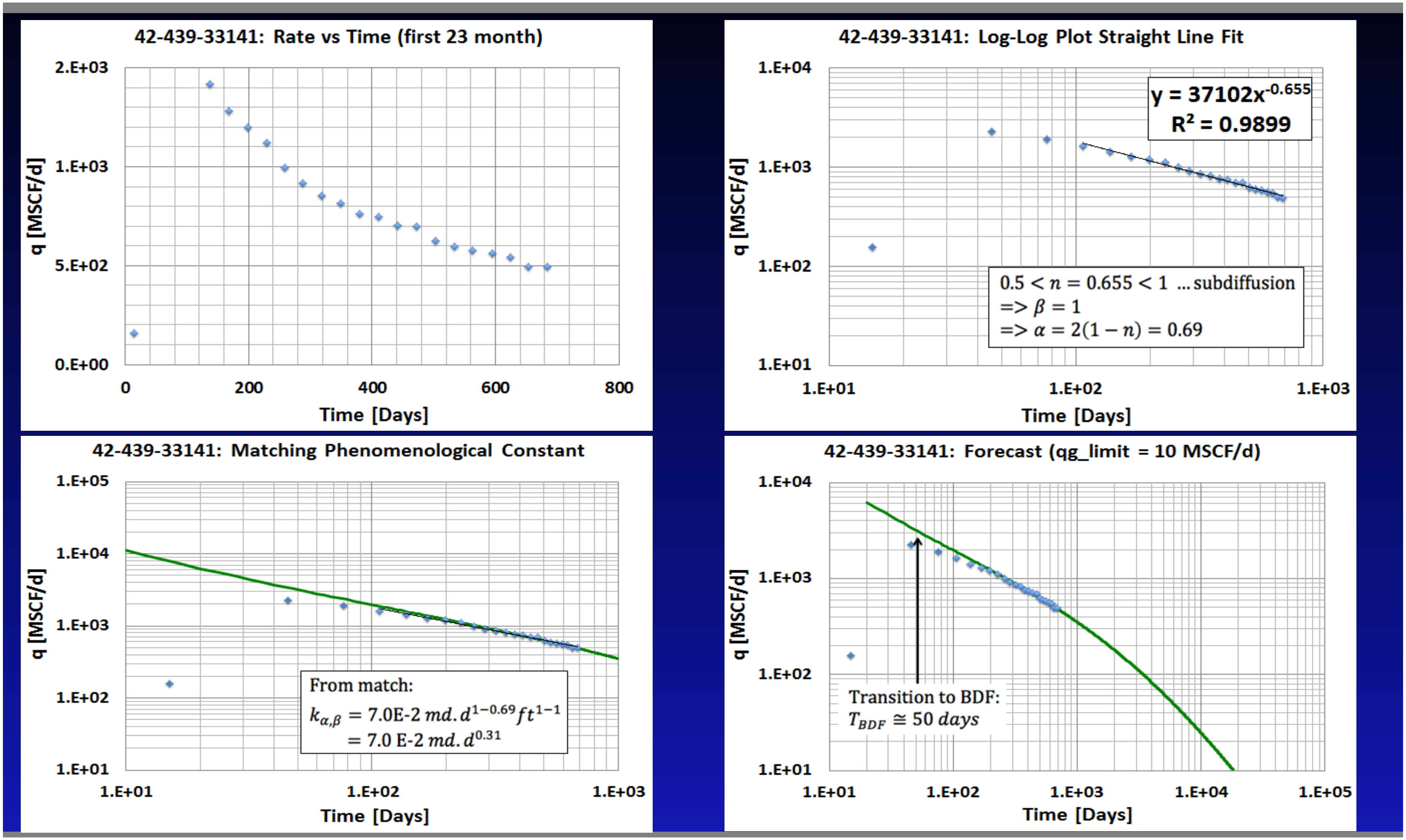

Application – Barnett Shale Gas Well 2

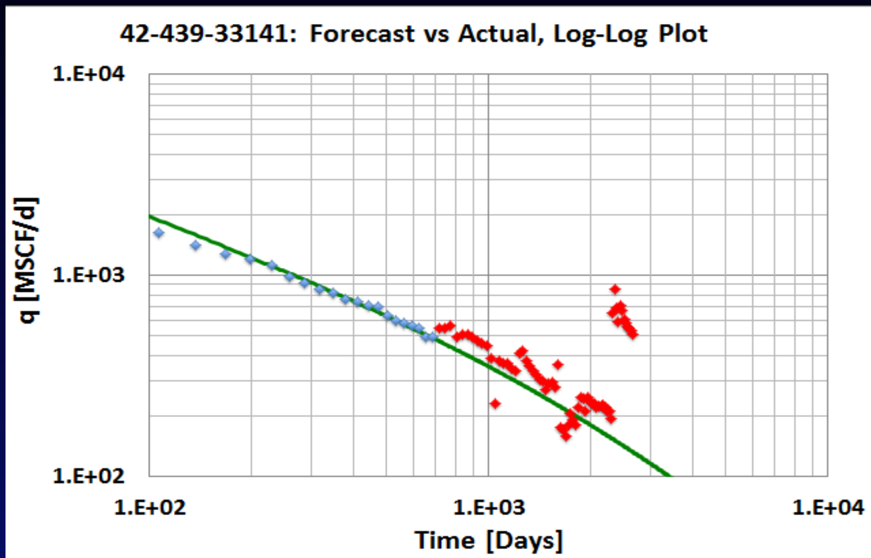

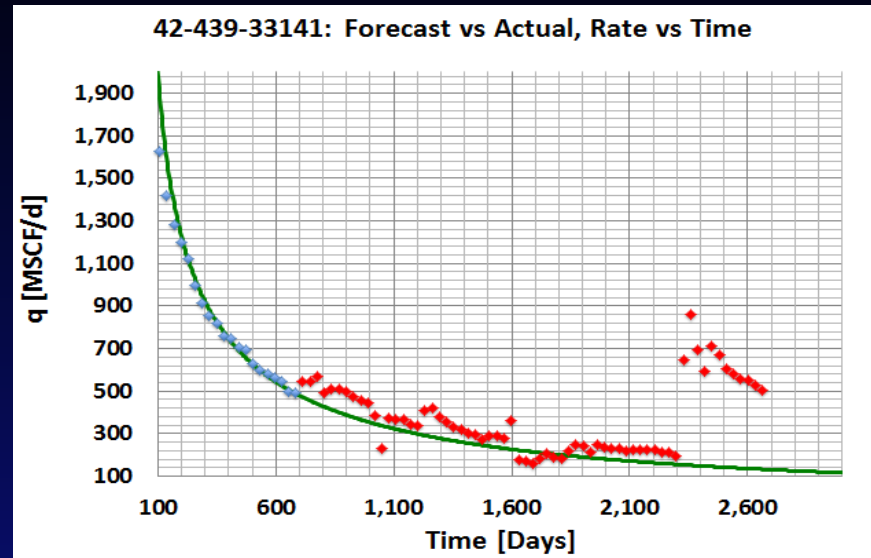

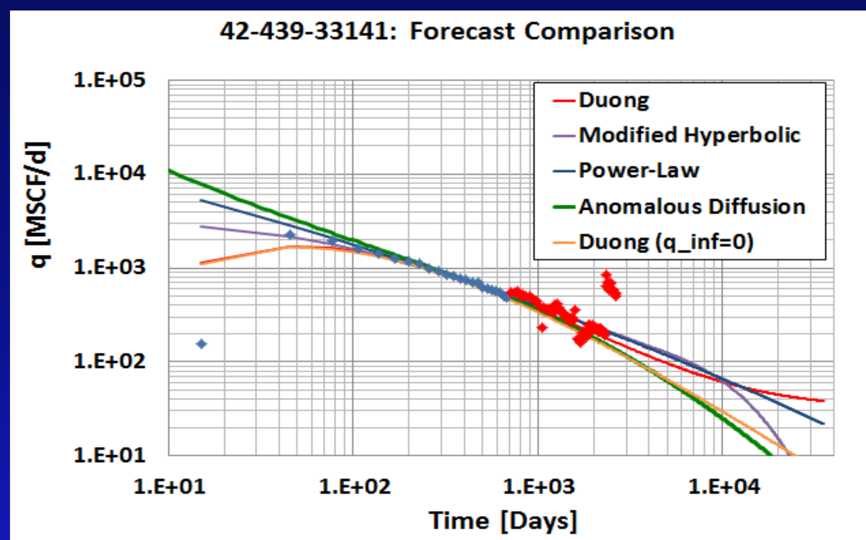

Conclusions

An anomalous diffusion based model has been developed for production data analysis in unconventional wells

Unlike existing empirical decline-curve analysis methods, this model is theoretically rigorous.

The complexity of the heterogeneous media and the flow mechanisms is captured in 3 parameters: α, β and $k_{\alpha,\beta}$

With limited completion, reservoir, and production data the flow characteristics of two Barnett shale gas wells were captured

The numerical model can be extended to incorporate:

- Multiphase flow
- Complex reservoir, fracture, well geometries
- Changing operating conditions

UNCONVENTIONAL RESERVOIR ENGINEERING PROJECT
Colorado School of Mines

Numerical Modeling of 1D Anomalous Diffusion

Ralf Holy
Colorado School of Mines

Outline

- Slightly compressible flow model
    - Linearized implicit scheme
    - Model validation (constant terminal rate & pressure solution)
    - Hydraulic fracture coupling
- Compressible flow model
    - Iterative implicit scheme
    - Model validation
- Multiphase flow model
    - IMPES formulation
    - Model validation

Slightly Compressible Flow Model

Initial boundary value problem

- Hydraulic fracture ¼ drainage volume

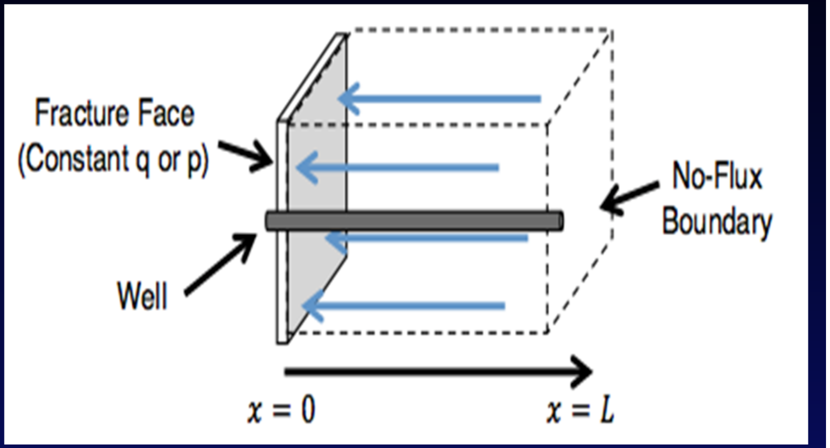

$$\frac{\partial}{\partial x}\left(\frac{k_{\alpha,\beta}}{\mu}\frac{\partial^{1-\alpha}}{\partial t^{1-\alpha}}\left(\frac{\partial^{\beta} p(x,t)}{\partial x^{\beta}}\right)\right) = \phi c_t \frac{\partial p(x,t)}{\partial t} \qquad \text{for } 0 < x < L, t > 0$$

$$p(x,0) = p_i \qquad \text{for } 0 \le x \le L$$ uniform initial pressure

$$u(L,t) = -\frac{k_{\alpha,\beta}}{\mu}\frac{\partial^{1-\alpha}}{\partial t^{1-\alpha}}\left(\frac{\partial^{\beta} p(L,t)}{\partial x^{\beta}}\right) = 0 \qquad \text{for } t \ge 0$$ no-flow boundary

$$u(0,t) = -\frac{k_{\alpha,\beta}}{\mu}\frac{\partial^{1-\alpha}}{\partial t^{1-\alpha}}\left(\frac{\partial^{\beta} p(0,t)}{\partial x^{\beta}}\right) = \frac{q_f B}{L_f h} \qquad \text{for } t > 0$$ constant rate boundary

or

$$p(0,t) = p_f \qquad \text{for } t > 0$$ constant pressure boundary

Slightly Compressible Flow Model

Time fractional derivative (Caputo, 1967)

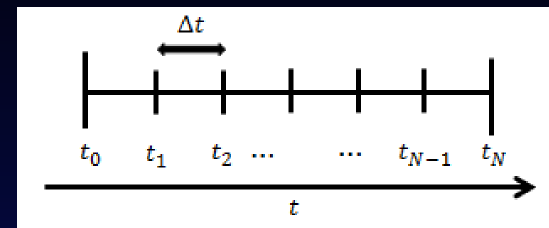

$$\left[\frac{\partial^{1-\alpha}}{\partial t^{1-\alpha}}\left(\frac{\partial^{\beta} p(x,t)}{\partial x^{\beta}}\right)\right]_{x_{i\mp 1/2}}^{n+1} = \frac{1}{\Gamma(\alpha)}\int_{t_0=0}^{t_{n+1}} \frac{\partial}{\partial \tau}\left(\frac{\partial^{\beta} p\left(x_{i\mp 1/2},\tau\right)}{\partial x^{\beta}}\right)(t_{n+1}-\tau)^{-(1-\alpha)}\,d\tau \qquad , n = 0,\ldots,N-1$$

(after Murio, 2008)

$$\cong \frac{1}{\Gamma(\alpha)}\sum_{k=1}^{n+1}\frac{\left(\frac{\partial^{\beta} p(x,t_k)}{\partial x^{\beta}} - \frac{\partial^{\beta} p(x,t_{k-1})}{\partial x^{\beta}}\right)}{\Delta t}\int_{(k-1)\Delta t}^{k\Delta t}(t_{n+1}-\tau)^{-(1-\alpha)}\,d\tau$$

$$= \sigma_{\alpha,\Delta t}\sum_{k=1}^{n+1}\omega_k^{(\alpha)}\left(\frac{\partial^{\beta} p\left(x_{i\mp 1/2},t_{n+2-k}\right)}{\partial x^{\beta}} - \frac{\partial^{\beta} p\left(x_{i\mp 1/2},t_{n+1-k}\right)}{\partial x^{\beta}}\right)$$

where $\sigma_{\alpha,\Delta t} = \frac{1}{\Gamma(1+\alpha)}\frac{1}{\Delta t^{1-\alpha}}$ and $\omega_1^{(\alpha)} = 1, \omega_k^{(\alpha)} = k^{\alpha} - (k-1)^{\alpha}$, $k = 2,\ldots,n+1$

Slightly Compressible Flow Model

Space fractional derivative:

- General 2-sided Caputo derivative (after Klimek and Lupa, 2011)

$$\frac{\partial^\beta p(x_{i+1/2}, t_{n+1})}{\partial x^\beta} = \vartheta\, {}_0^C D_{x_{i+1/2}}^\beta - (1-\vartheta)\, {}_{x_{i+1/2}}^{\quad C} D_L^\beta \qquad 0 < \beta, \vartheta < 1$$

ϑ… bias (or weighting) factor: allows for consideration of upstream/downstream flux dependencies

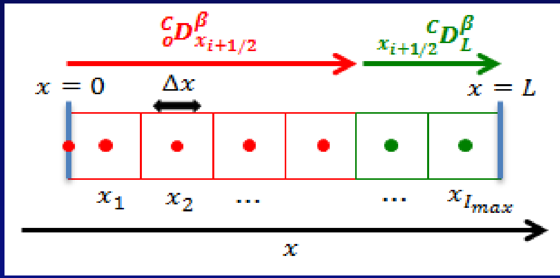

- Left sided derivative (after Caputo, 1967)

$${}_0^C D_{x_{i+1/2}}^\beta = \frac{1}{\Gamma(1-\beta)} \int_0^{x_{i+1/2}} \frac{\partial p(\xi, t_{n+1})}{\partial \xi} \left(x_{i+1/2} - \xi\right)^{-\beta} d\xi$$

$$\cong \sigma_{\beta,\Delta x} \left\{ 2\left(P_1^{n+1} - P_f^{n+1}\right)\omega_{i+1}^{(\beta)} + \sum_{m=1}^{i} \omega_m^{(\beta)} \left(P_{i+2-m}^{n+1} - P_{i+1-m}^{n+1}\right) \right\}$$

where $\sigma_{\beta,\Delta x} = \frac{1}{\Gamma(2-\beta)} \frac{1}{\Delta x^\beta}$ and $\omega_1^{(\beta)} = 1\,, \omega_m^{(\beta)} = m^{1-\beta} - (m-1)^{1-\beta} \quad , m > 1$

Slightly Compressible Flow Model

Space fractional derivative:

- Right sided derivative (after Kilbas et al., 2006)

$$
{}_{x_{i+1/2}}^{\;\;C}D_L^{\beta} = \frac{-1}{\Gamma(1-\beta)} \int_{x_{i+1/2}}^{L} \frac{\partial P(\xi, t_{n+1})}{\partial \xi} (\xi - x_{i+1/2})^{-\beta}\, d\xi
$$

$$
\cong -\sigma_{\beta,\Delta x} \sum_{m=1}^{Imax-i} \omega_m^{(\beta)} \left(P_{i+m}^{n+1} - P_{i+m-1}^{n+1}\right)
$$

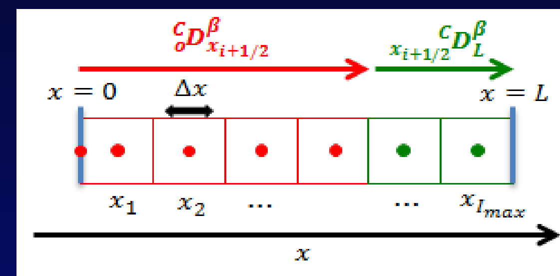

- General two-sided finite difference approximation:

$$
\frac{\partial^{\beta} p(x_{i+1/2}, t_{n+1})}{\partial x^{\beta}} = \sigma_{\beta,\Delta x} \left\{ \begin{array}{l} \vartheta \left[2\left(P_1^{n+1} - P_f^{n+1}\right)\omega_{i+1}^{(\beta)} + \displaystyle\sum_{m=1}^{i} \omega_m^{(\beta)} \left(P_{i+2-m}^{n+1} - P_{i+1-m}^{n+1}\right) \right] \\ +(1-\vartheta) \displaystyle\sum_{m=1}^{Imax-i} \omega_m^{(\beta)} \left(P_{i+m}^{n+1} - P_{i+m-1}^{n+1}\right) \end{array} \right\}
$$

Compressible Flow Model

Assumptions

- Conventional PVT correlations apply
  - Sutton (1985): pseudo-critical properties based on specific gravity
  - Dranchuck and Abou-Kassem (1975): z-factor
  - Lee et al. (1966): viscosity
- Single-point upstream weighting using fractional potentials

$$\left(\frac{1}{\mu B}\right)_{i+\frac{1}{2}}^{n+1,v} = \begin{cases} (1/\mu B)_{i+1}^{n+1,v} & \text{for } \left[\frac{\partial^{1-\alpha}}{\partial t^{1-\alpha}}\left(\frac{\partial^{\beta} P(x,t)}{\partial x^{\beta}}\right)\right]_{i+\frac{1}{2}}^{n+1,v} > 0 \\ (1/\mu B)_{i}^{n+1,v} & \text{for } \left[\frac{\partial^{1-\alpha}}{\partial t^{1-\alpha}}\left(\frac{\partial^{\beta} P(x,t)}{\partial x^{\beta}}\right)\right]_{i+\frac{1}{2}}^{n+1,v} < 0 \end{cases}$$

Model Validation – Constant Terminal Pressure

Gas model verification

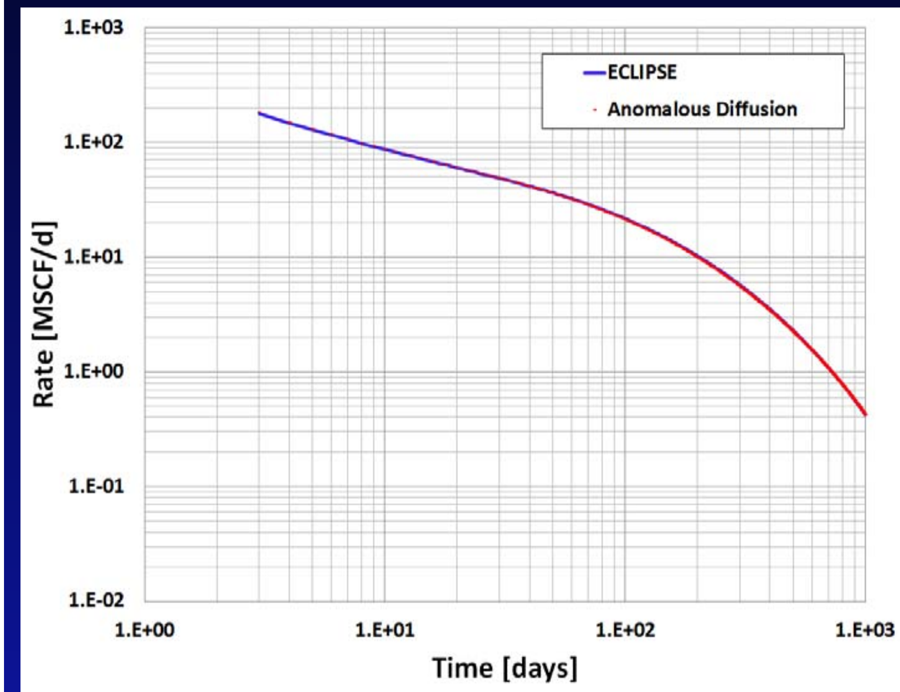

ECLIPSE comparison for normal diffusion case

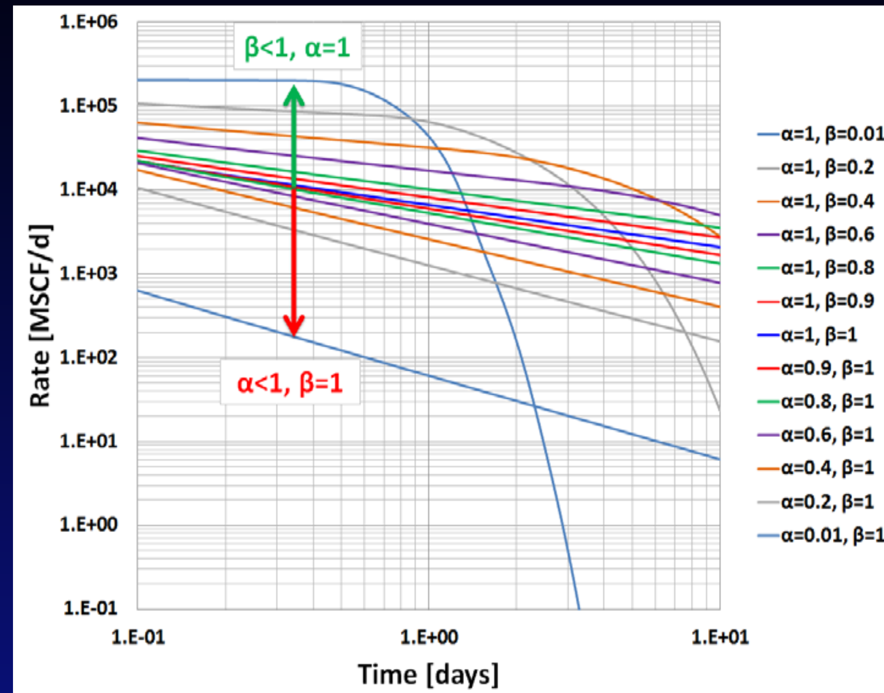

Transient slope validation with analytical slightly compressible flow model

Transient Slopes		
α, β	Analytical	Numerical
α=1, β=0.01	0.010	0.011
α=1, β=0.2	0.167	0.175
α=1, β=0.4	0.286	0.295
α=1, β=0.6	0.375	0.384
α=1, β=0.8	0.444	0.453
α=1, β=0.9	0.474	0.479
α=1, β=1	0.500	0.504
α=0.9, β=1	0.550	0.555
α=0.8, β=1	0.600	0.600
α=0.6, β=1	0.700	0.706
α=0.4, β=1	0.800	0.807
α=0.2, β=1	0.900	0.907
α=0.01, β=1	0.995	0.999

Multiphase Flow Model

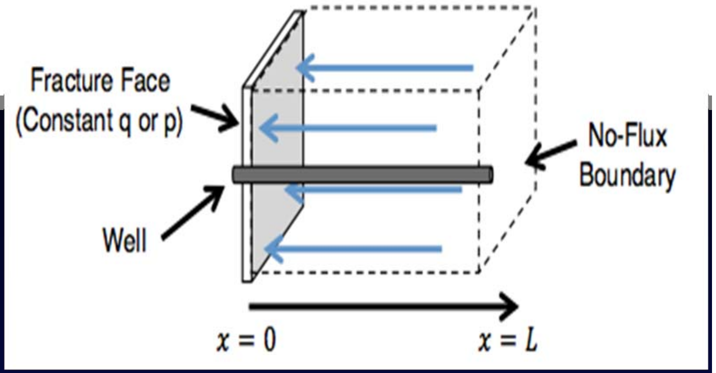

Oil + water 1D flow – constant terminal pressure

- Assumptions
  - Capillary pressure and rel. perms defined in conventional way
  - Same set of exponents α and β used for oil and water flux
  - $p_o(0,t) = p_w(0,t) = p_f(t)$
- Oil Phase:
  - Flux: $u_m = -k_{\alpha,\beta} \dfrac{k_{rm}}{\mu_m} \dfrac{\partial^{1-\alpha}}{\partial t^{1-\alpha}} \left(\dfrac{\partial^\beta p_m}{\partial x^\beta} \right)$ $\quad m = o \text{ or } w$
  - Global pressure eq. ($C_{P_c} = 1$ if $\partial p_c / \partial t$ negligible over sim. Step)

$$\left\{ \begin{aligned} & B_o \frac{\partial}{\partial x}\left(\frac{k_{\alpha,\beta} k_{ro}}{B_o \mu_o} \frac{\partial^{1-\alpha}}{\partial t^{1-\alpha}} \left(\frac{\partial^\beta p_o}{\partial x^\beta} \right) \right) \\ & + \frac{B_w}{C_{P_c}} \frac{\partial}{\partial x}\left(\frac{k_{\alpha,\beta} k_{rw}}{B_w \mu_w} \frac{\partial^{1-\alpha}}{\partial t^{1-\alpha}} \left(\frac{\partial^\beta (p_o - p_c)}{\partial x^\beta} \right) \right) \end{aligned} \right\} = \phi \left(S_o c_f + S_o c_o + \frac{S_w c_f + S_w c_w}{C_{P_c}} \right) \frac{\partial p_o}{\partial t}$$

Multiphase Flow Model

- Single-point upstream weighting using fractional potentials

$$\left(k_{ro,w}/\mu_{o,w}\right)^n_{i+\frac{1}{2}} = \begin{cases} \left(k_{ro,w}/\mu_{o,w}\right)^n_{i+1} & for \left[\dfrac{\partial^{1-\alpha}}{\partial t^{1-\alpha}}\left(\dfrac{\partial^{\beta} p_{o,w}(x,t)}{\partial x^{\beta}}\right)\right]^n_{i+\frac{1}{2}} > 0 \\ \left(k_{ro}/\mu_{o,w}\right)^n_{i} & for \left[\dfrac{\partial^{1-\alpha}}{\partial t^{1-\alpha}}\left(\dfrac{\partial^{\beta} p_{o,w}(x,t)}{\partial x^{\beta}}\right)\right]^n_{i+\frac{1}{2}} < 0 \end{cases}$$

- Solve for oil saturations at t_{n+1}:

$$S_{o_i}^{\,n+1} = S_{o_i}^{\,n}\left[1-\left(c_f+c_o\right)\left(P_{o_i}^{\,n+1}-P_{o_i}^{\,n}\right)\right] + \Delta t\left(\frac{B_o}{\phi}\frac{1}{\Delta x}\right)^n_i \left(\begin{array}{l} +\left[\left(\dfrac{k_{\alpha,\beta}k_{ro}}{B_o\mu_o}\right)_{i+\frac{1}{2}}\right]^n \left[\dfrac{\partial^{1-\alpha}}{\partial t^{1-\alpha}}\left(\dfrac{\partial^{\beta} P_o(x,t)}{\partial x^{\beta}}\right)\right]^{n+1}_{i+\frac{1}{2}} \\ -\left[\left(\dfrac{k_{\alpha,\beta}k_{ro}}{B_o\mu_o}\right)_{i-\frac{1}{2}}\right]^n \left[\dfrac{\partial^{1-\alpha}}{\partial t^{1-\alpha}}\left(\dfrac{\partial^{\beta} P_o(x,t)}{\partial x^{\beta}}\right)\right]^{n+1}_{i-\frac{1}{2}} \end{array}\right)$$

Model Validation – Constant Terminal Pressure

Multiphase model verification

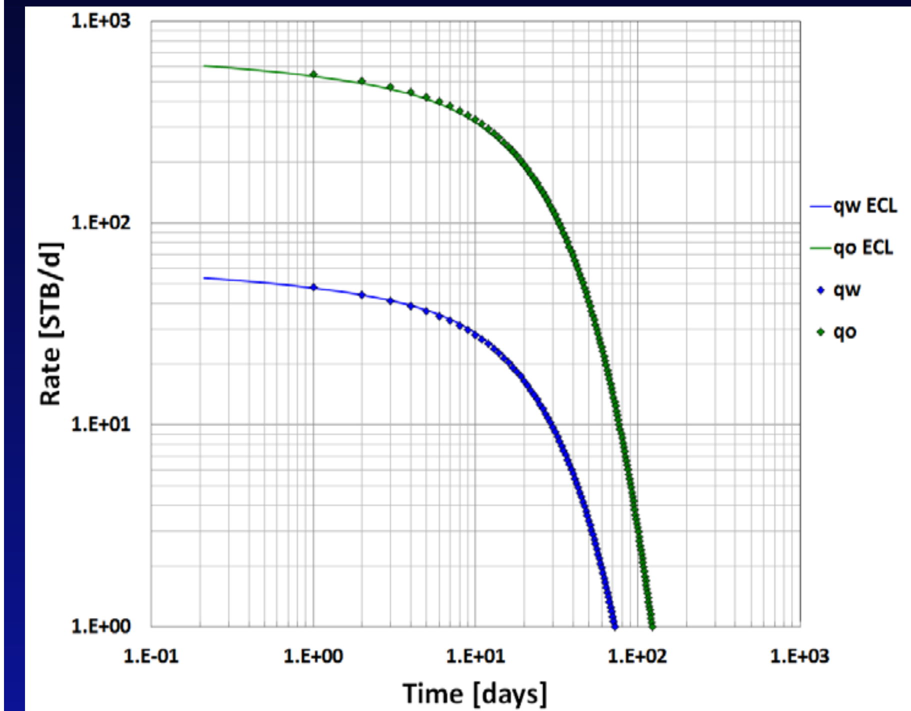

ECLIPSE comparison for normal diffusion case

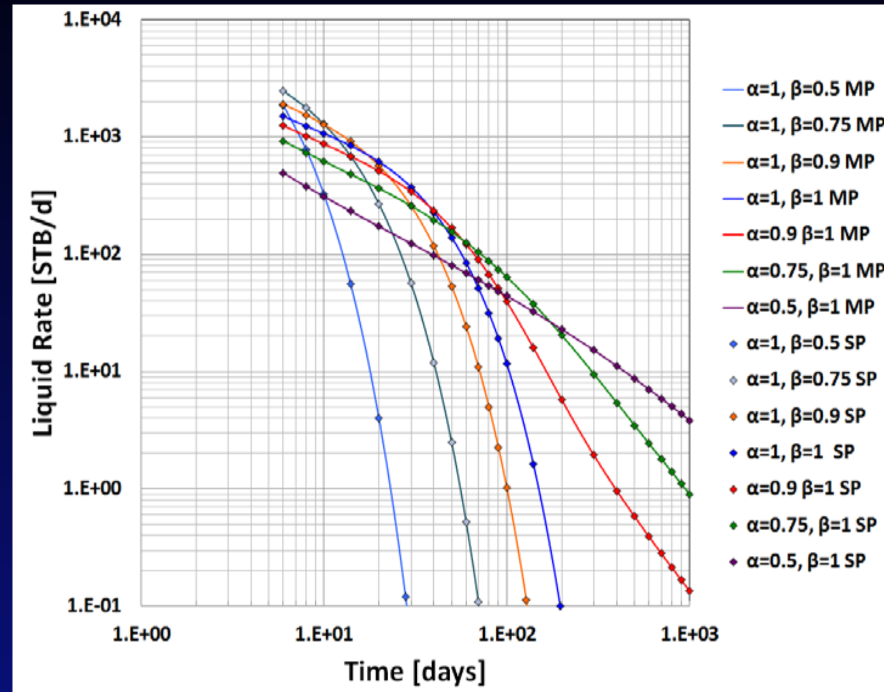

Single phase vs multiphase liquid rate for

$$\frac{k_{ro}}{\mu_o} + \frac{k_{rw}}{\mu_w} = 1\,, c_o = c_w, B_o = B_w$$

Model Validation – Constant Terminal Pressure

Sensitivity on exponents α and β , (β =1)

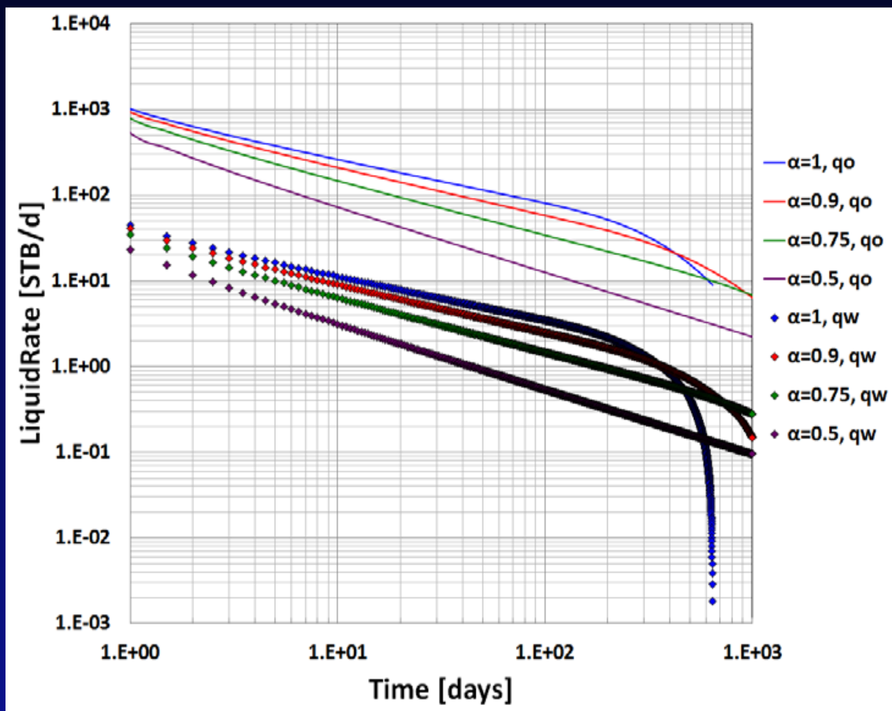

Sub-diffusion (α < 1)

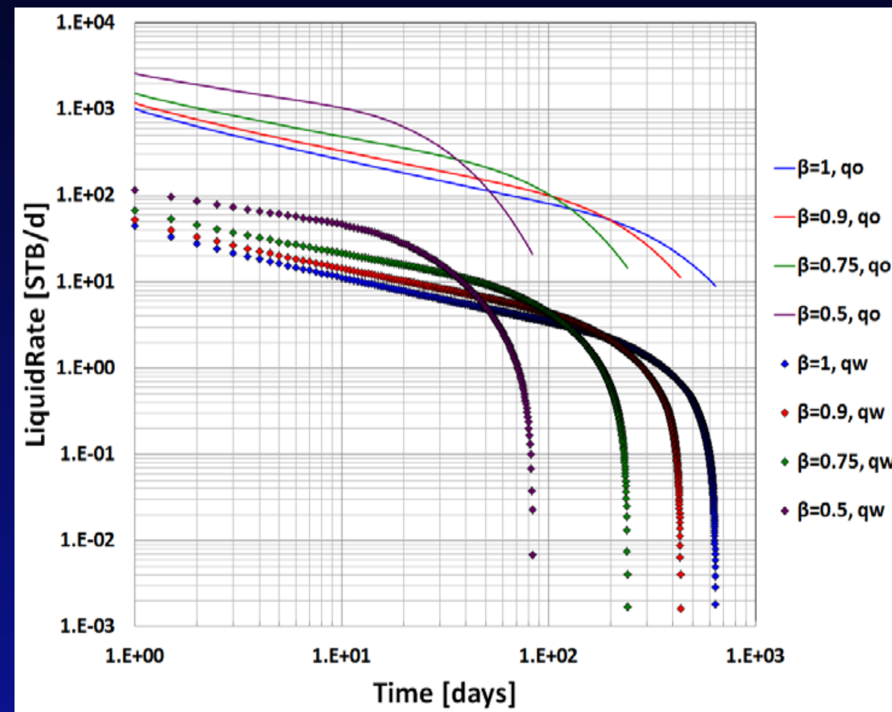

Super-diffusion (β < 1)

Research Summary

Gas Flow Inside Nano-Fluidic Chips

Elham Parsa, Colorado School of Mines

Outline

- Background
- Tasks Report
- Literature Review
- Laboratory Experiments
- Modeling
- Conclusion

Background

- Prediction of unconventional reservoir life depends on the understanding of the phase behavior of hydrocarbons inside.
- Unconventional reservoirs have abundant nano-pores in which phase behaviors of hydrocarbons deviate from the expected conventional behaviors i.e. condensation/ vaporization can happen at conditions different than those measured in PVT cells.
- Objective of this study: Direct visualization of phase change of confined hydrocarbon fluids inside the nano-fluidic chips.

Tasks Report

Completed and reported:

- Propane condensation experiments inside the nano-fluidic chips (confinement).
- Comparing the experimental results with standard database and Kelvin equation.

Currently undertaken :

- Propane condensation experiments inside the micro-fluidic chips (Bulk).
- Building an insulated box around the experimental set up in order to minimize the temperature issue.
- investigating the pressure sensors use, instead of pressure gauges.

Final (expected) outcome:

- Repeating the bulk and nano-fluidic chips experiments in the insulated set up at different temperatures.
- Kelvin equation can duplicate our experimental results.

Experiment Setup

- Condensing the %99.99 pure propane gas into the micro/nano-fluidic chips
- Observing the condensation with microscope
- Different temperatures
- Different nano-channels sizes

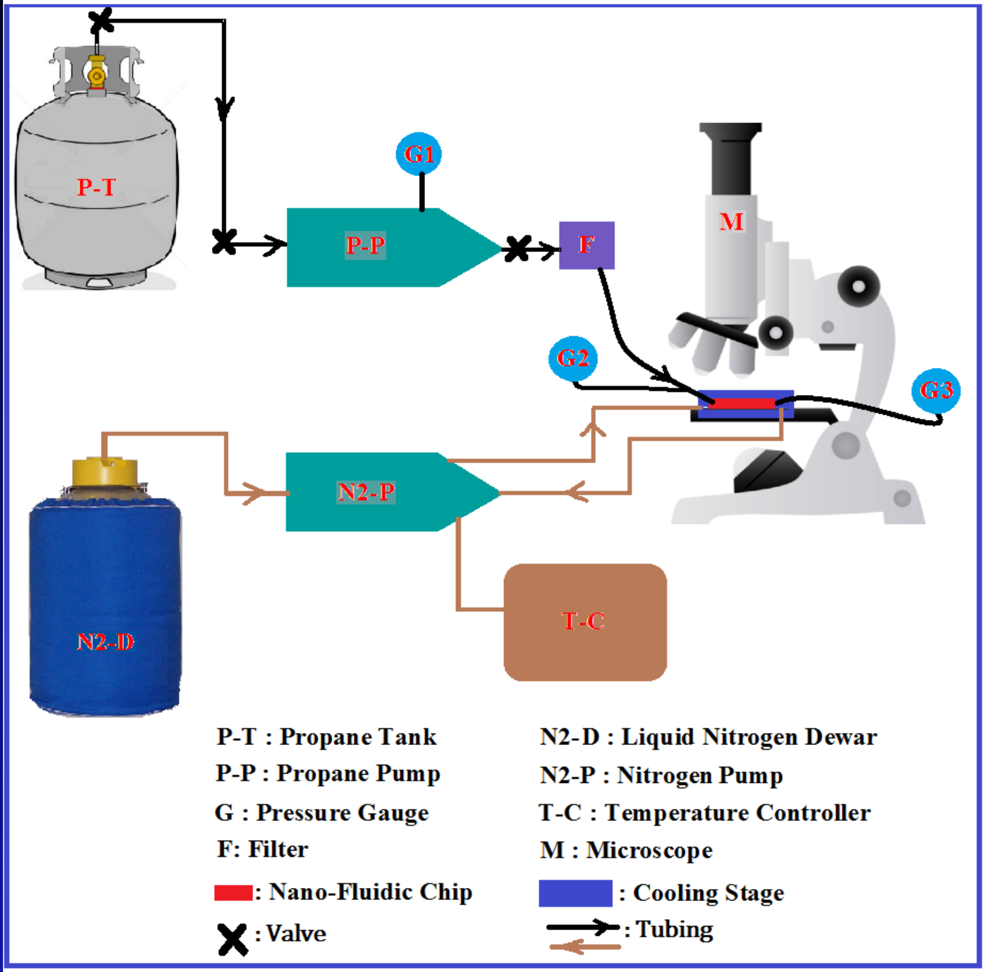

Different Nano-Fluidic Chips

- Ionic bonding the silicon chip to the Pyrex plate at 300 C and 800 volts.
- Gluing the coned ports to the holes on silicon chip


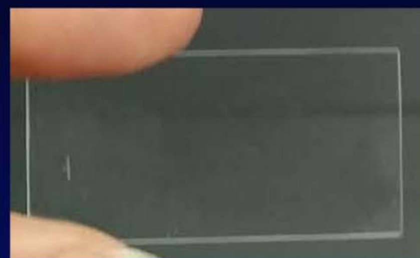

- Random pattern channels (30 nm or 300 nm depth)
- Parallel pattern channels (10 nm, 50 nm and 500 nm depth)

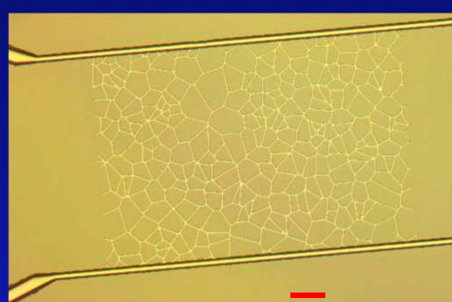

100 micrometer

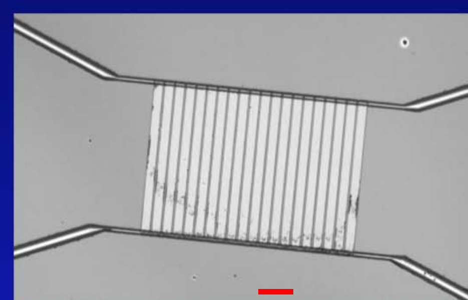

200 micrometer

Laboratory Experiment

Bulk:

- Condensing the propane in micro-channels (bulk)
- Reproduction of standard bulk vapor pressures (NIST database)

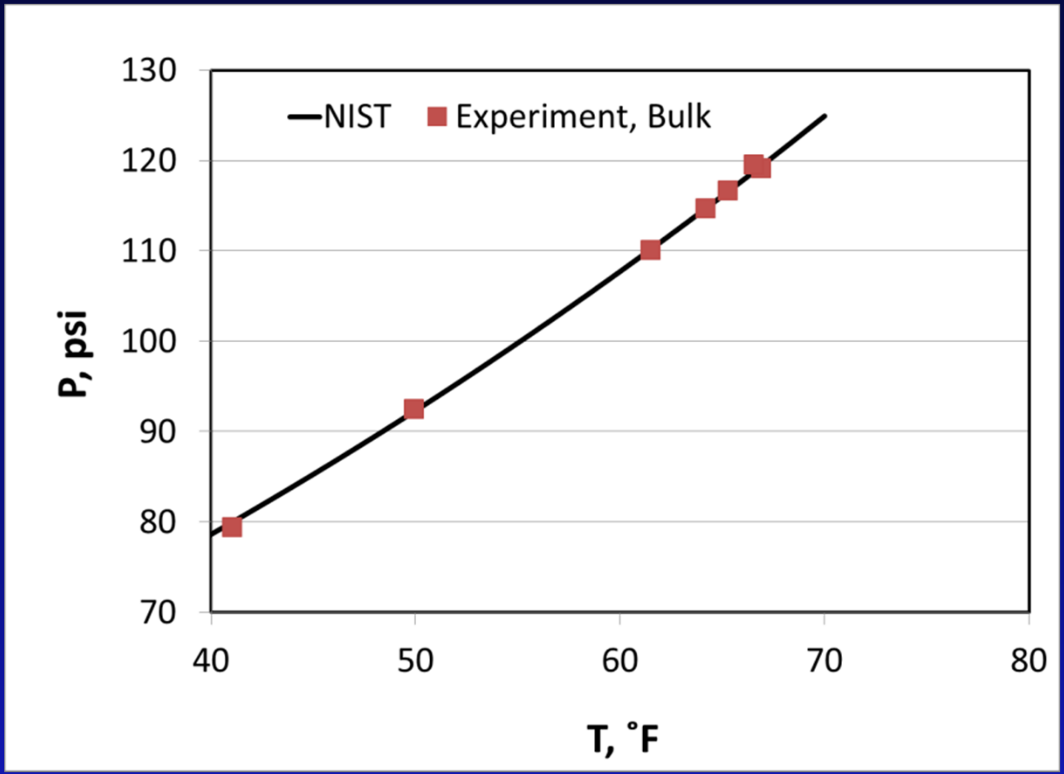

Laboratory Experiment

Confinement:

- Condensing the propane in nano-channels (confinement)
- At 500 nm channels, we were able to duplicate the NIST bulk value
- At 300, 50, 30 and 10 nm channels we observed lower condensation pressures than NIST

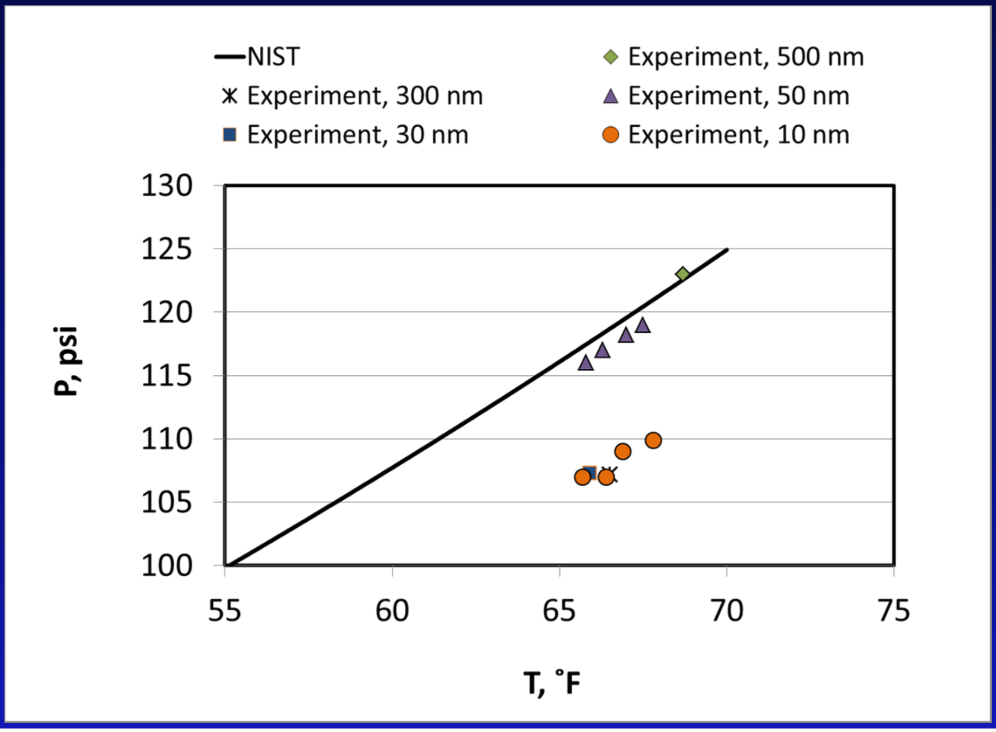

Modeling: Kelvin Equation

Kelvin equation includes the effect of confinement on condensation pressure.

$$\ln\left(\frac{P_s}{P_{ss}}\right) = -\frac{v^l \sigma}{RT}\left(\frac{1}{r_1} + \frac{1}{r_2}\right)$$

P_{ss} : Standard saturation pressure

P_s: Confined saturation pressure

v^l : Liquid molar volume

σ : Interfacial tension

r_1 and r_2 : Pore width and depth

R: Gas constant

T: Temperature

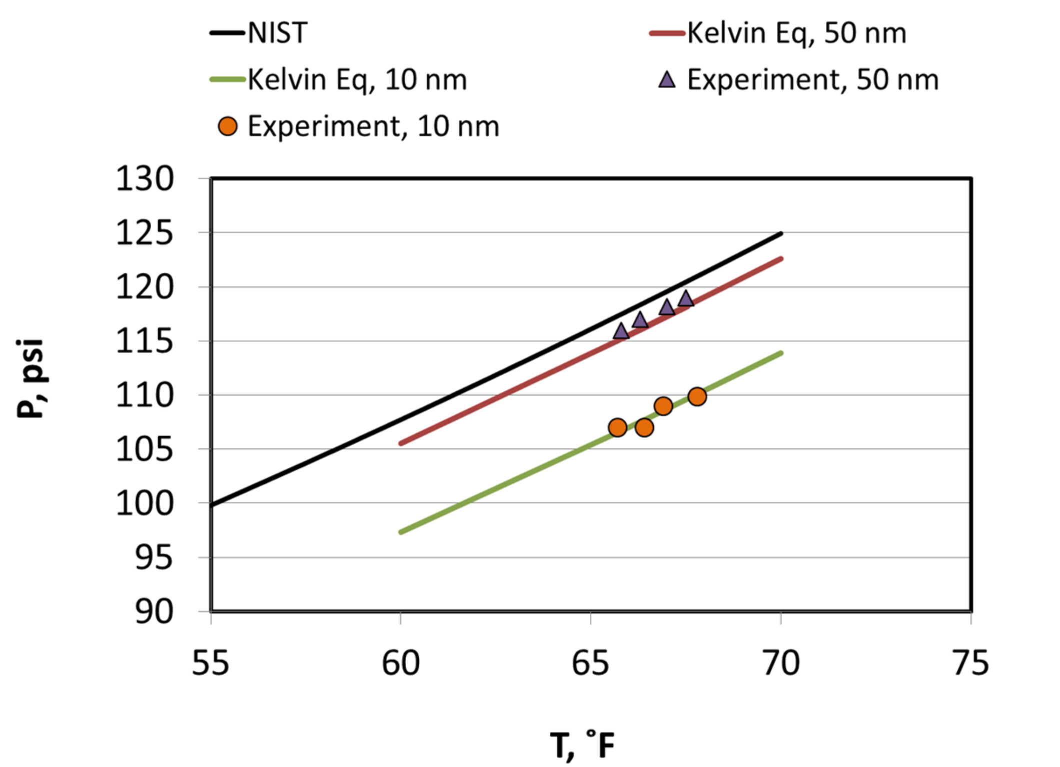

Modeling: Kelvin Equation

- In random pattern channels, condensation happened in the corners first.
- Kelvin equation does not includes the effect of corners on condensation pressure.

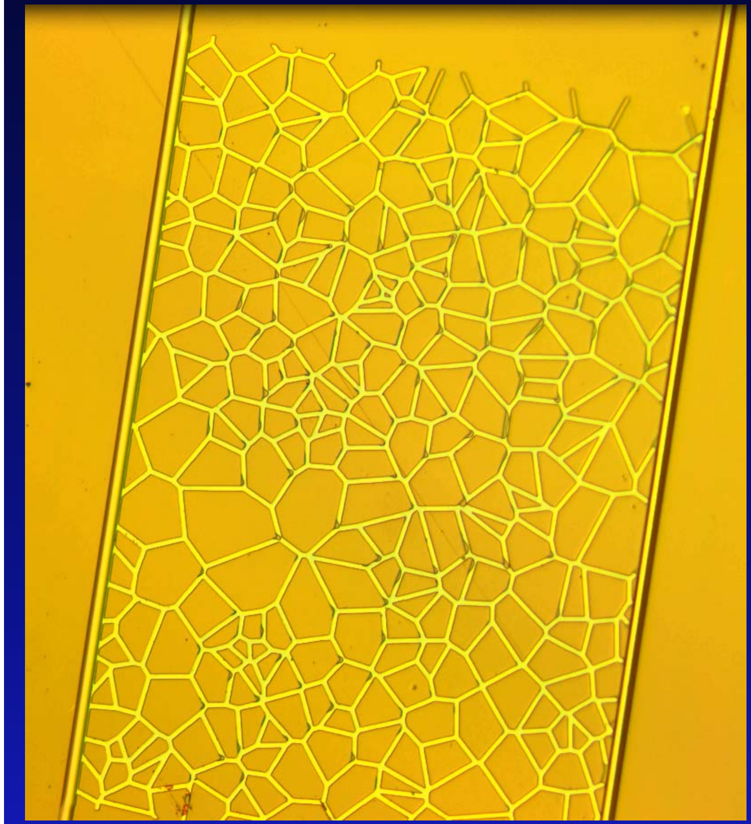

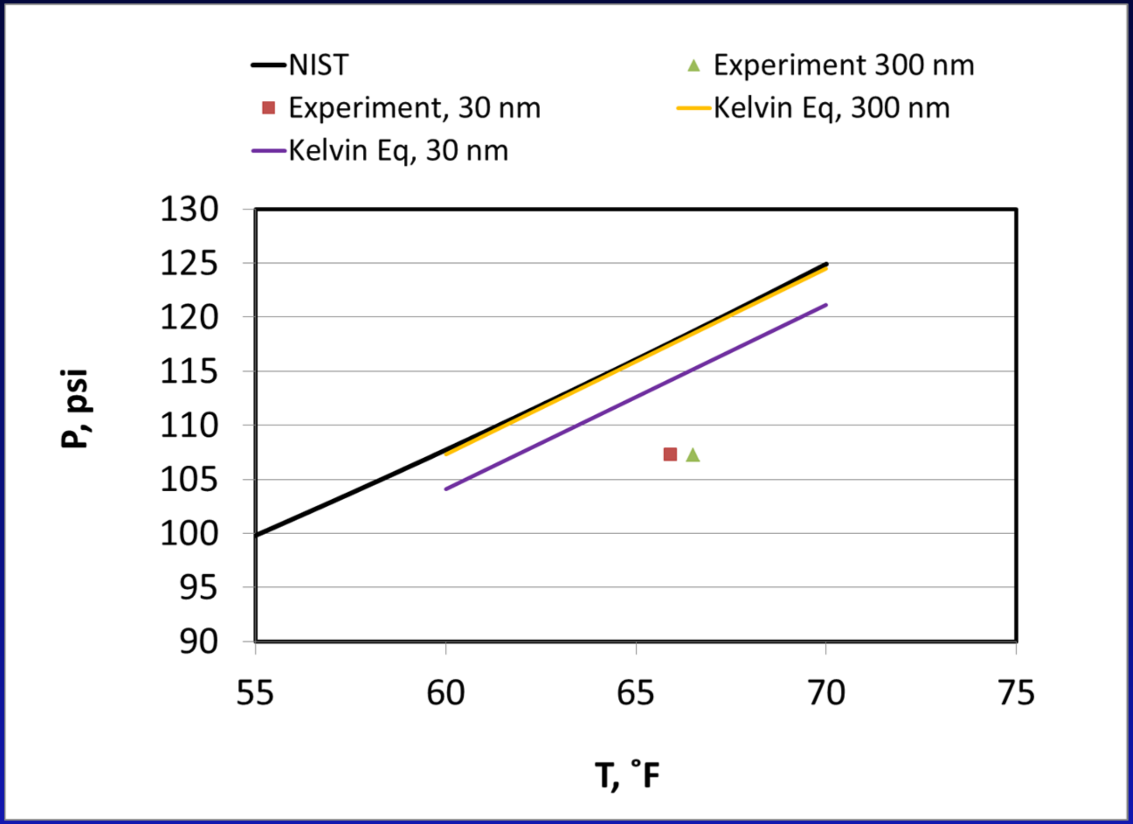

Insulated Box

- Room temperature is higher than cooling stage temperature
- Chip temperature is not exactly the temperature of the cooling stage, leading to errors
- Building an insolated box, with an AC unit, around the set up to provide better environmental control

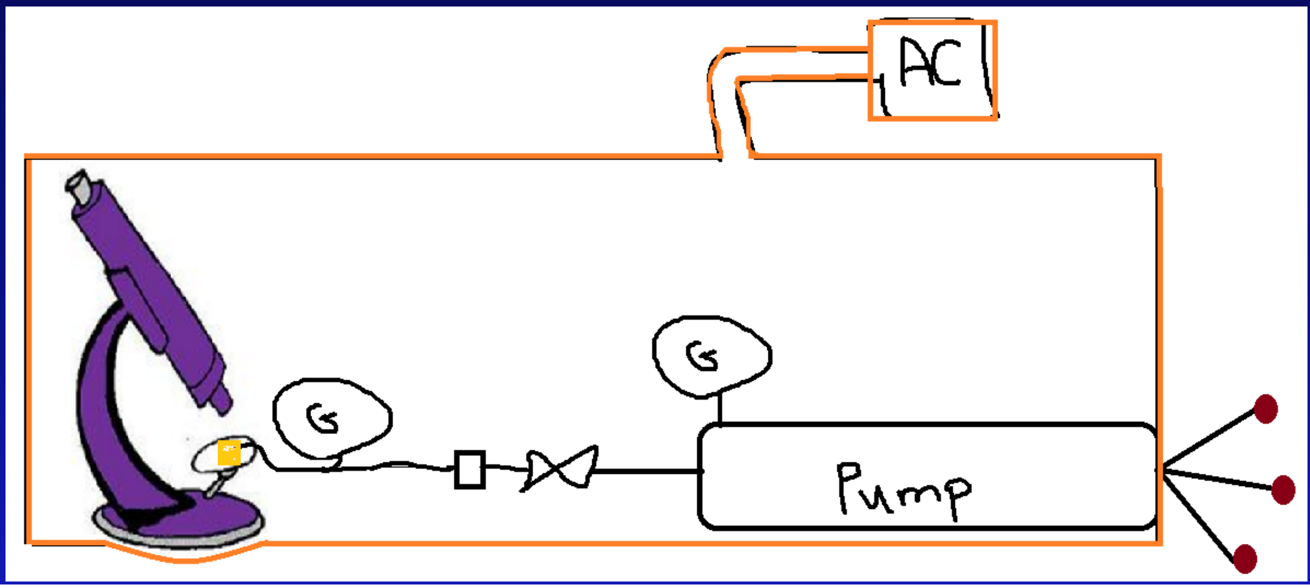

Conclusion

- Reproduced the standard (bulk) vapor pressure of propane
- Based on our experiments at 300 nm and smaller confinements, propane saturation pressure is less than its bulk value (most literature say that confinement effect starts at 10 nm or less)
- Kelvin equation can predict our experimental results in parallel nano-channels
- Kelvin equation couldn’t predict our experimental results in random pattern nano-channels

THANK YOU

Research Summary

Impact of Confinement on Flow: Black Oil Simulation

Tugce Calisgan, Colorado School of Mines

Scope of Research

Firincioglu et al. (2013)

- single porosity
- 2D model
- vertical wells
- single Pcgo distribution

New study

- multi porosity
- 3D model
- vertical/horizontal wells
- different Pcgo distribution
- realistic case study
- history match

Verify the impact of confined PVT behavior (pore size impact) on flow in unconventional reservoirs using a black oil simulator

Application – Simulation Model

- Dual-porosity concept assumes discrete matrix blocks in the continuous fracture network formed by intersecting horizontal and vertical fractures (Warren and Root, 1963)
- Extension of the dual-porosity formulation to n-porosity is performed in two different approaches: parallel (matrix-fracture) and serial (matrix-matrix-fracture)

Serial

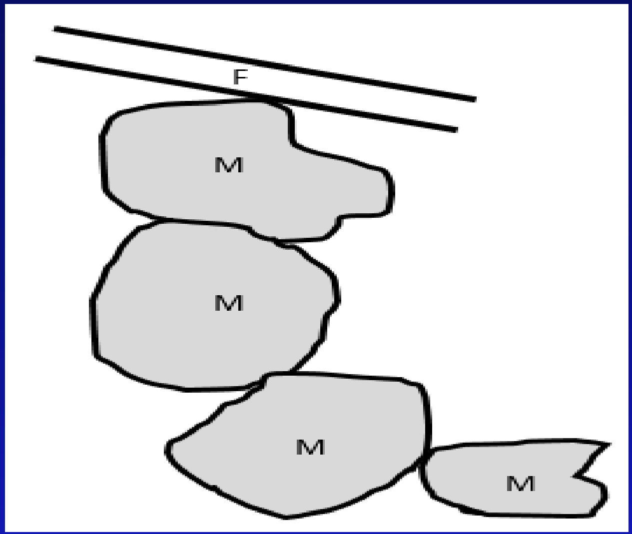

Parallel

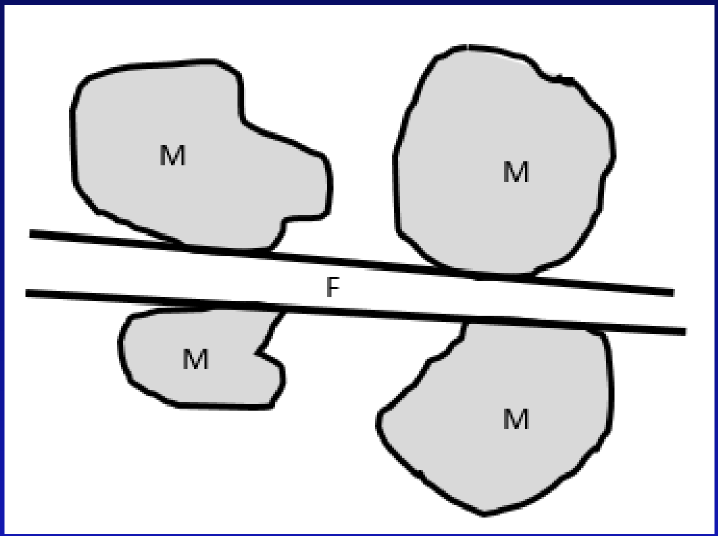

Application – Case Design

- 10mD matrix permeability & 20% matrix porosity
- Bulk P_b = 975 psi; R_s = 158 SCF/STB
- Initially undersaturated

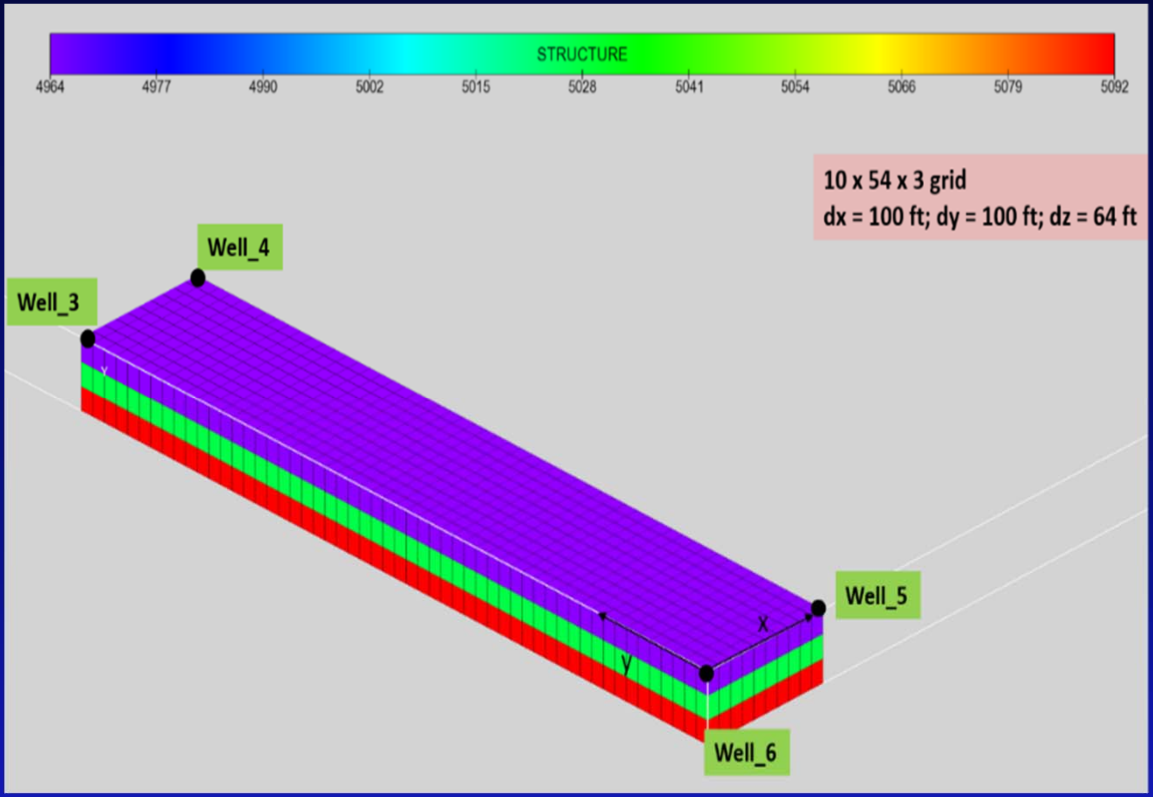

Application – Case Design

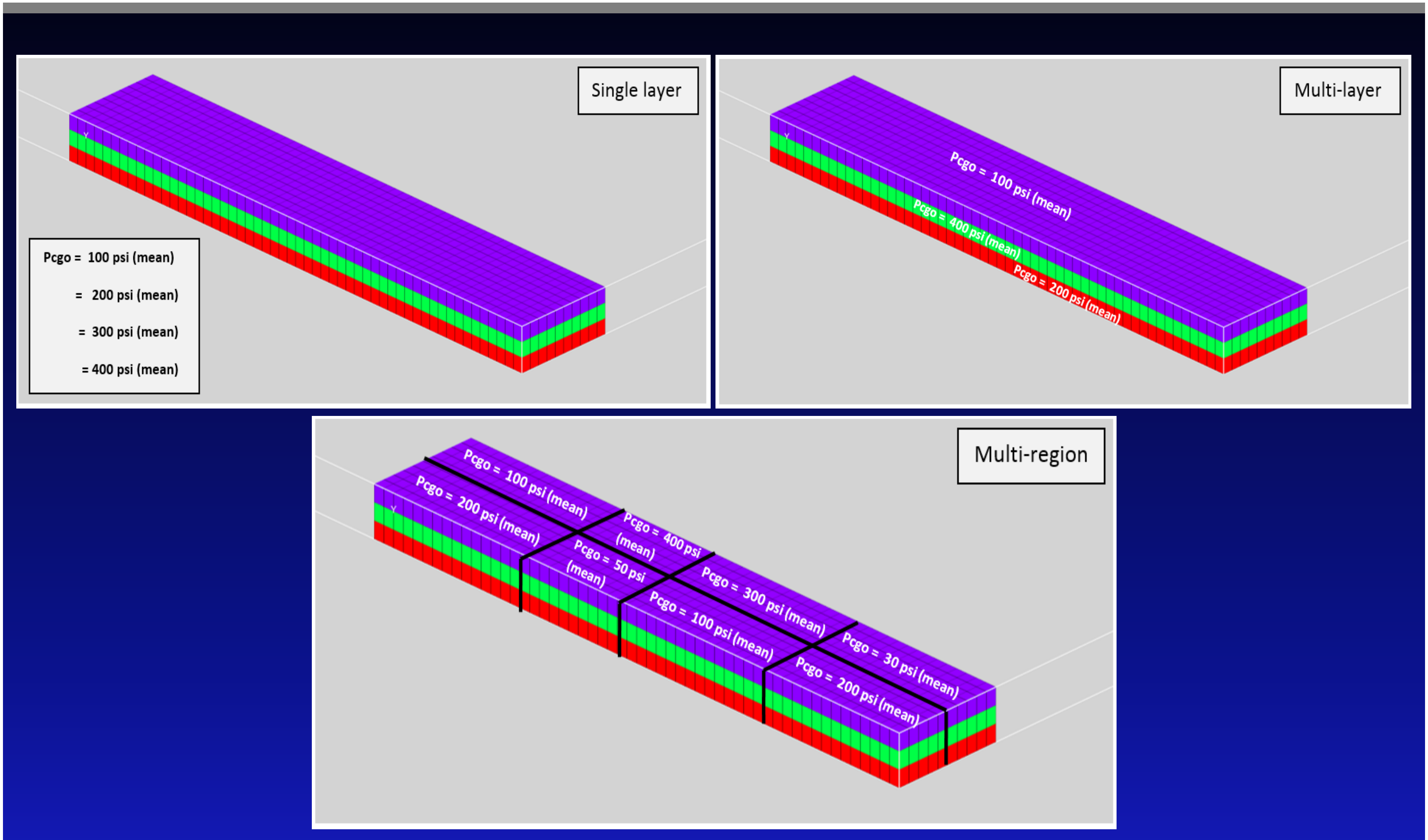

Results – Impact of different Pcgo distributions

Single porosity system

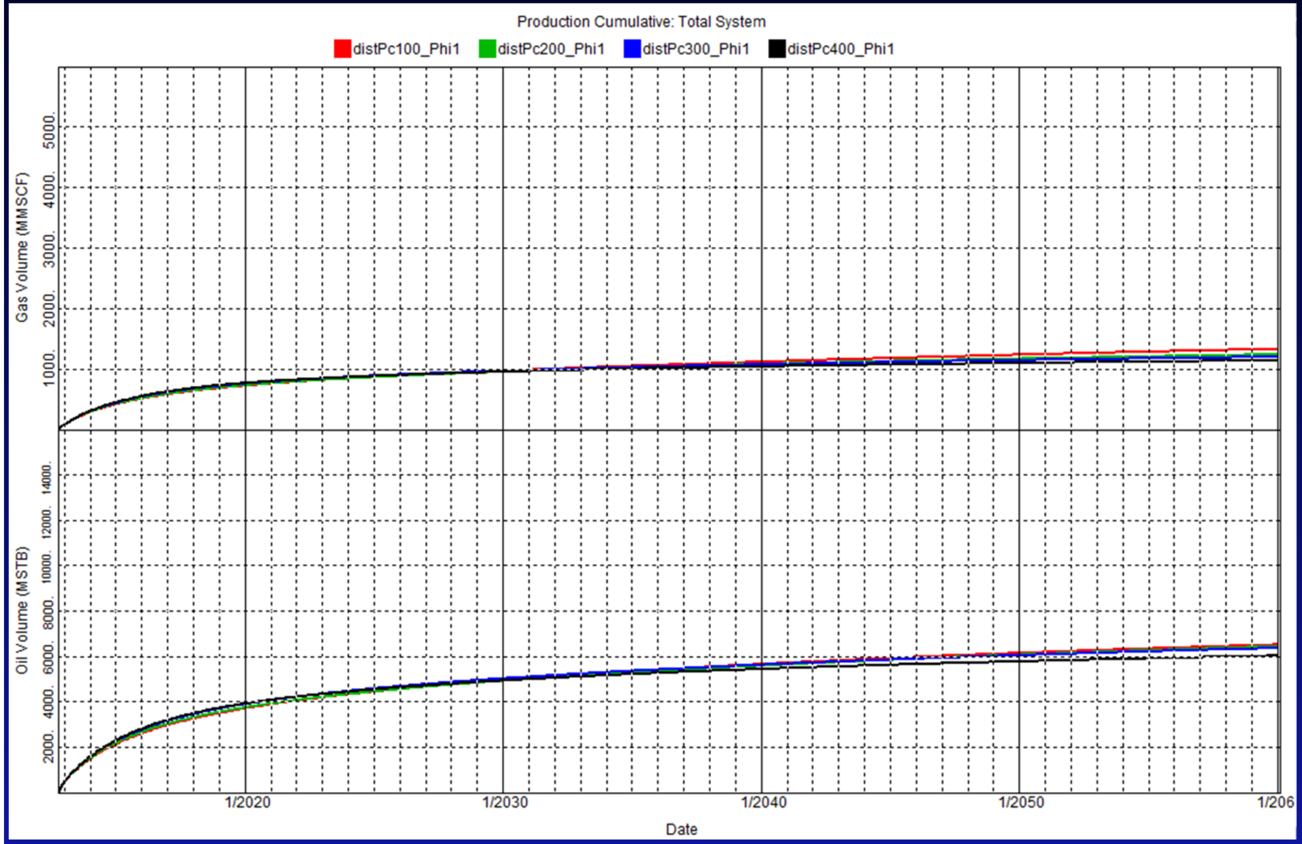

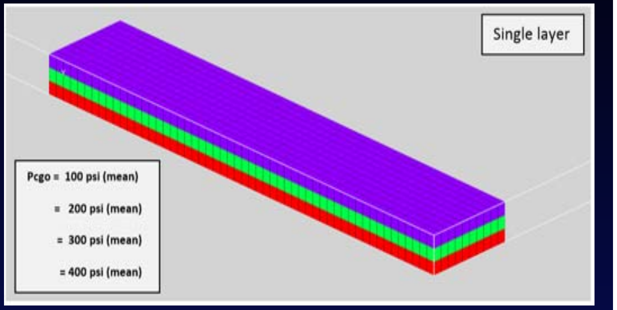

Results – Impact of different Pcgo distributions

Single porosity system

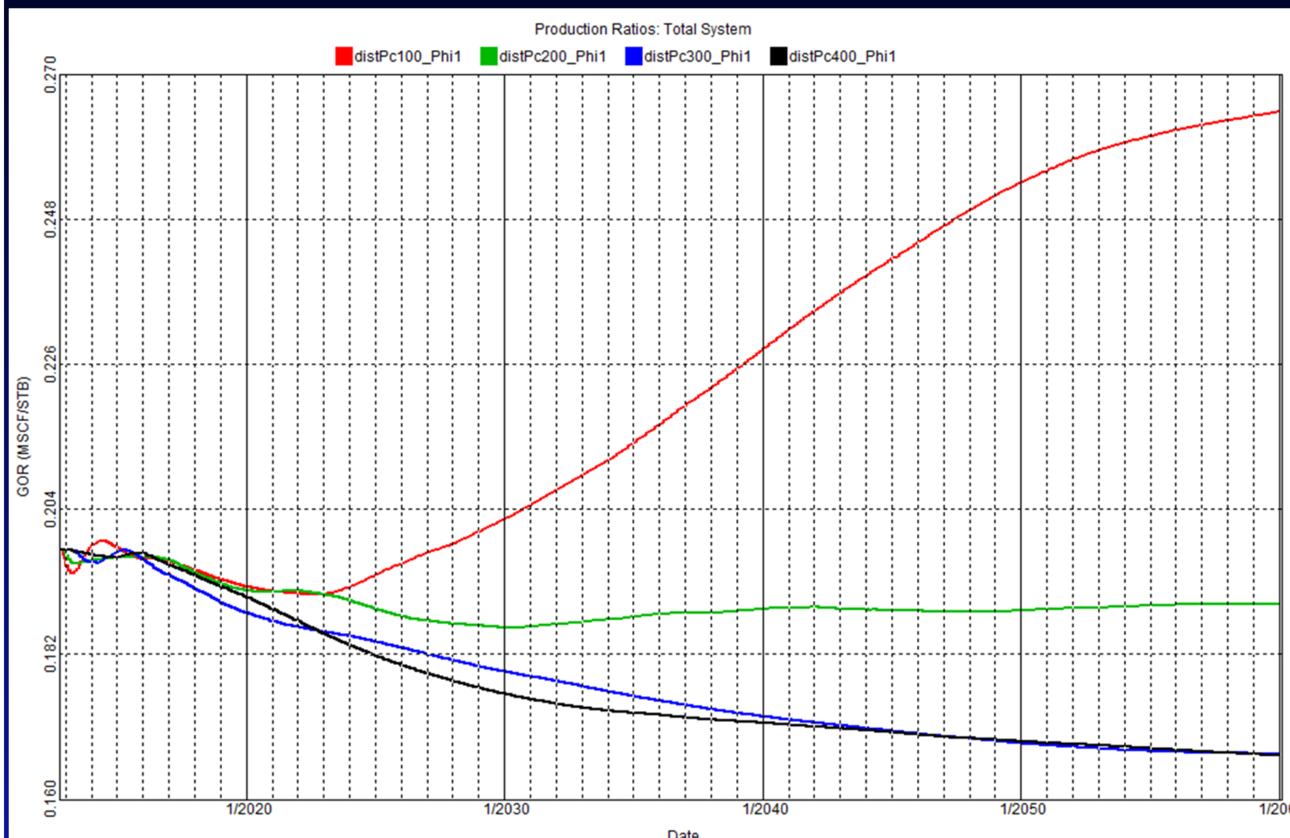

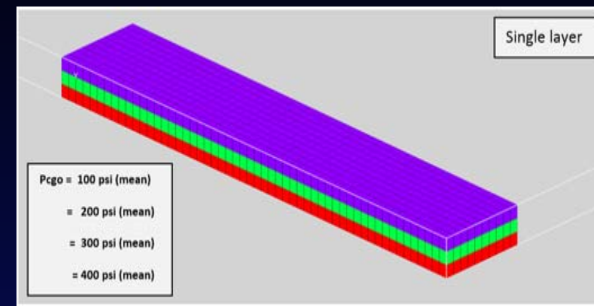

Results – Impact of different Pcgo distributions

Single porosity system

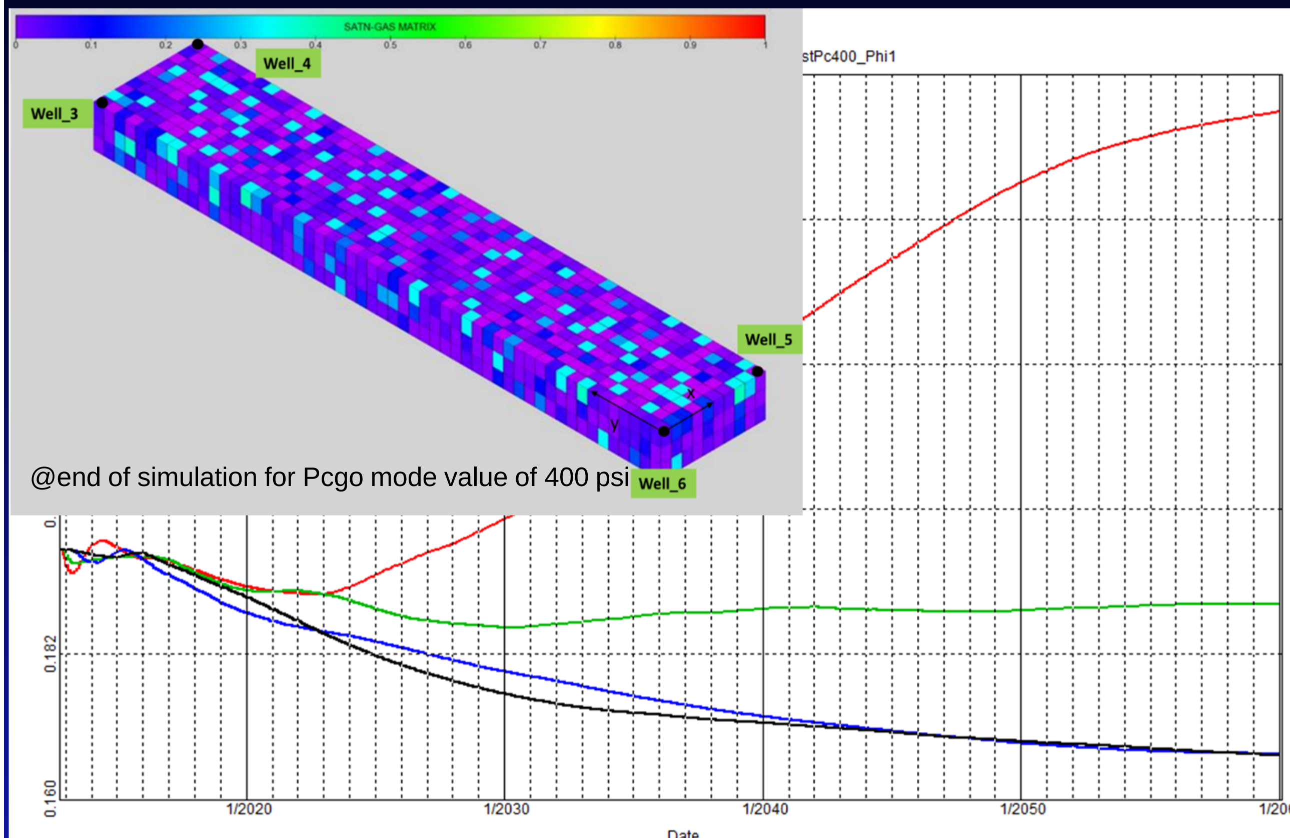

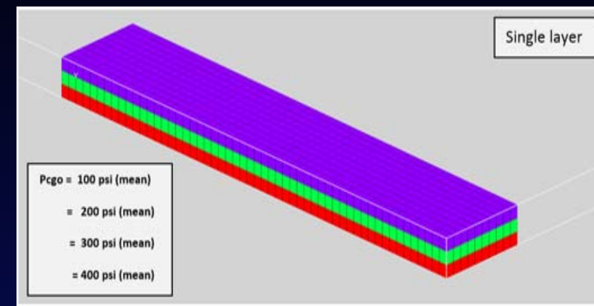

Results – Impact of different Pcgo distributions

Single porosity system

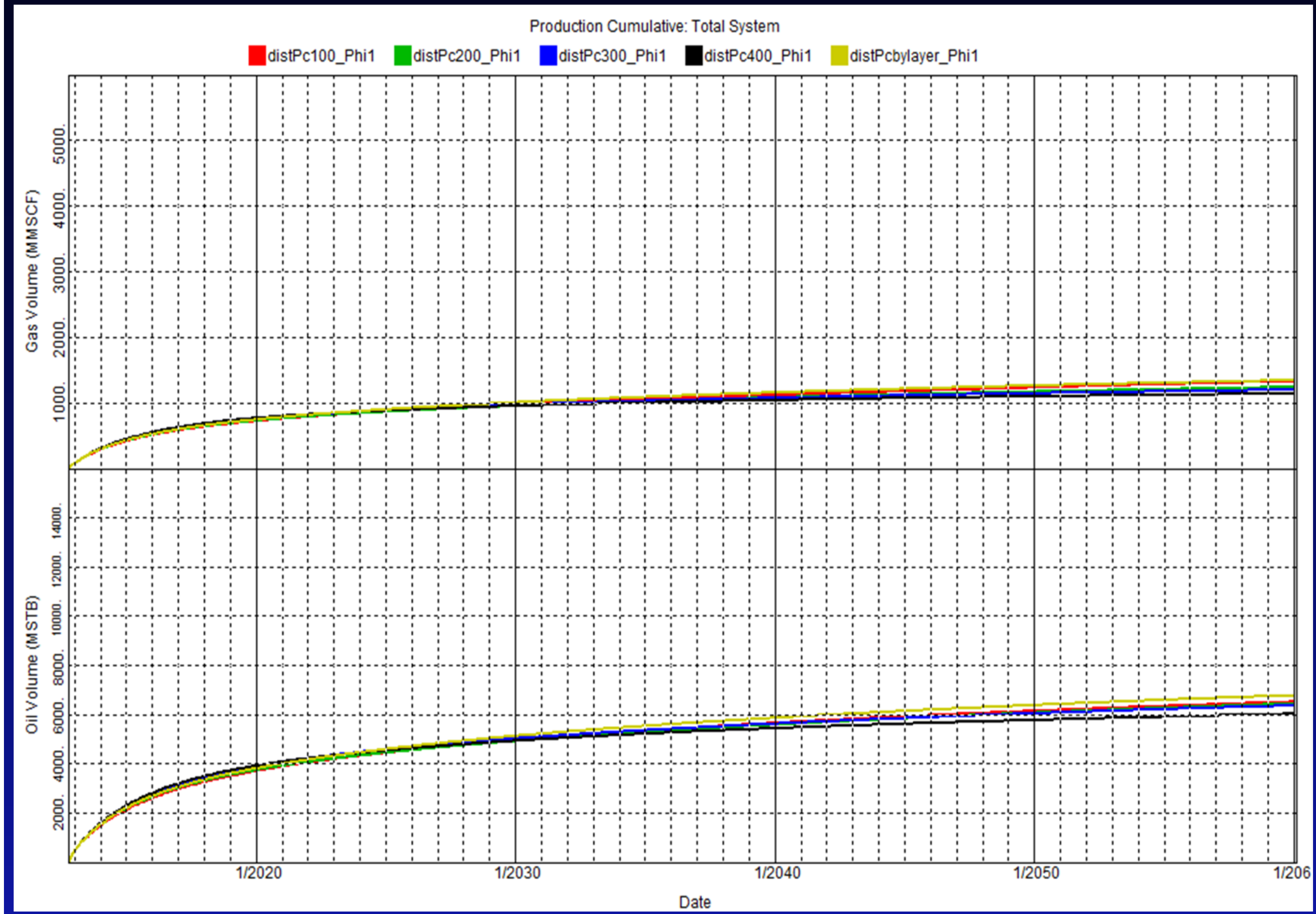

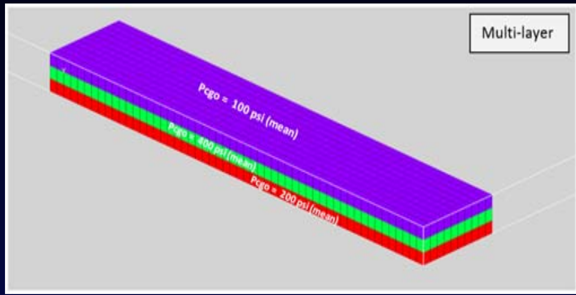

Results – Impact of different Pcgo distributions

Single porosity system

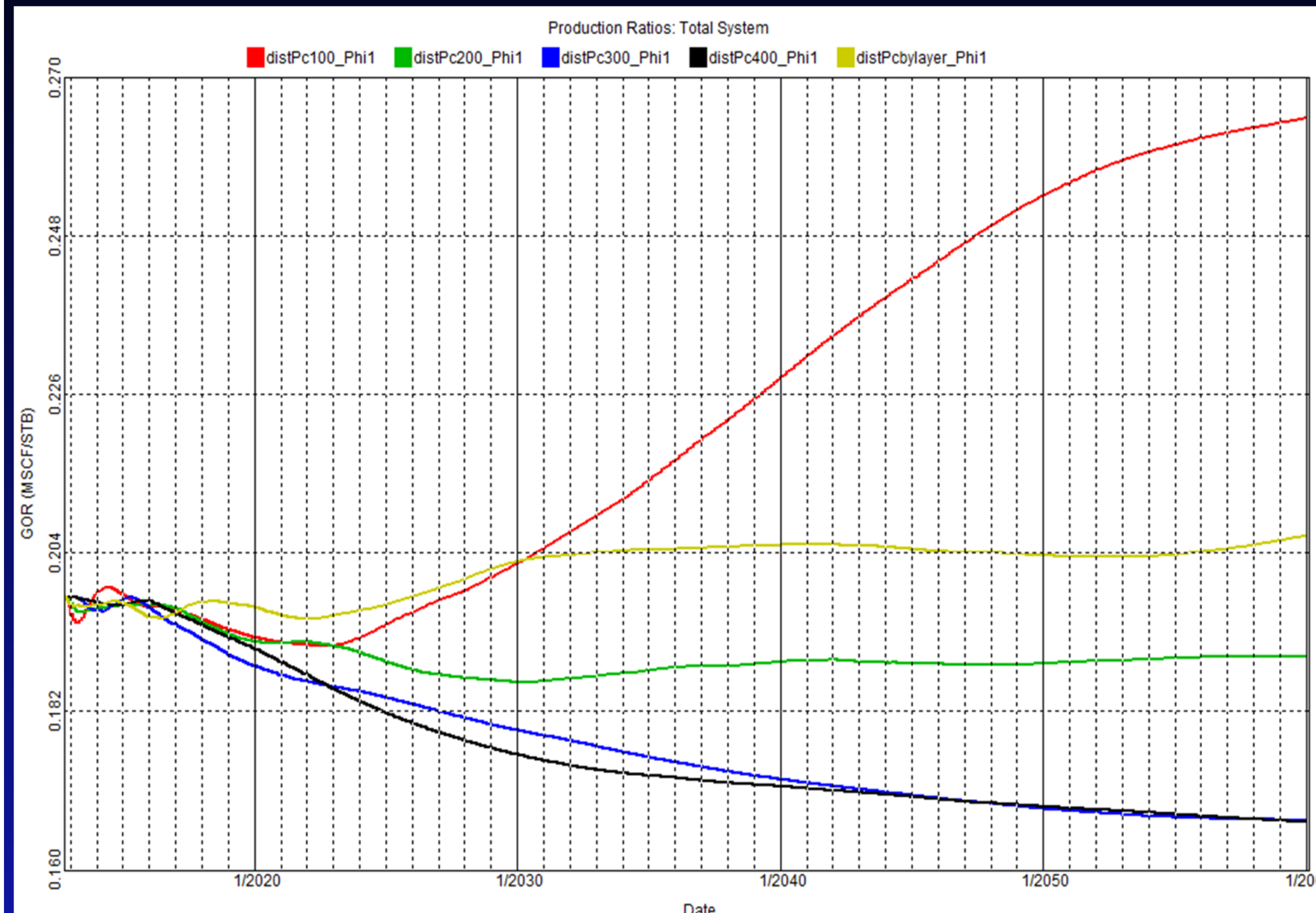

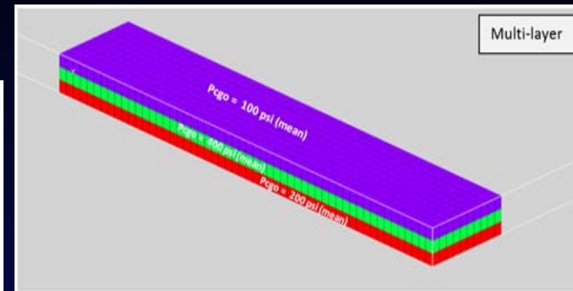

Results – Impact of different Pcgo distributions

Single porosity system

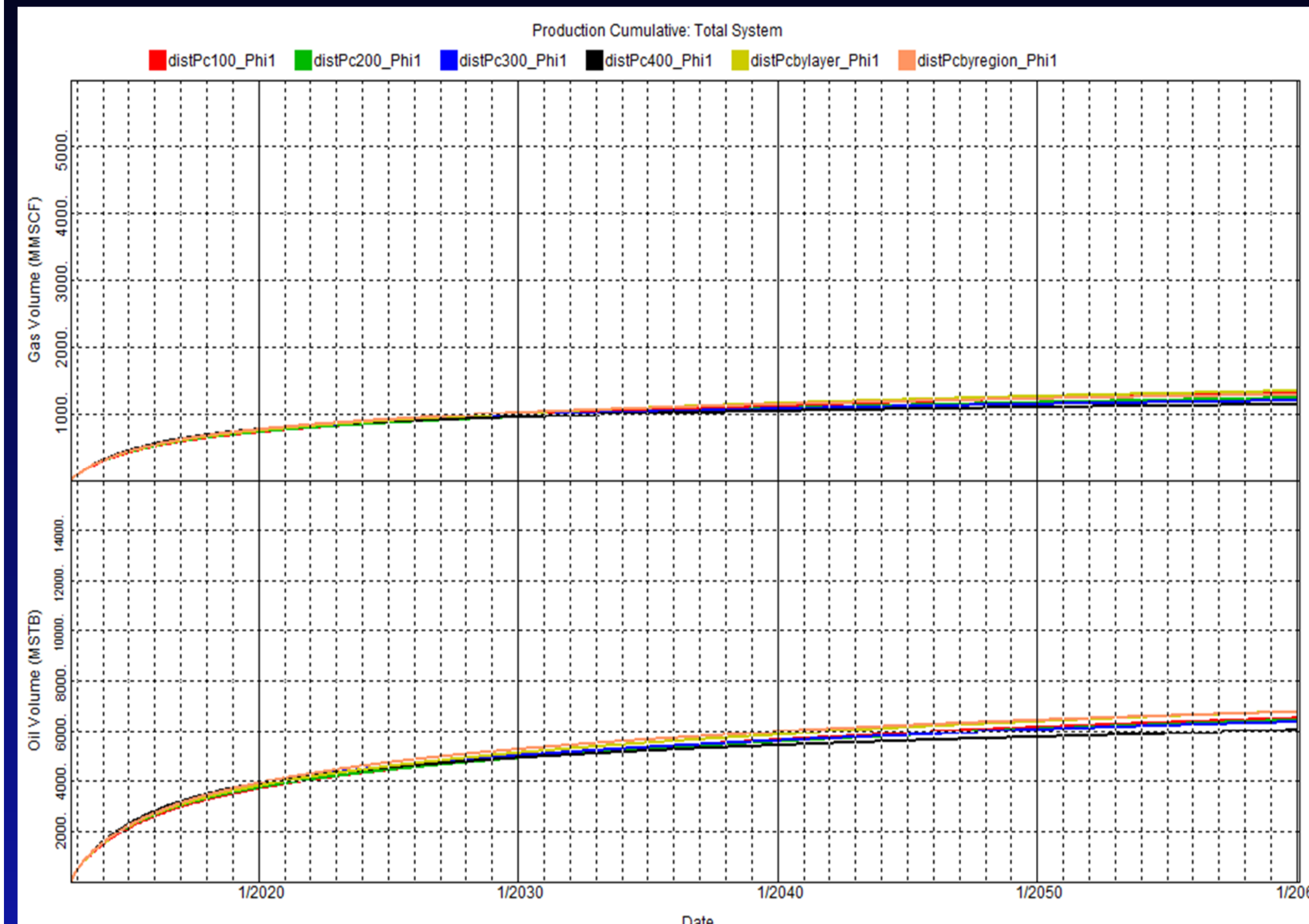

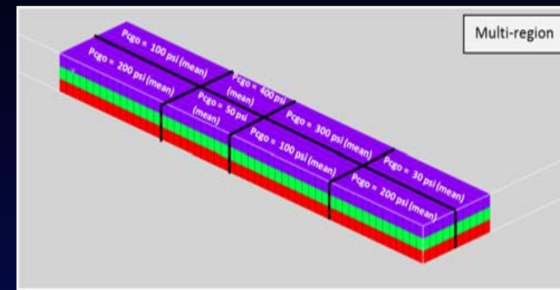

Results – Impact of different Pcgo distributions

Single porosity system

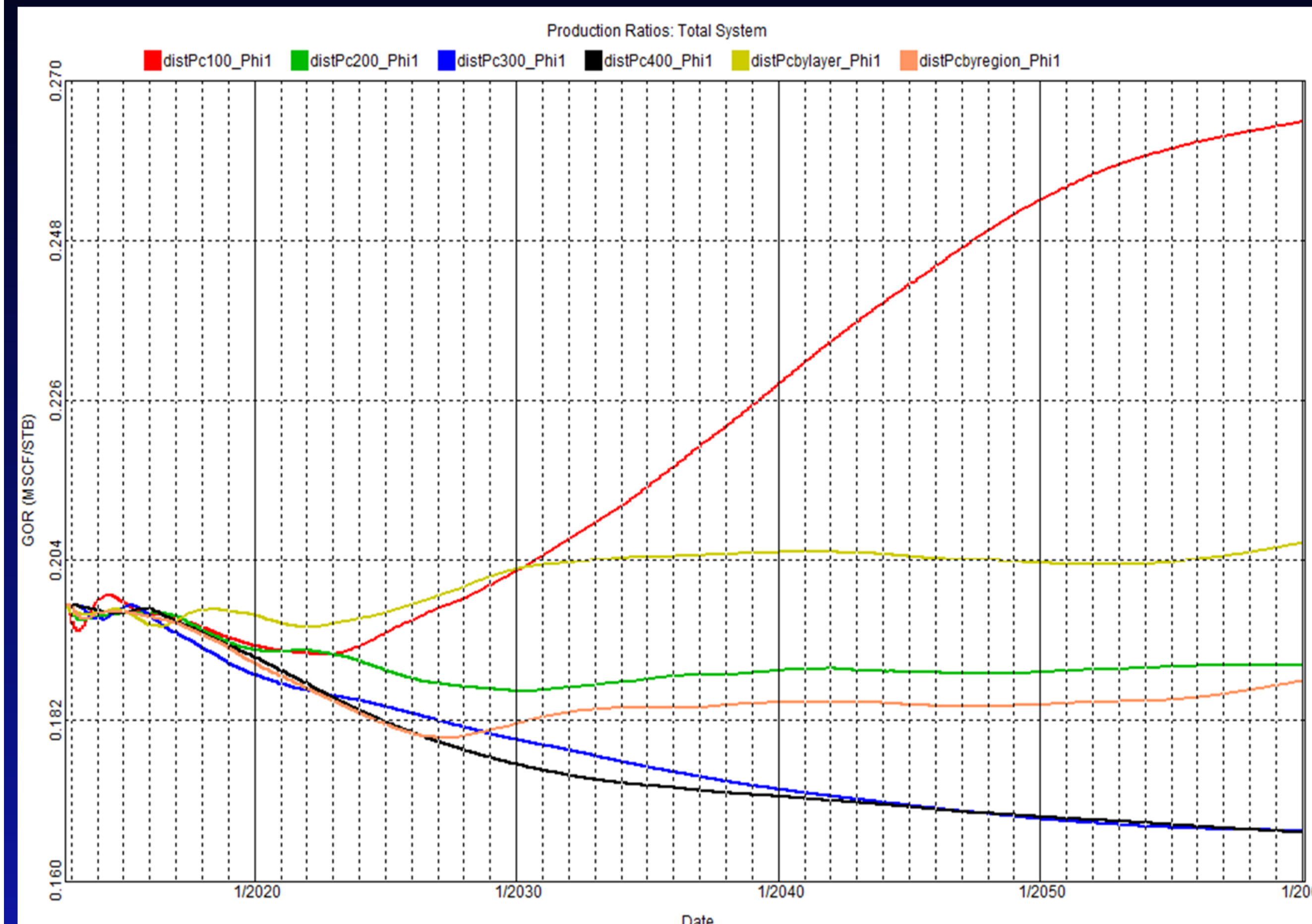

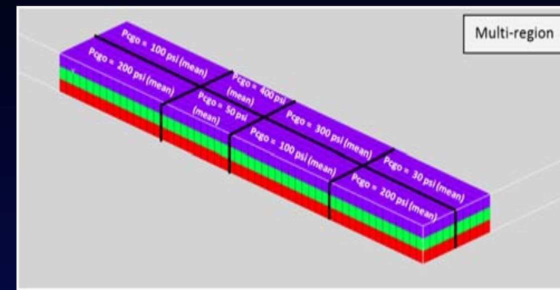

Results – Impact of different Pcgo distributions

Dual porosity system

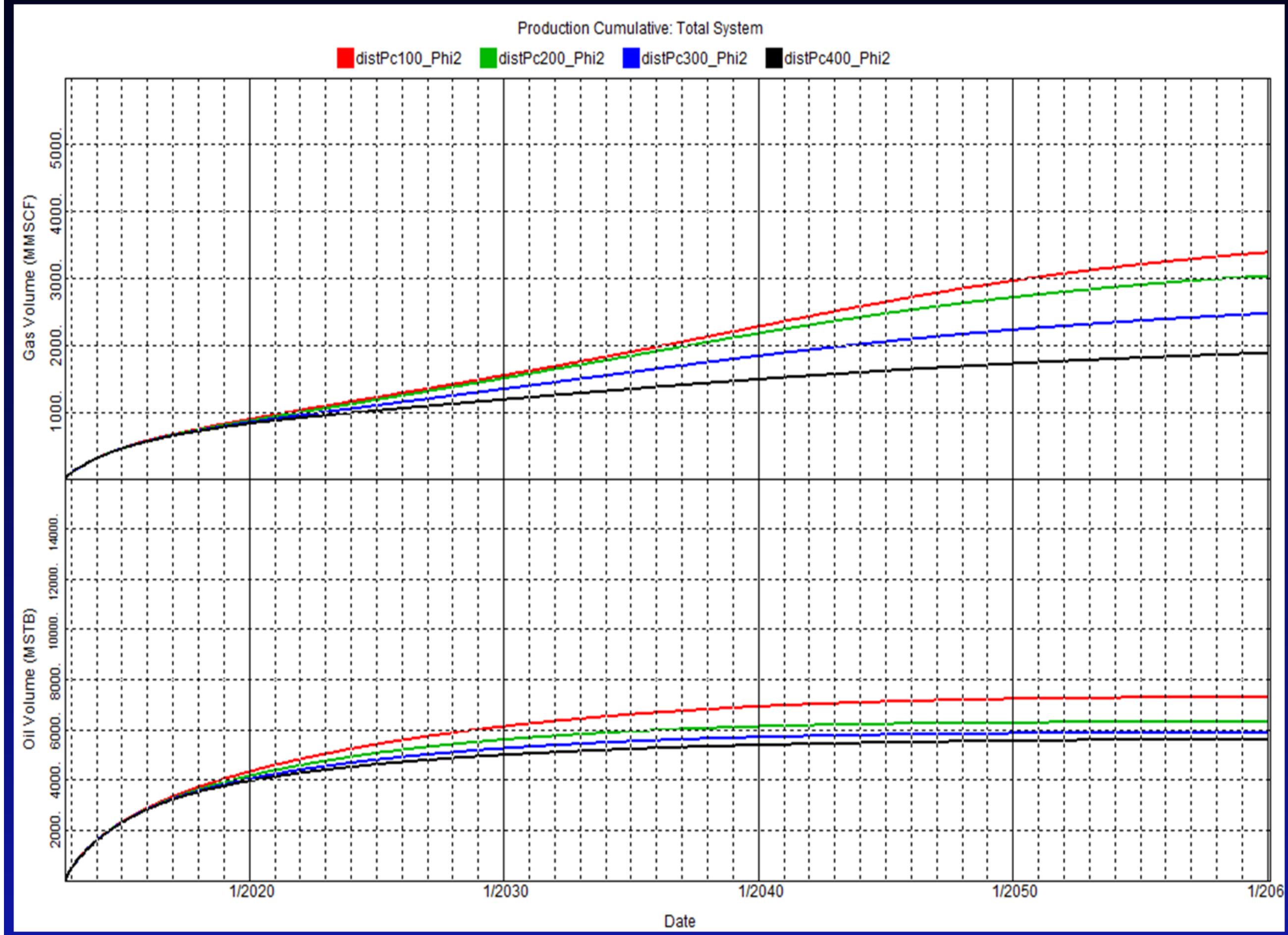

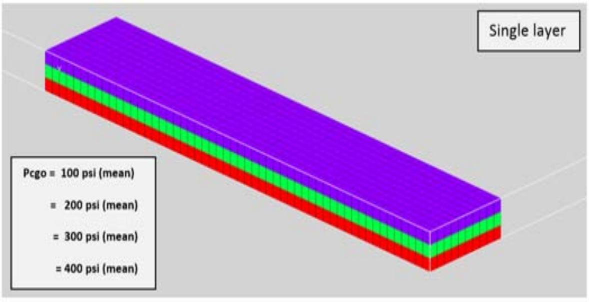

Pc ⬆ (pore size ⬇)

recovery ⬇

Results – Impact of different Pcgo distributions

Dual porosity system

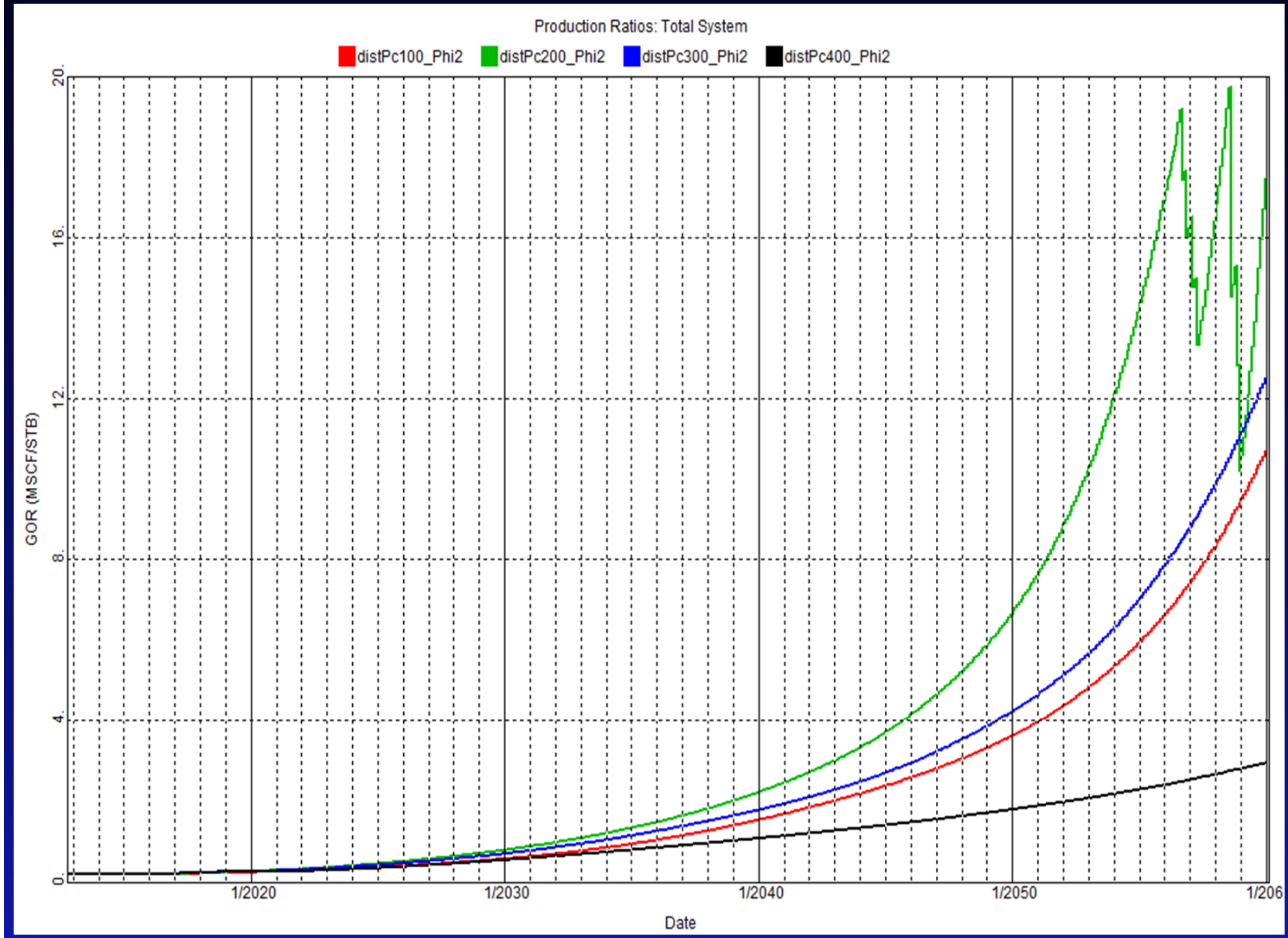

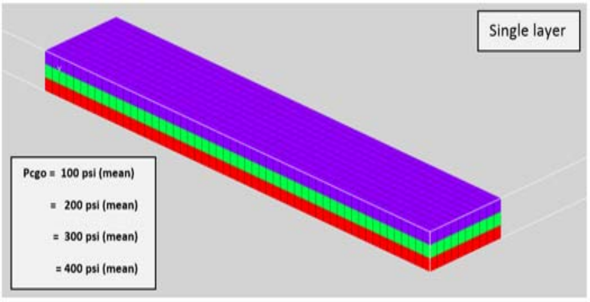

Pc (pore size)

recovery

Results – Impact of different Pcgo distributions

Dual porosity system

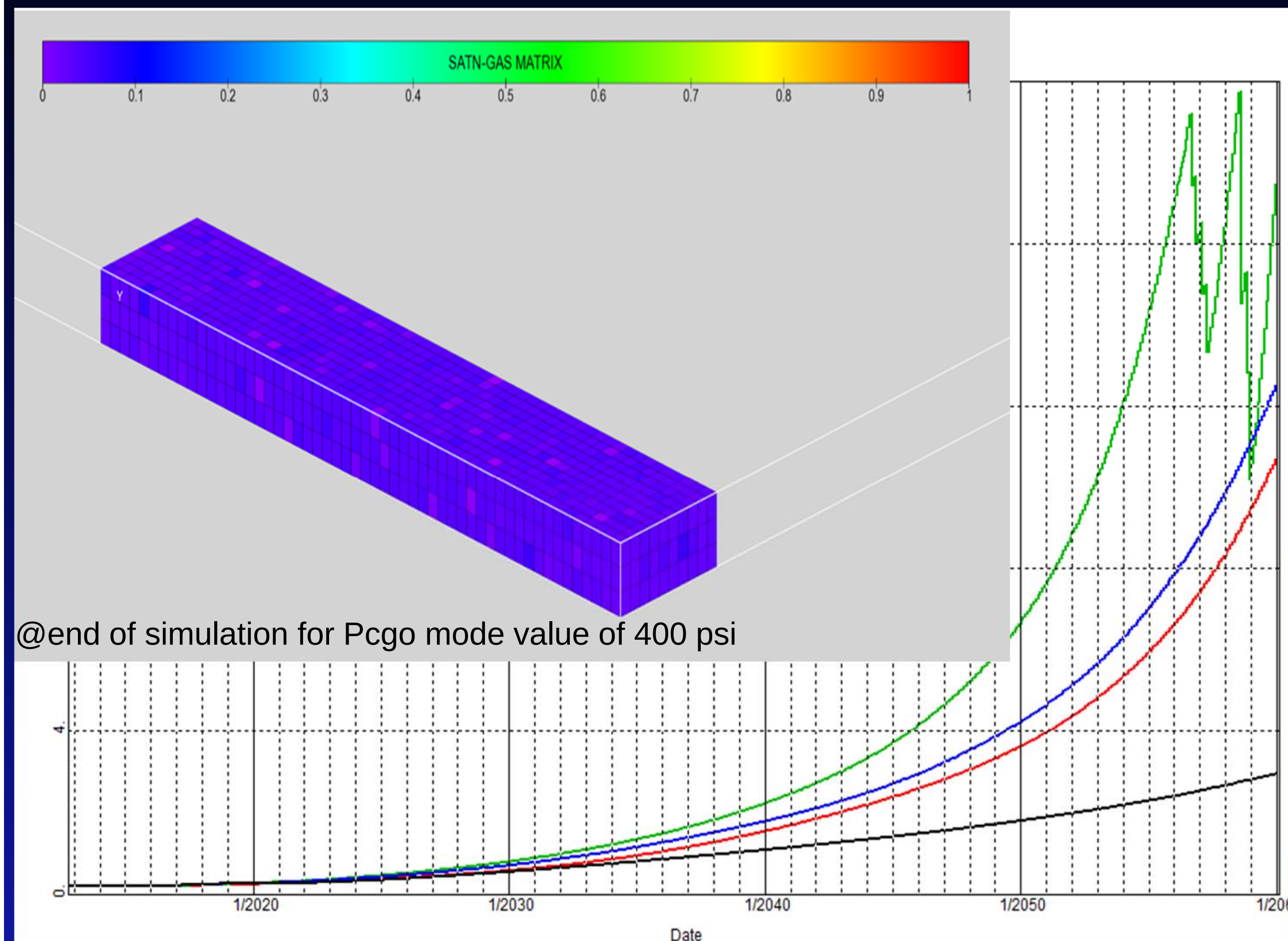

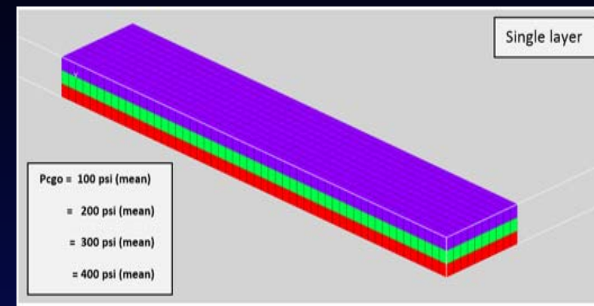

Pc ⬆ (pore size ⬇)

recovery ⬇

Results – Impact of different Pcgo distributions

Dual porosity system

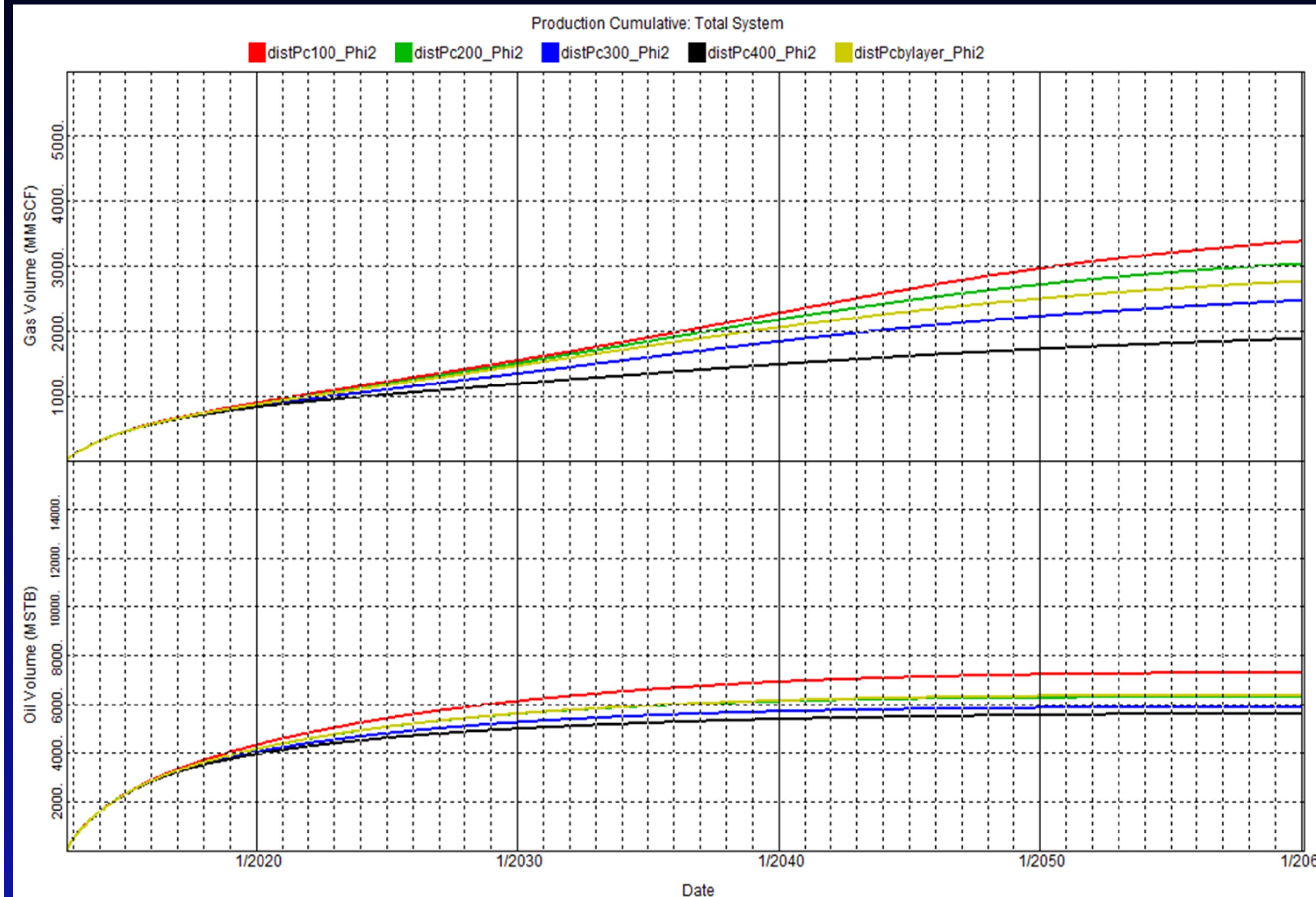

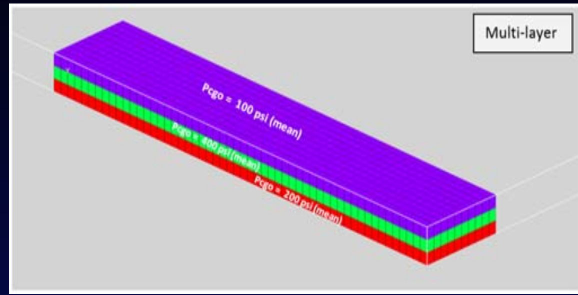

Results – Impact of different Pcgo distributions

Dual porosity system

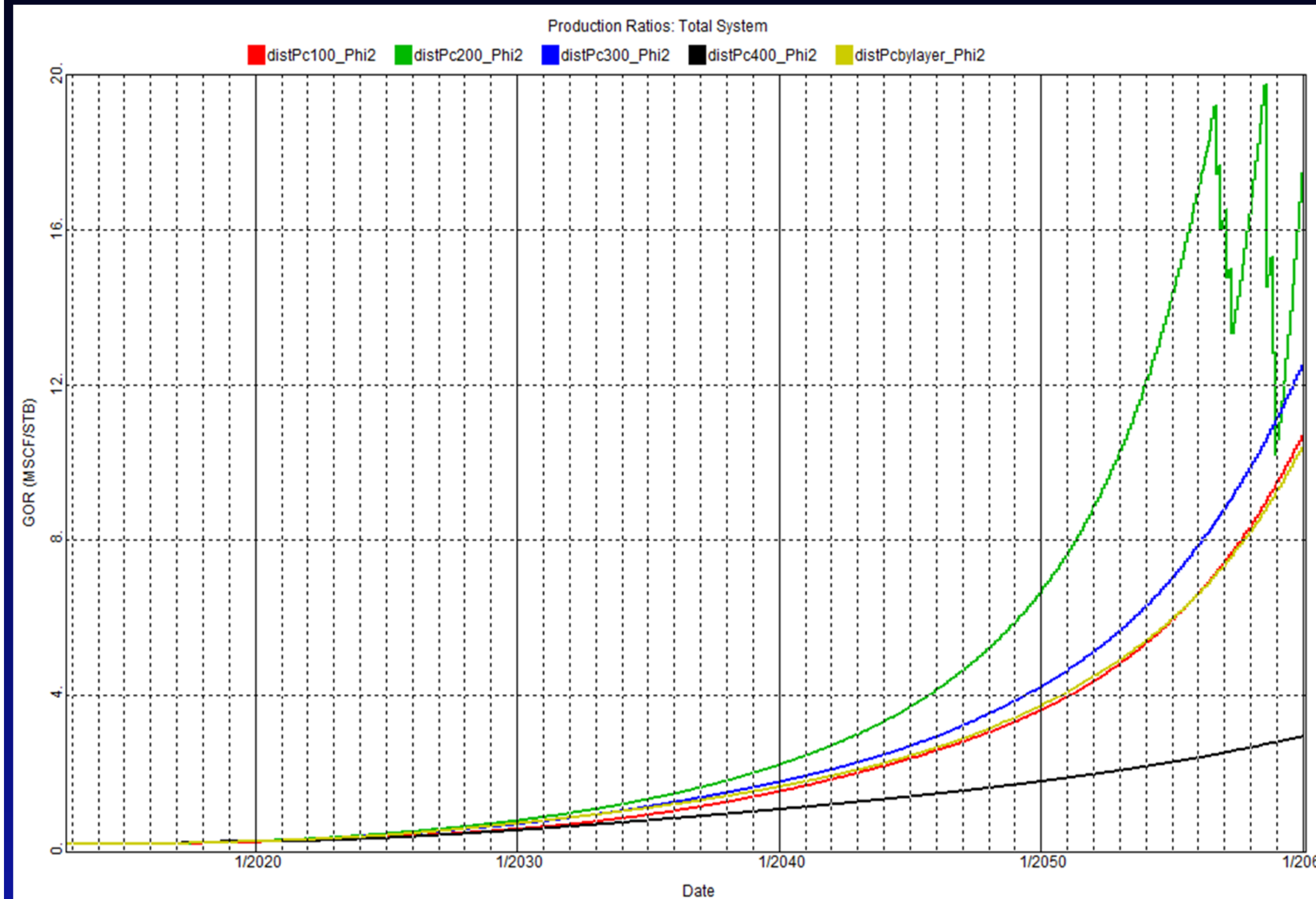

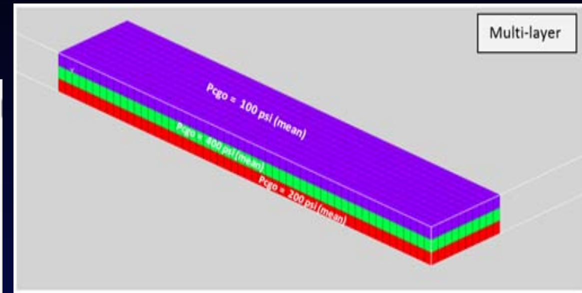

Results – Impact of different Pcgo distributions

Dual porosity system

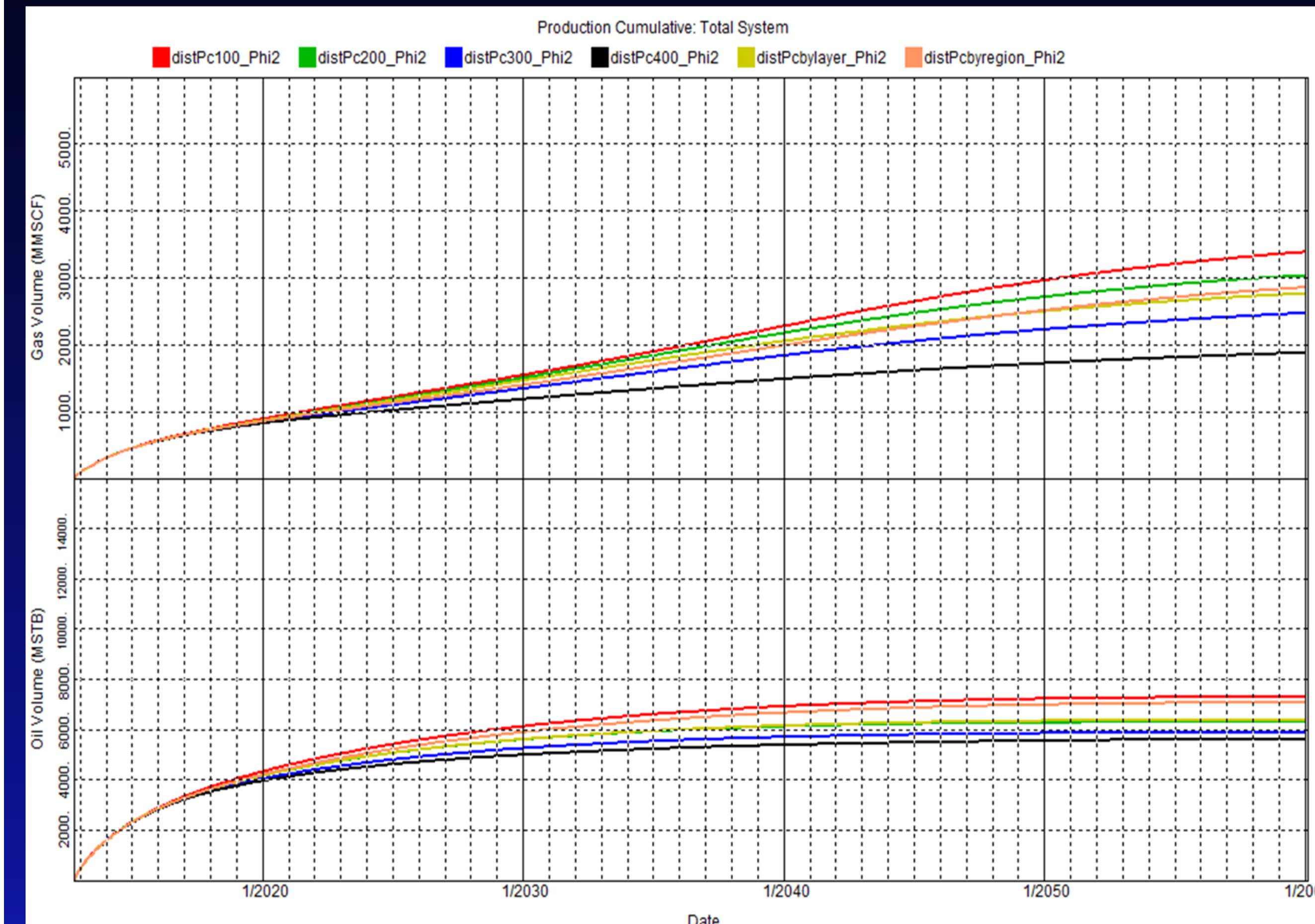

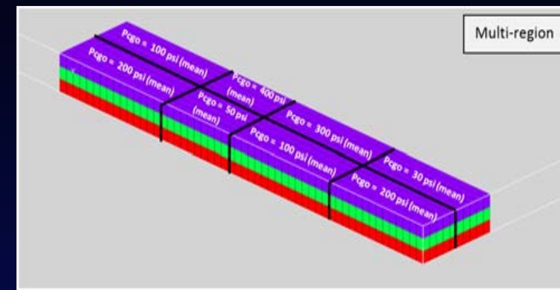

Results – Impact of different Pcgo distributions

Dual porosity system

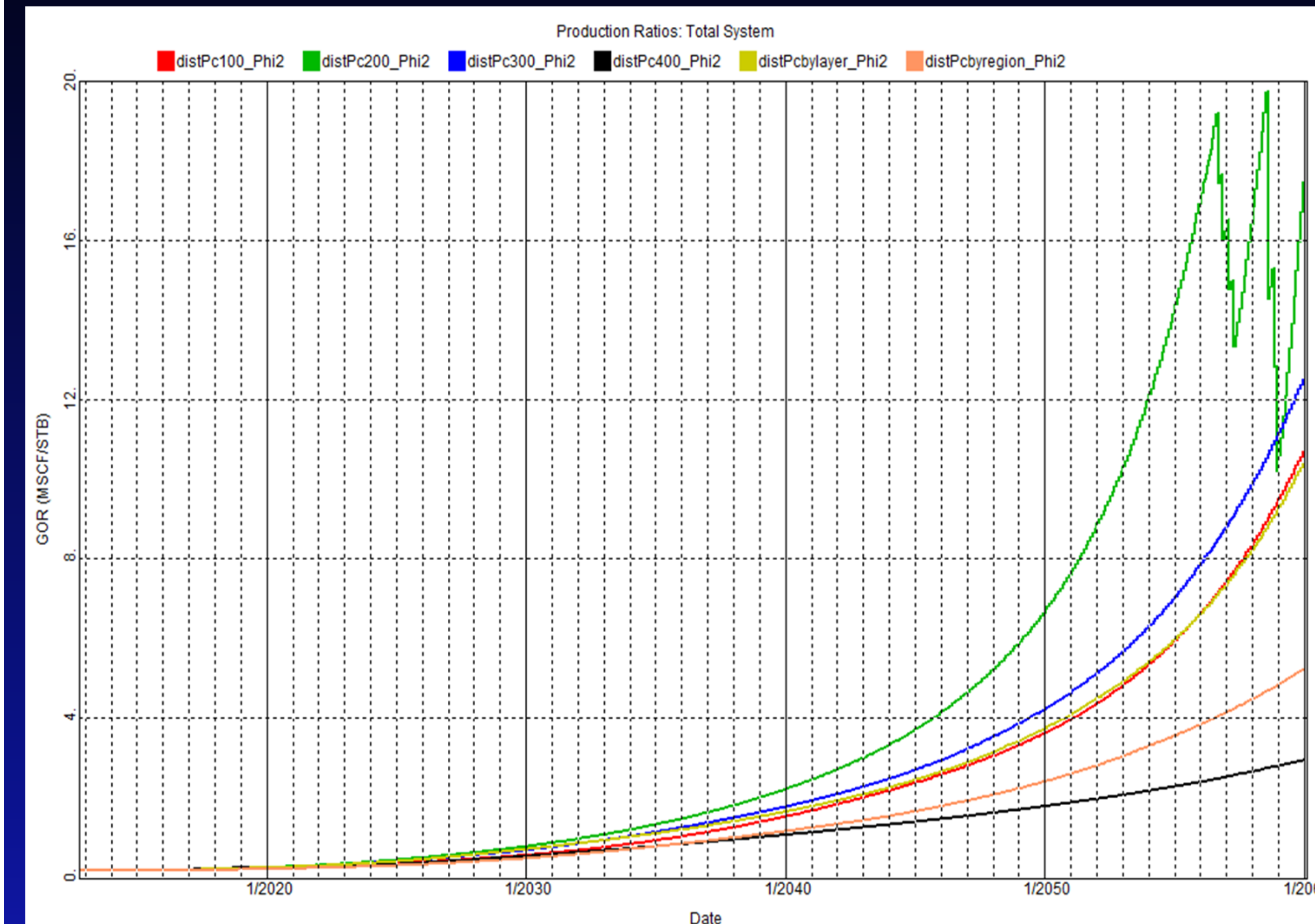

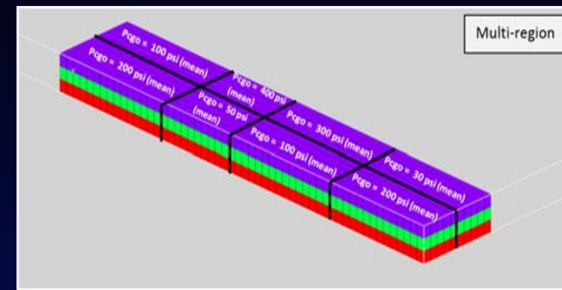

Results – Impact of different Pcgo distributions

Triple porosity system

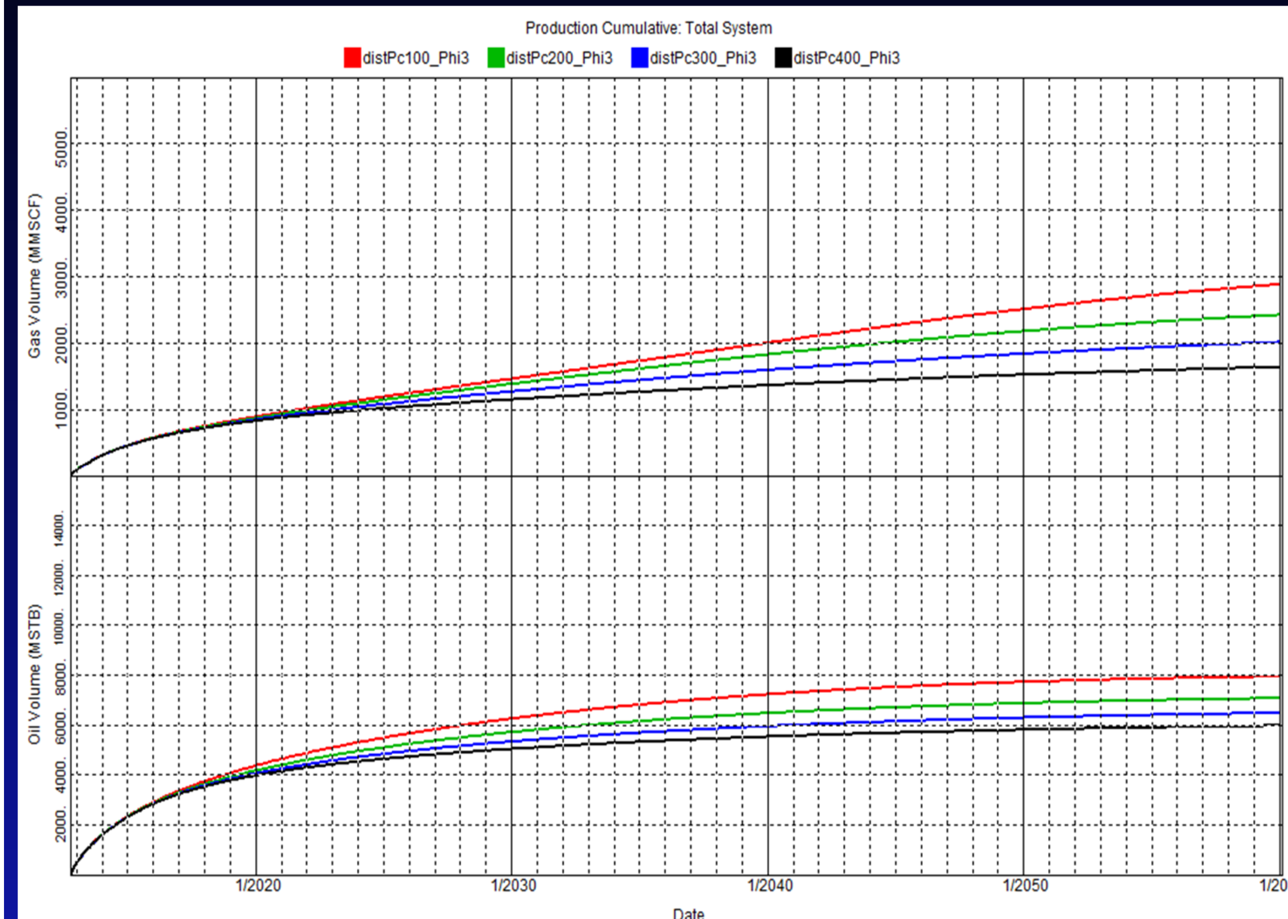

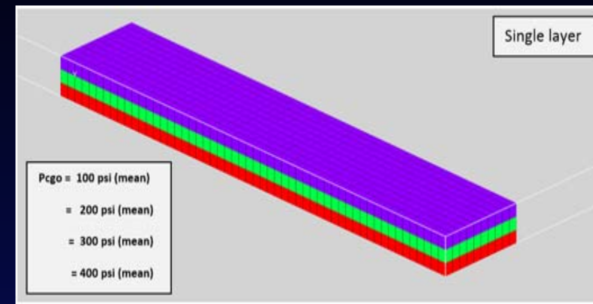

Pc ⬆ (pore size ⬇)

recovery ⬇

Results – Impact of different Pcgo distributions

Triple porosity system

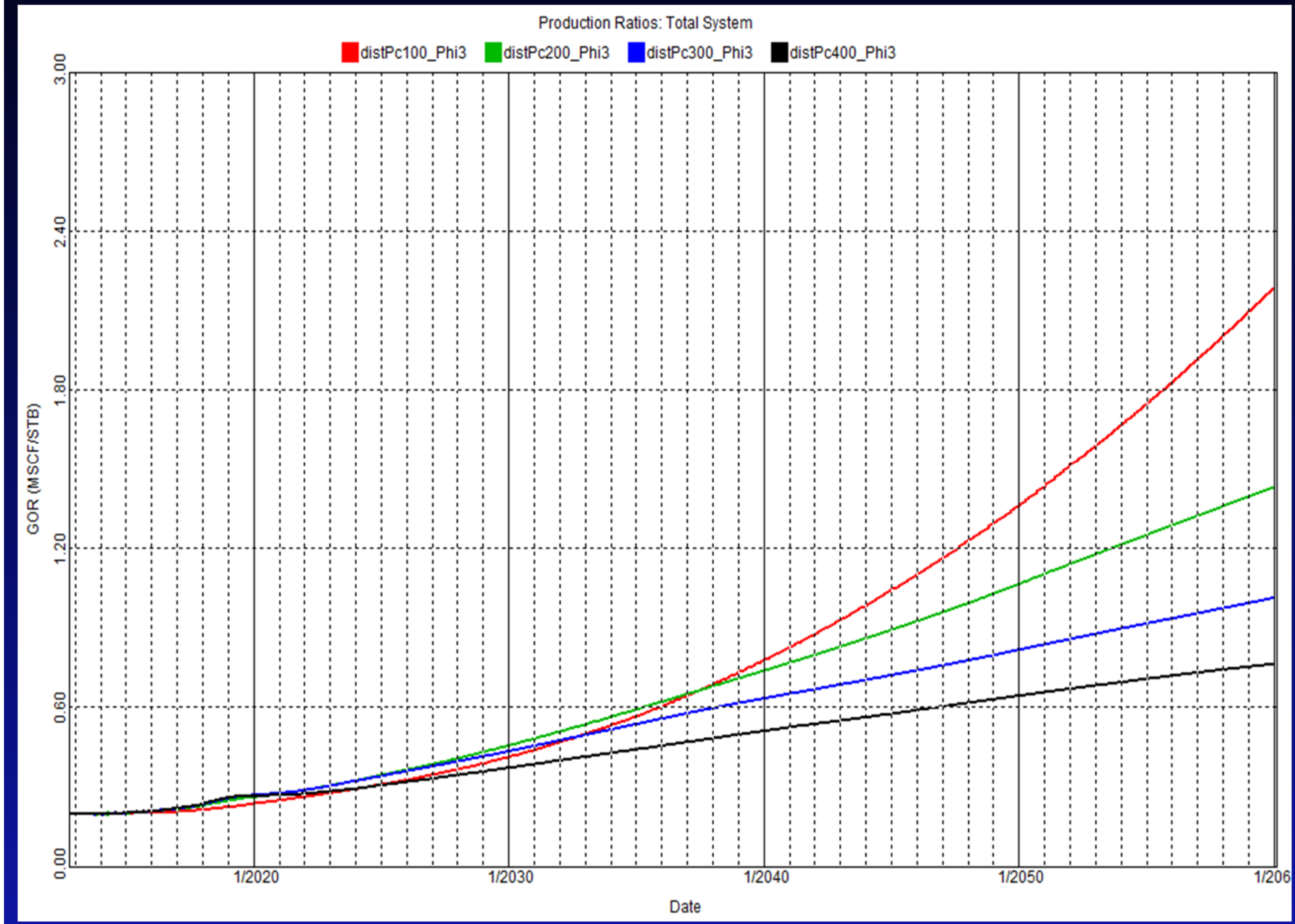

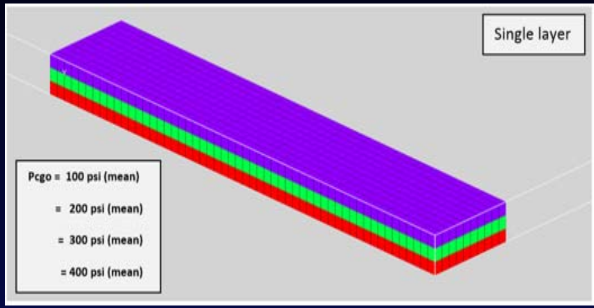

Pc ⬆ (pore size ⬇)

recovery ⬇

Results – Impact of different Pcgo distributions

Triple porosity system

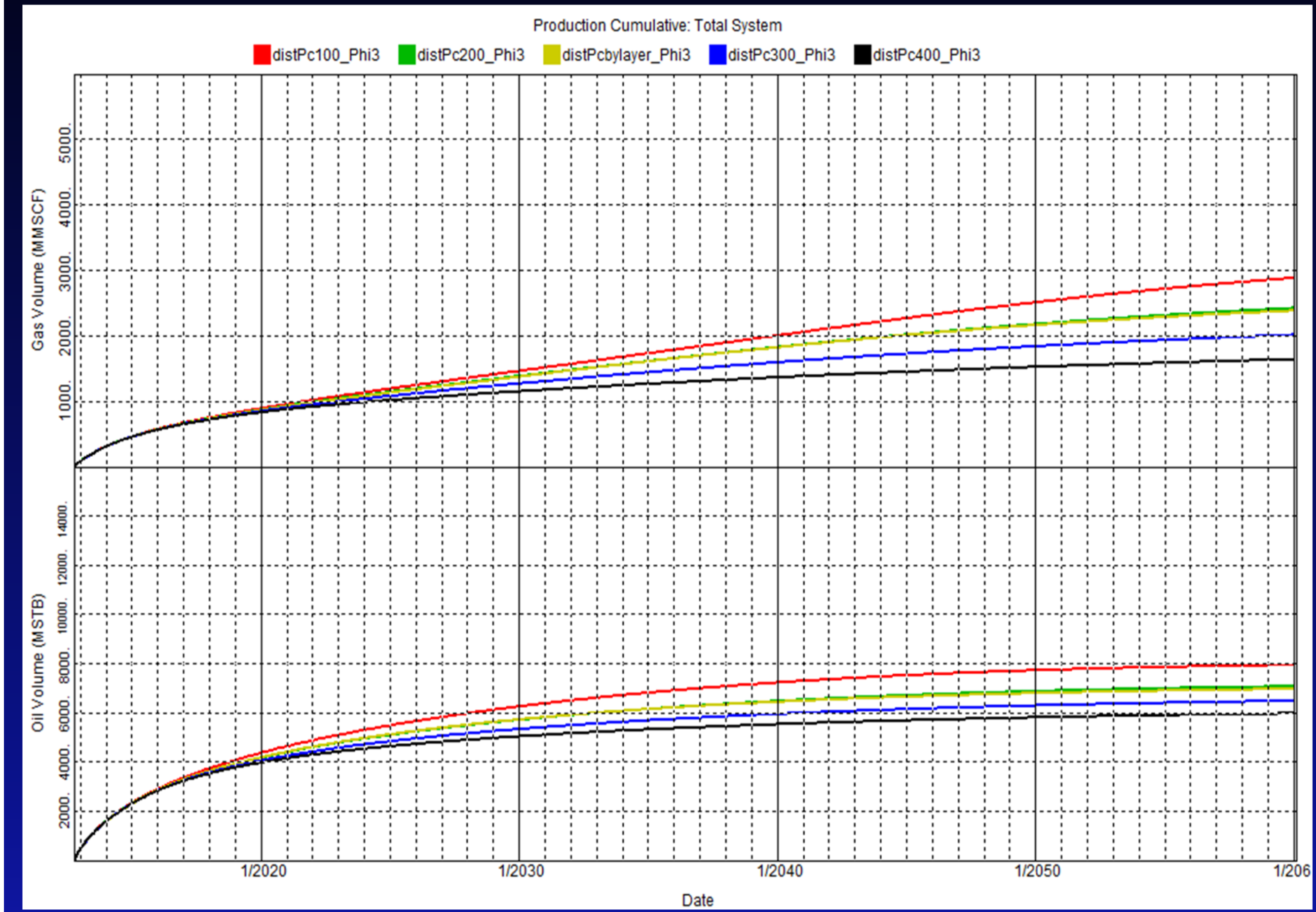

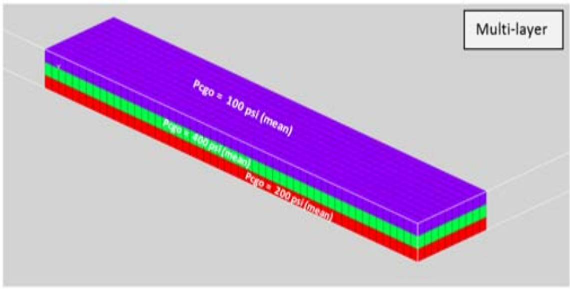

Results – Impact of different Pcgo distributions

Triple porosity system

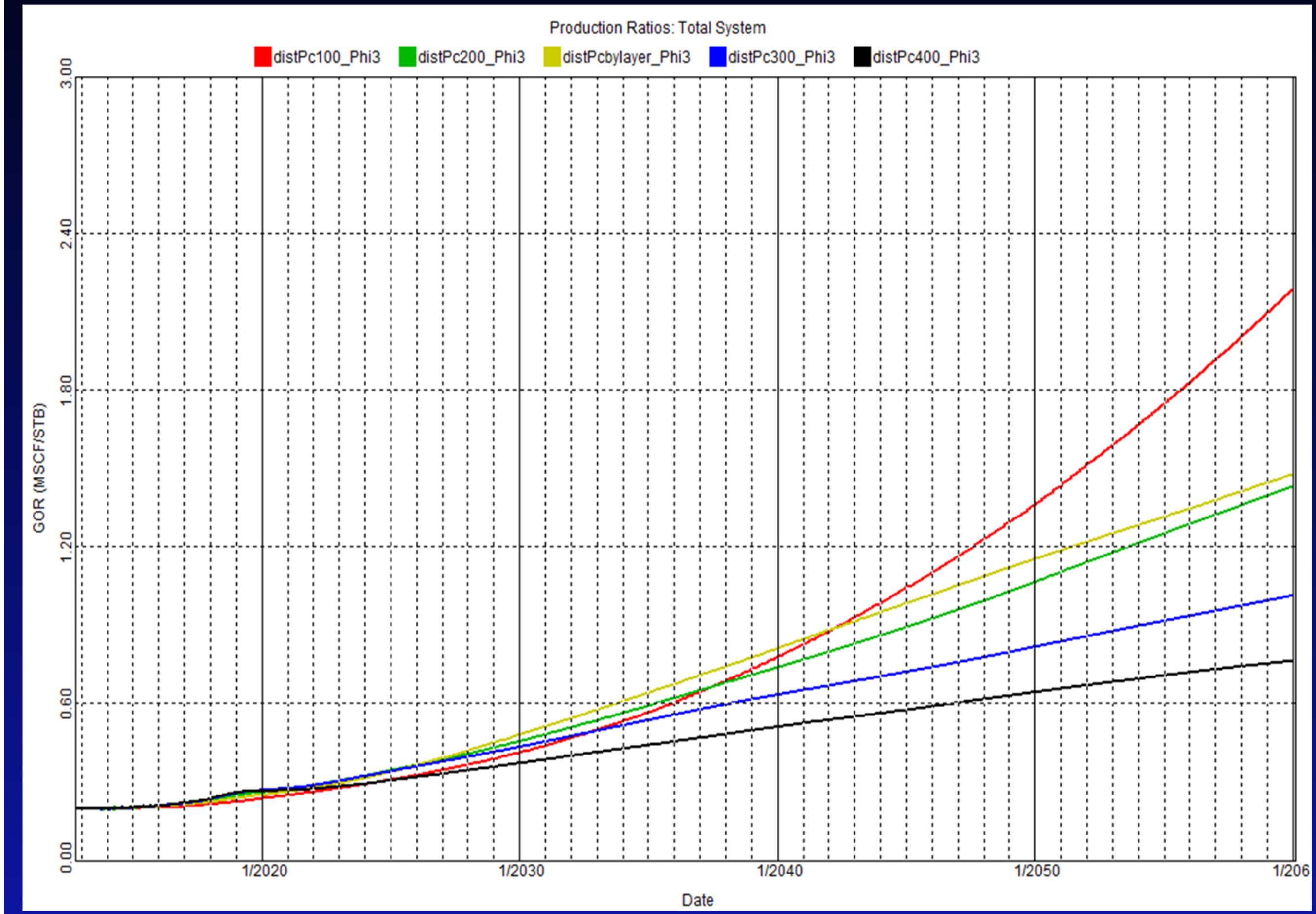

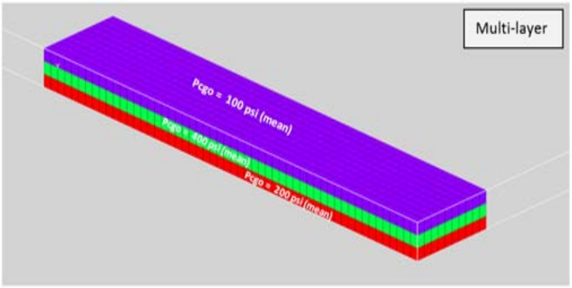

Results – Impact of different Pcgo distributions

Triple porosity system

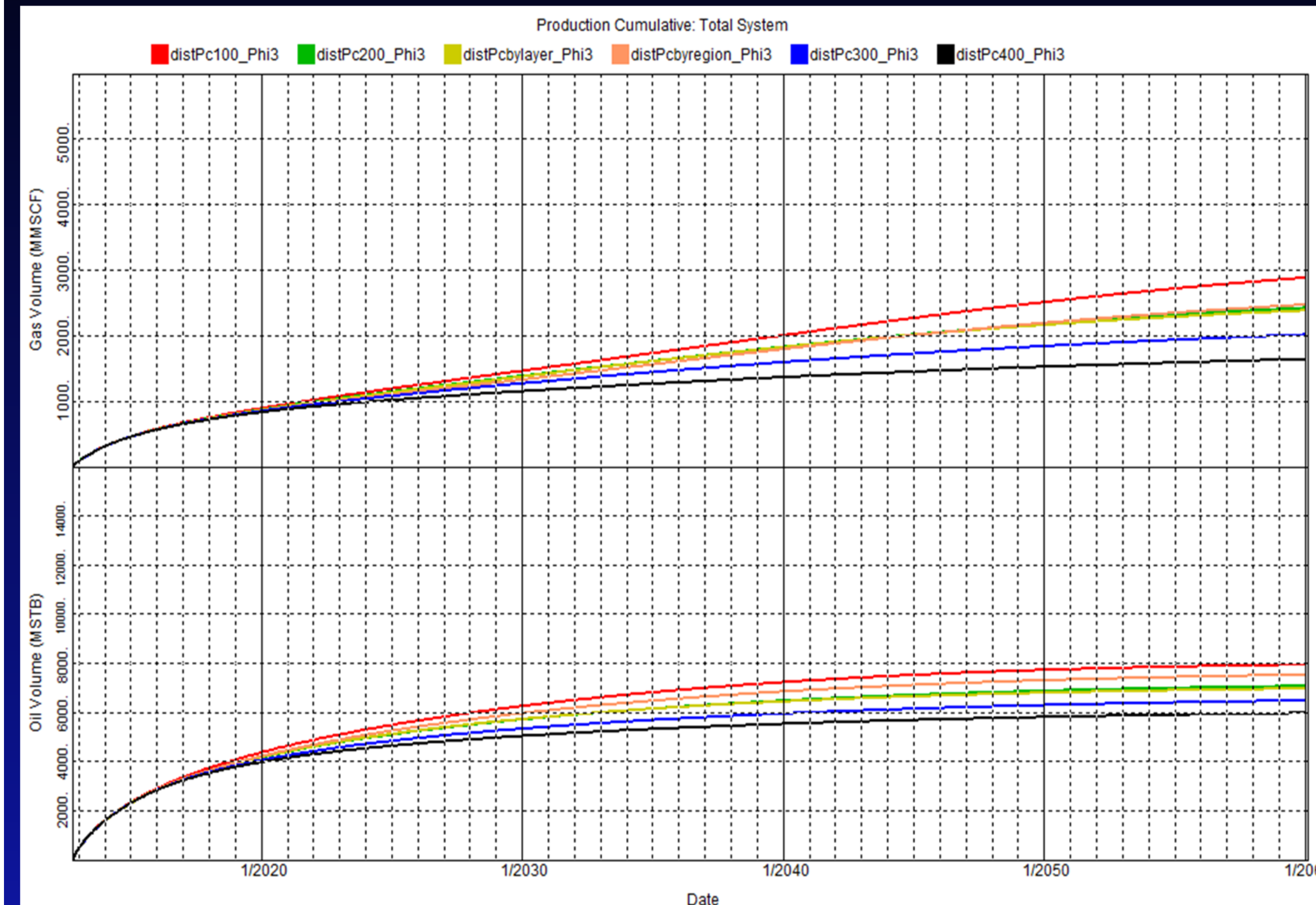

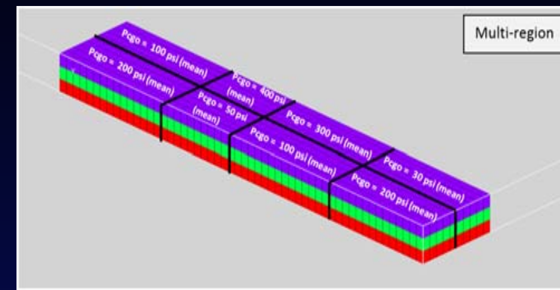

Results – Impact of different Pcgo distributions

Triple porosity system

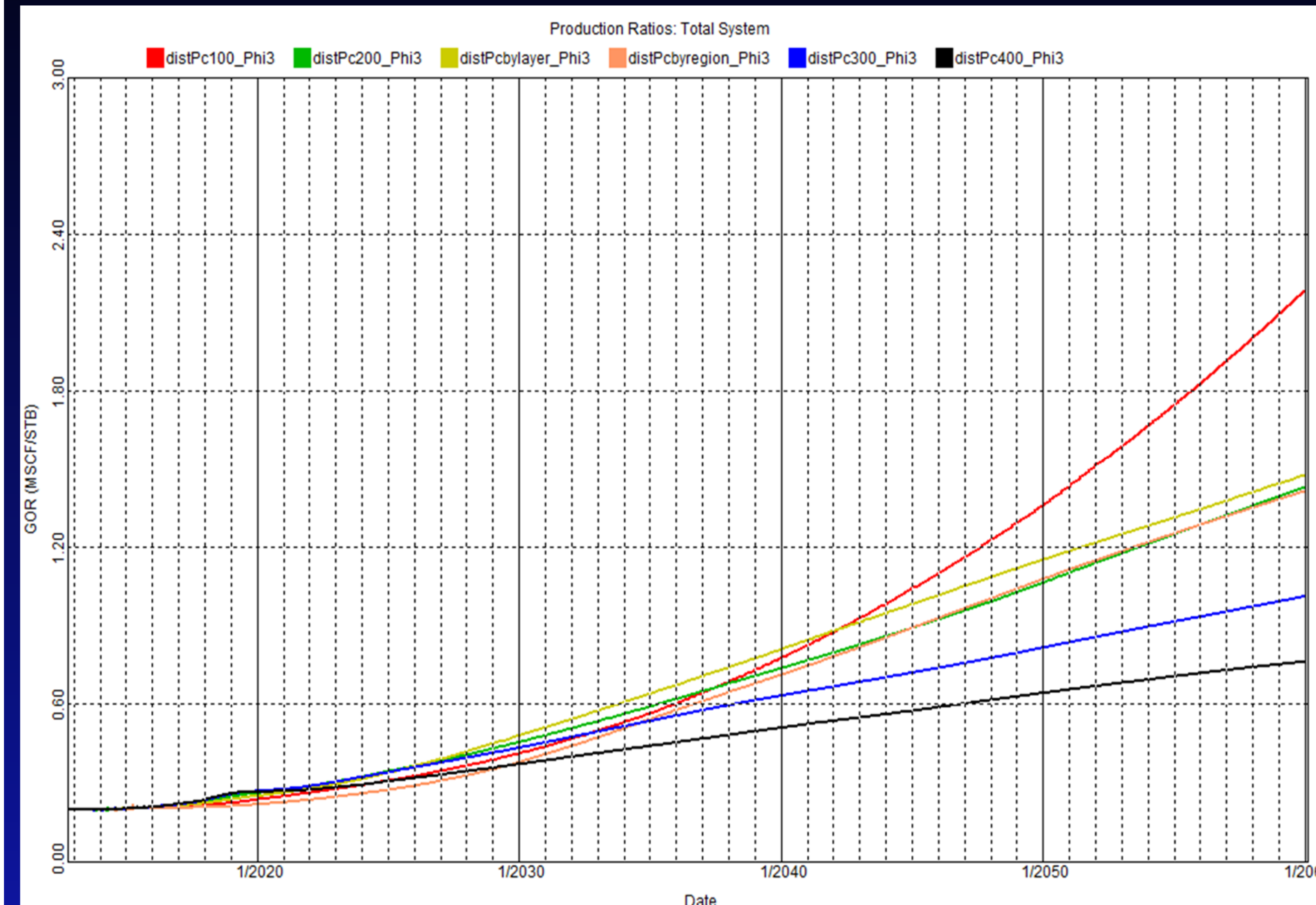

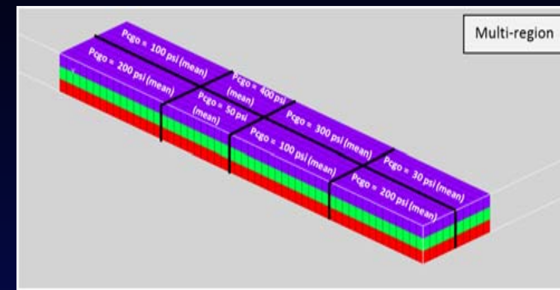

Results – Impact of different Pcgo distributions

Quintuple (serial connection) porosity system

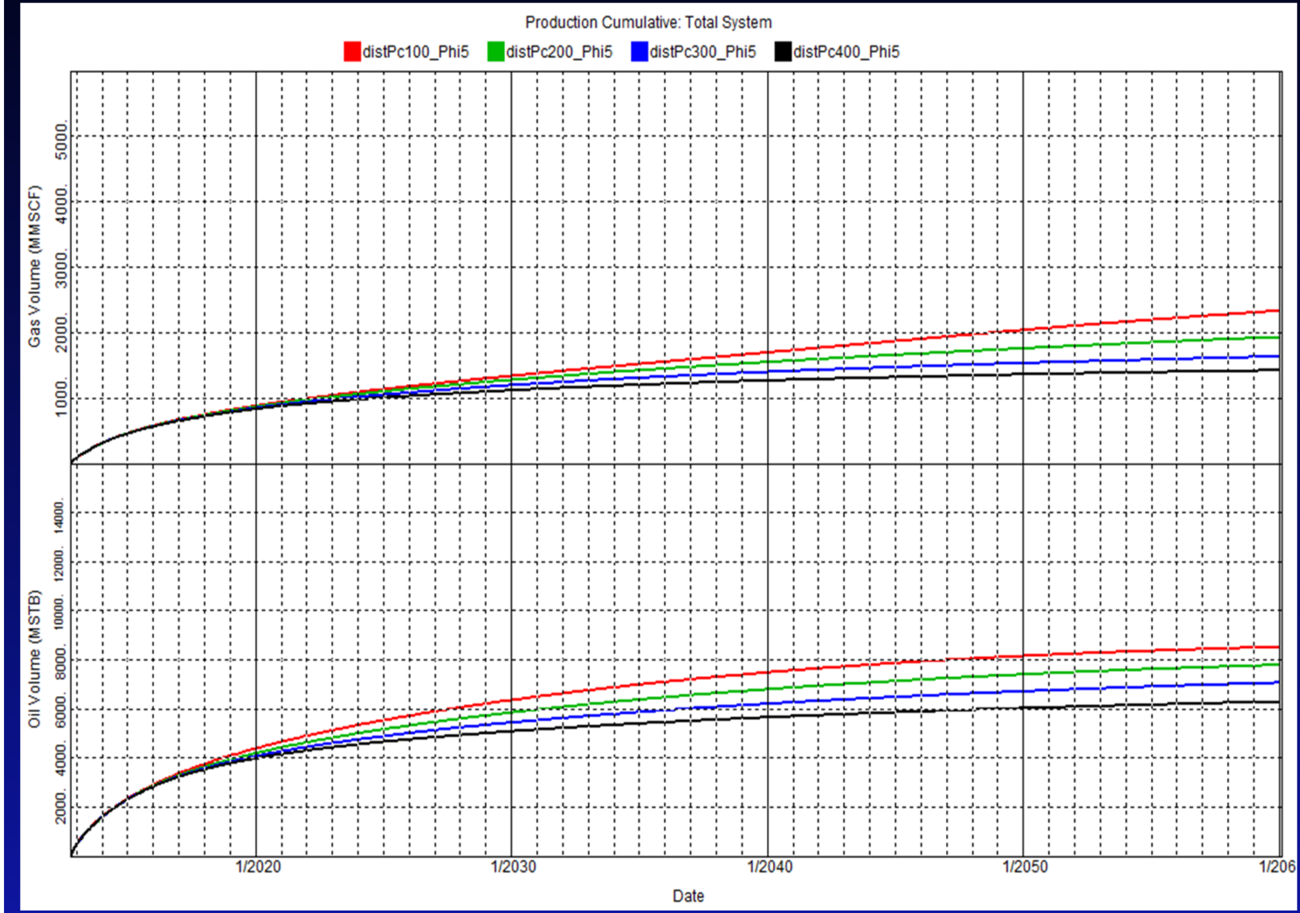

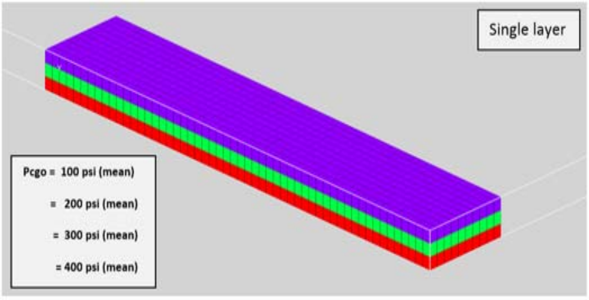

Pc ⬆ (pore size ⬇)

recovery ⬇

Results – Impact of different Pcgo distributions

Quintuple (serial connection) porosity system

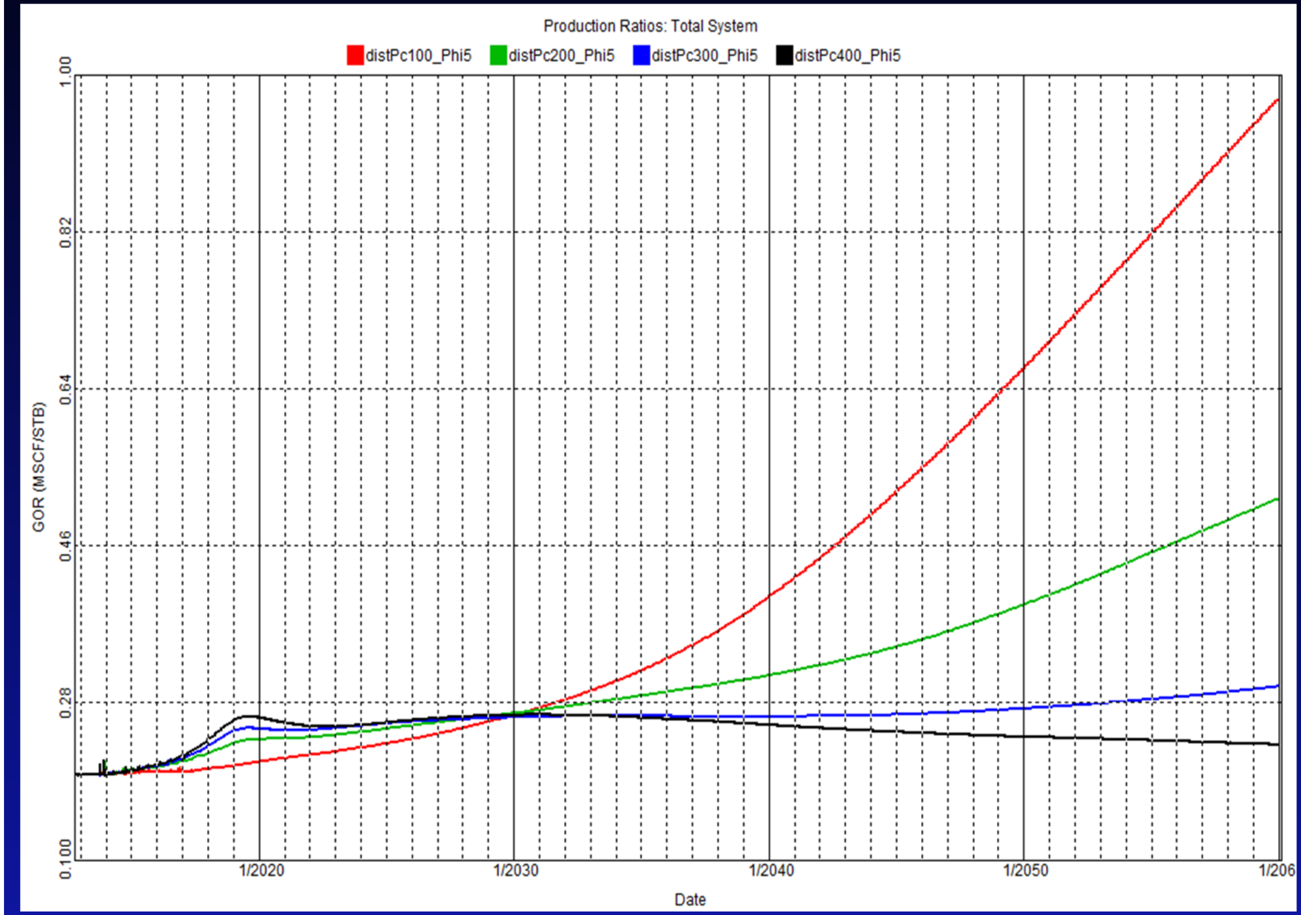

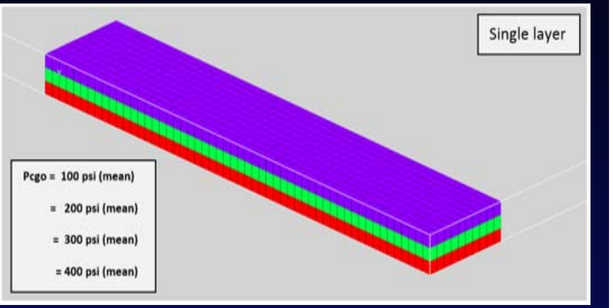

Pc ⬆ (pore size ⬇)

recovery ⬇

Results – Impact of multi porosity systems

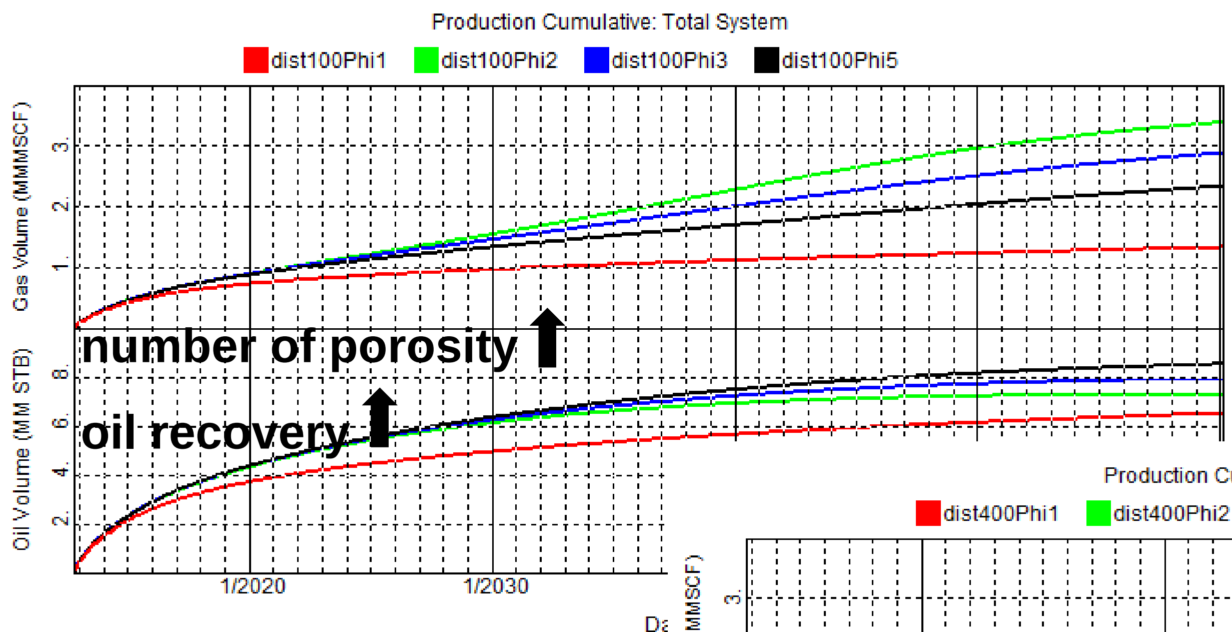

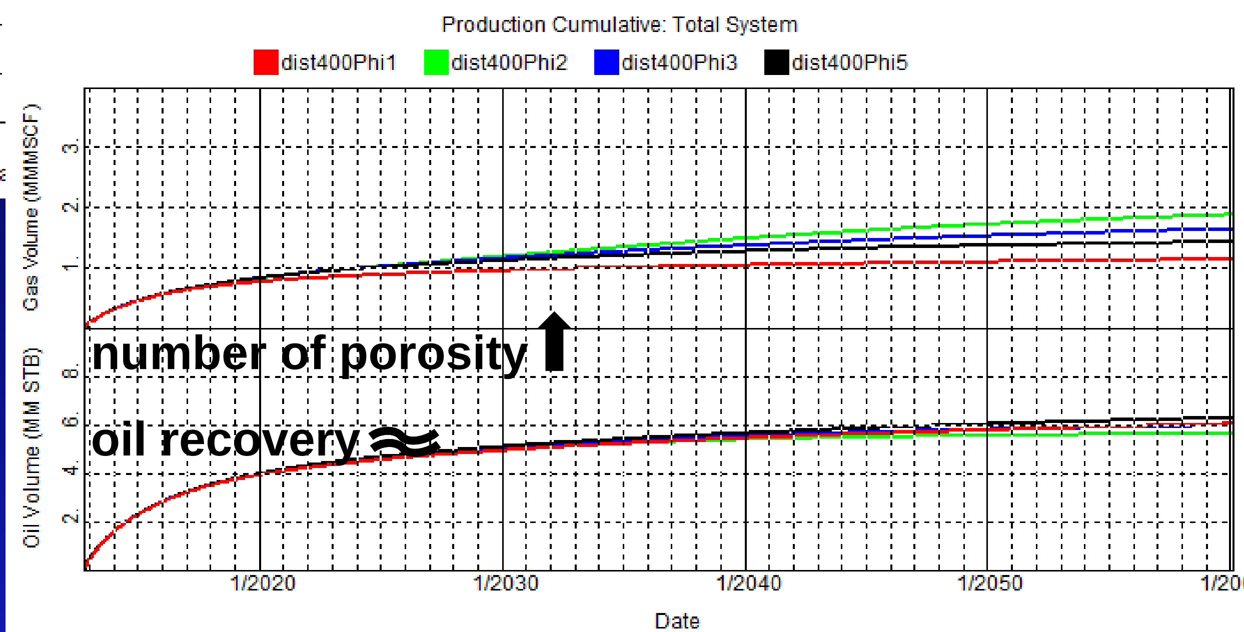

For smaller pore sizes; oil recovery is not a function of number of porosity connections

Results – Impact of different Pcgo distributions

Quintuple (serial connection) porosity system

dist1400Phi5 case:

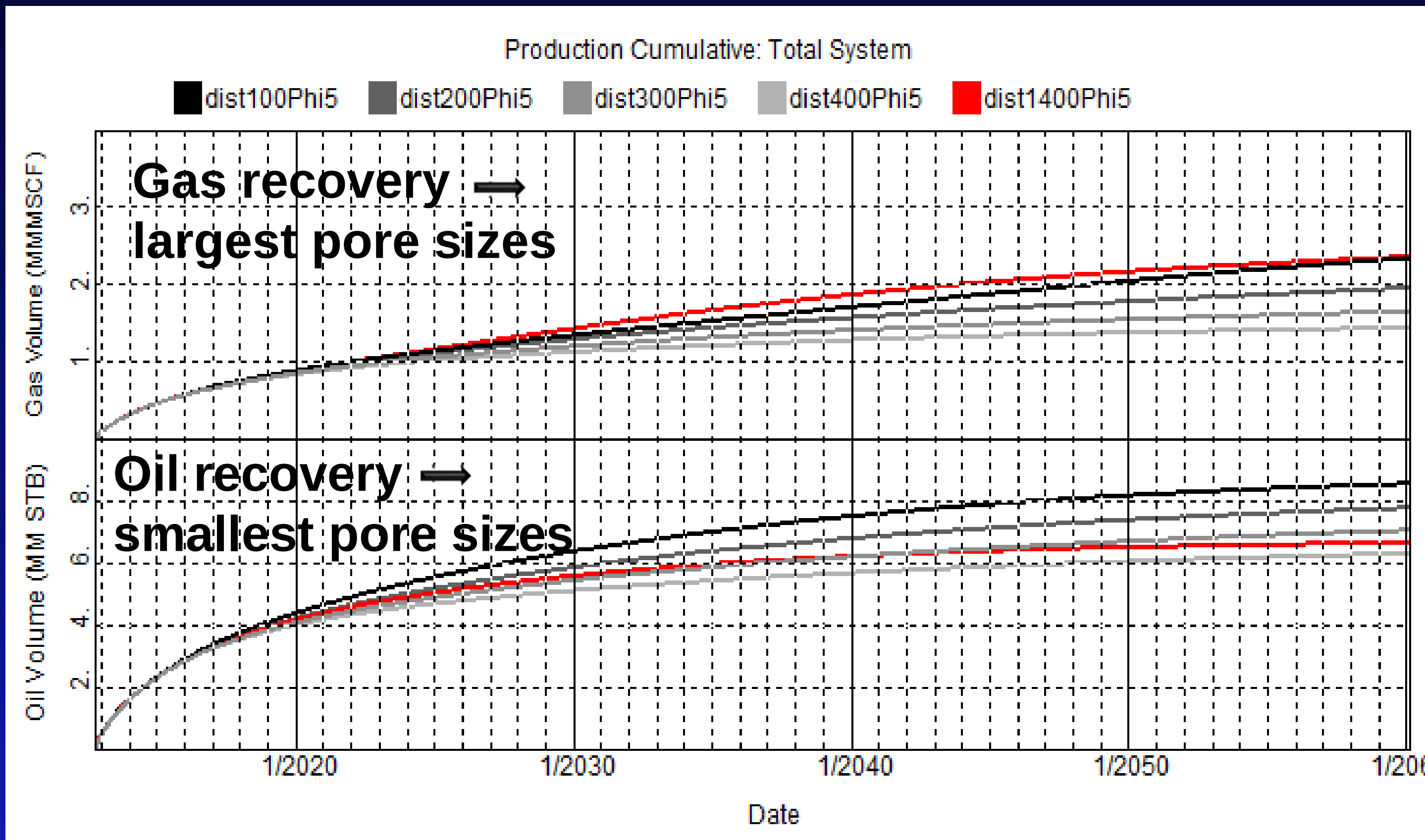

Results – Sensitivity of serial and parallel connection

Quintuple porosity system

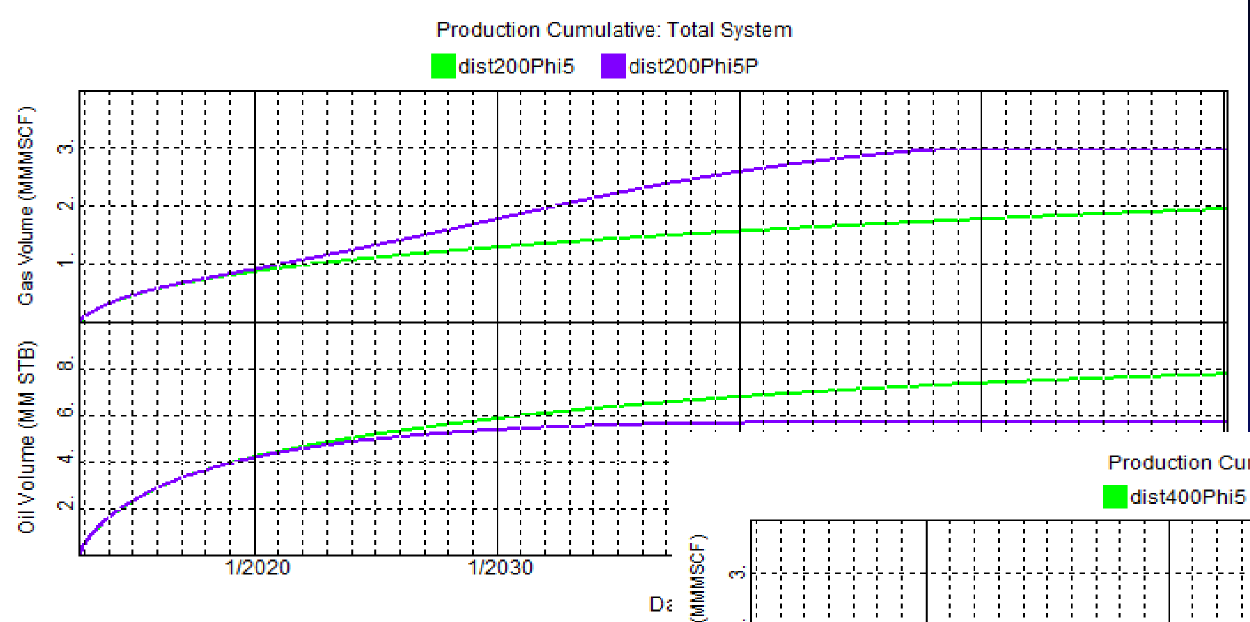

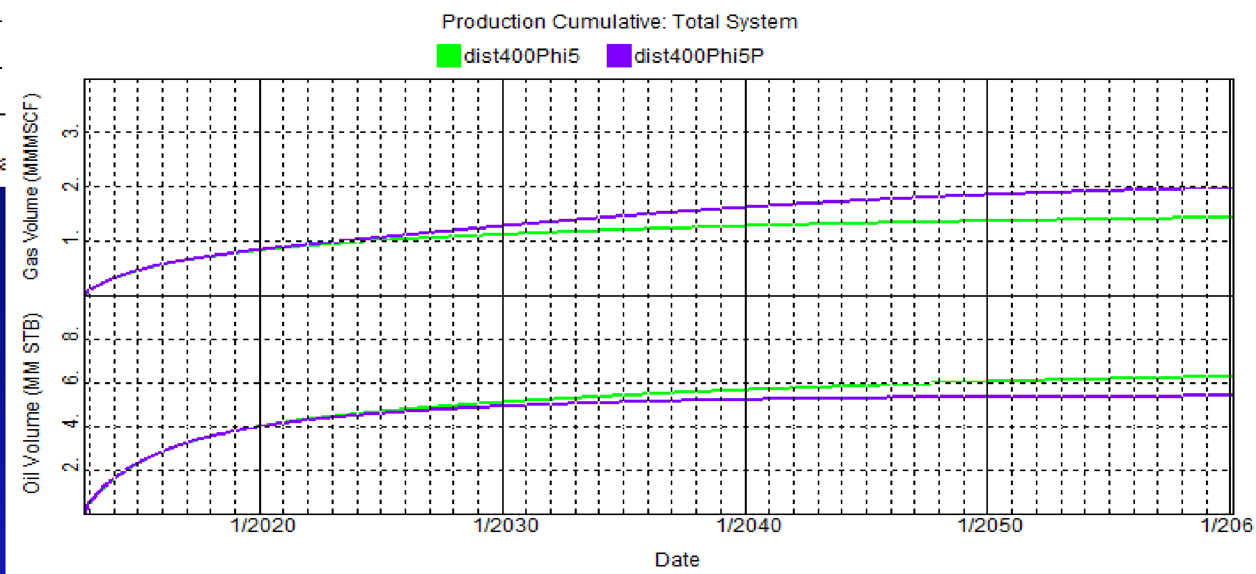

Results – Sensitivity of serial and parallel connection

Quintuple porosity system

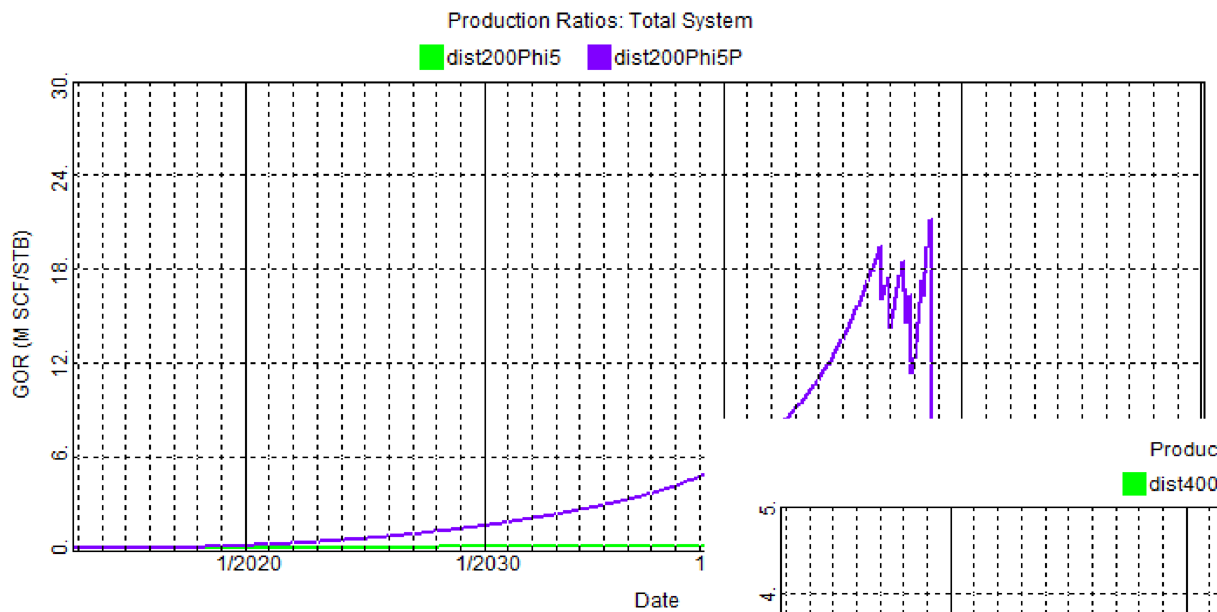

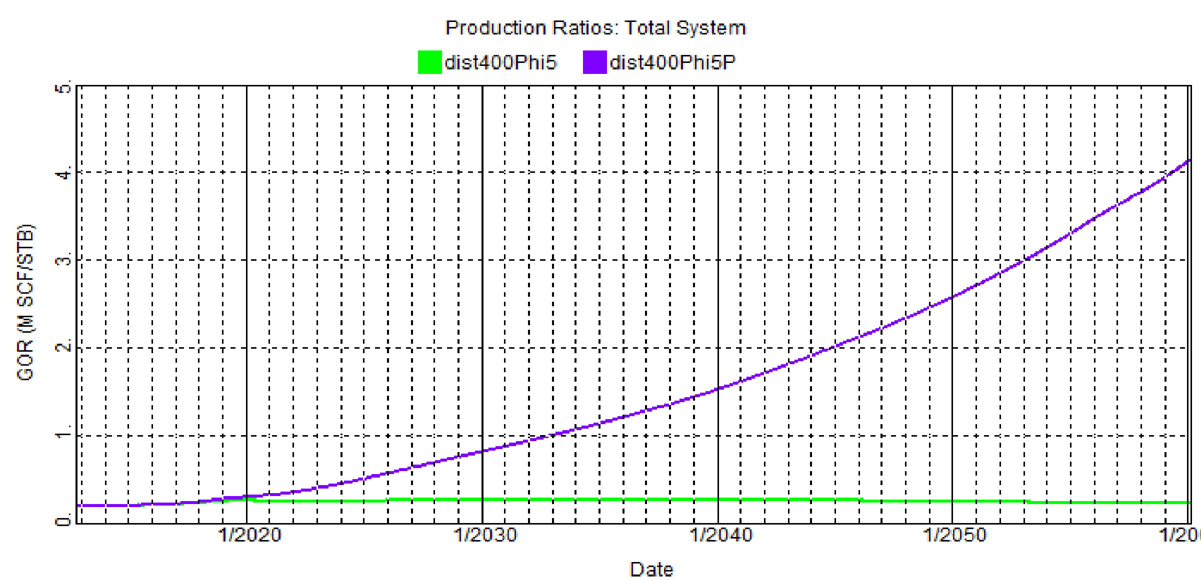

Conclusions

- Predicted production profiles from single porosity models do not show any sensitivity to bubble point suppression formulations
- Dual-porosity models predict highest cumulative gas production profiles
- At large uniform pores, serial n-porosity models predict highest cumulative oil production profiles
- When serially connected matrix Pcgo model is organized in a manner to approximate the natural connectivity of large and small pores, the predicted cumulative oil production profile is higher and the predicted cumulative gas production profile is significantly higher than single-porosity models
- Parallel connected n-porosity models match the results obtained by simpler dual-porosity models

Future Work

Horizontal well model:

- New 5-phi model: include four different rock types with realistic unconventional porosity and permeability values
- New dual-phi model: use averaged values find in new 5-phi model / compare

History match:

- Work with real model ➡ history match ➡ prediction
  - Frac property enhancement around the wells to represent hydraulic fracturing
  - Add more layers (bigger grid size)
  - Compare / show the confinement impact

Questions?

Thank you

Research Summary

Potential of Thermal Methods to Enhanced Recovery in Unconventional Oil Reservoirs

Jamila Huseynova

Agenda

Tight unconventional reservoirs display membrane properties.

- Determine the composition distribution.
- Determine the size of hydrocarbon molecular components.
- Establishing filtration properties

Two phase compositional flow model

- Derivation of model
- Mathematical description
- Solution approach

Methodology

van der Waals Equation of State

$$\left[P + \frac{a}{V_m^2}\right][V_m - b] = RT$$

$$a = \frac{27\,R^2 T_c^2}{64\,P_c}$$

$$b = \frac{RT_c}{8\,P_c}$$

$$V = \frac{b}{N_A}$$

'a' represents attraction between the particles
'b' represents molecular volume

Methodology

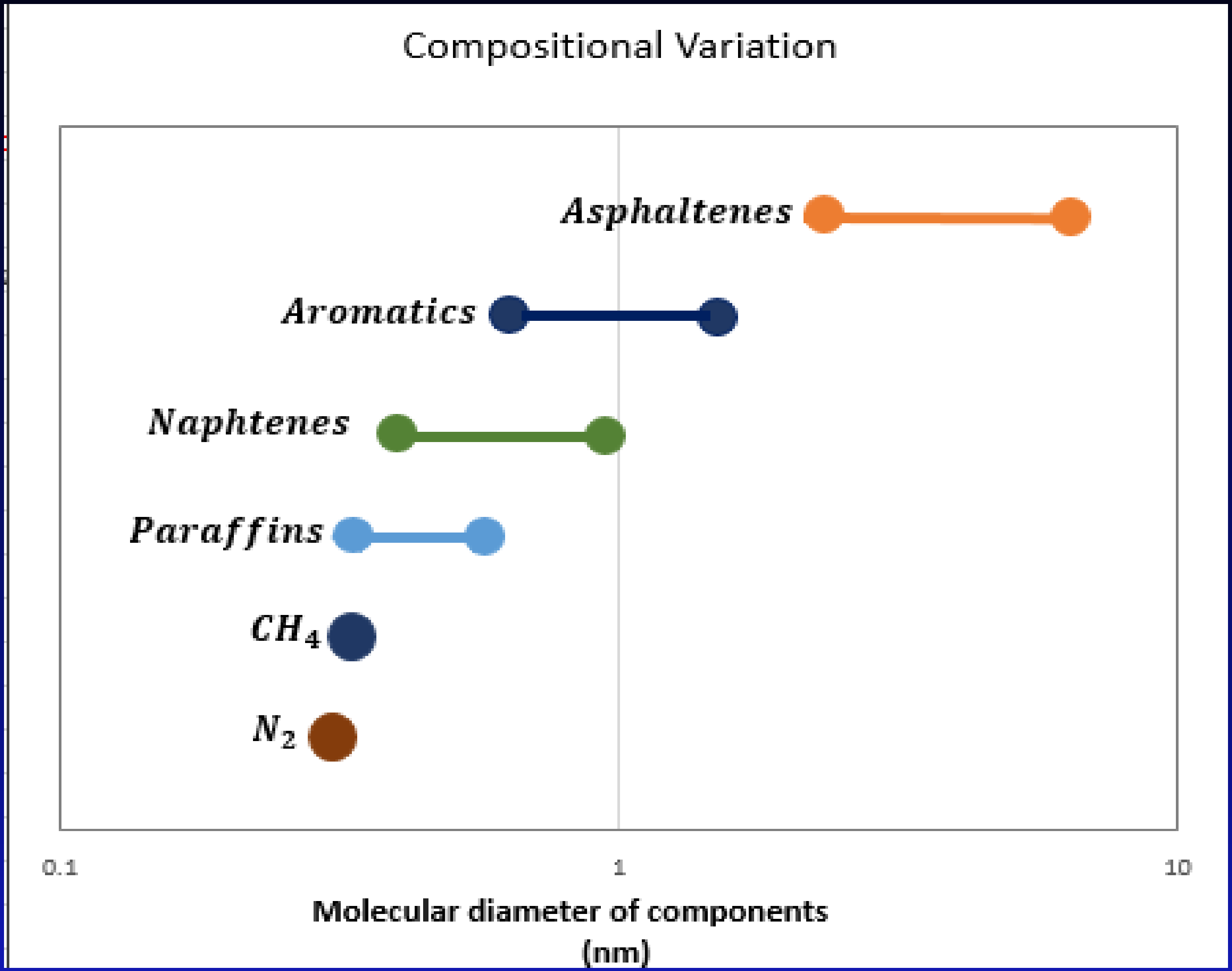

Problem Statement

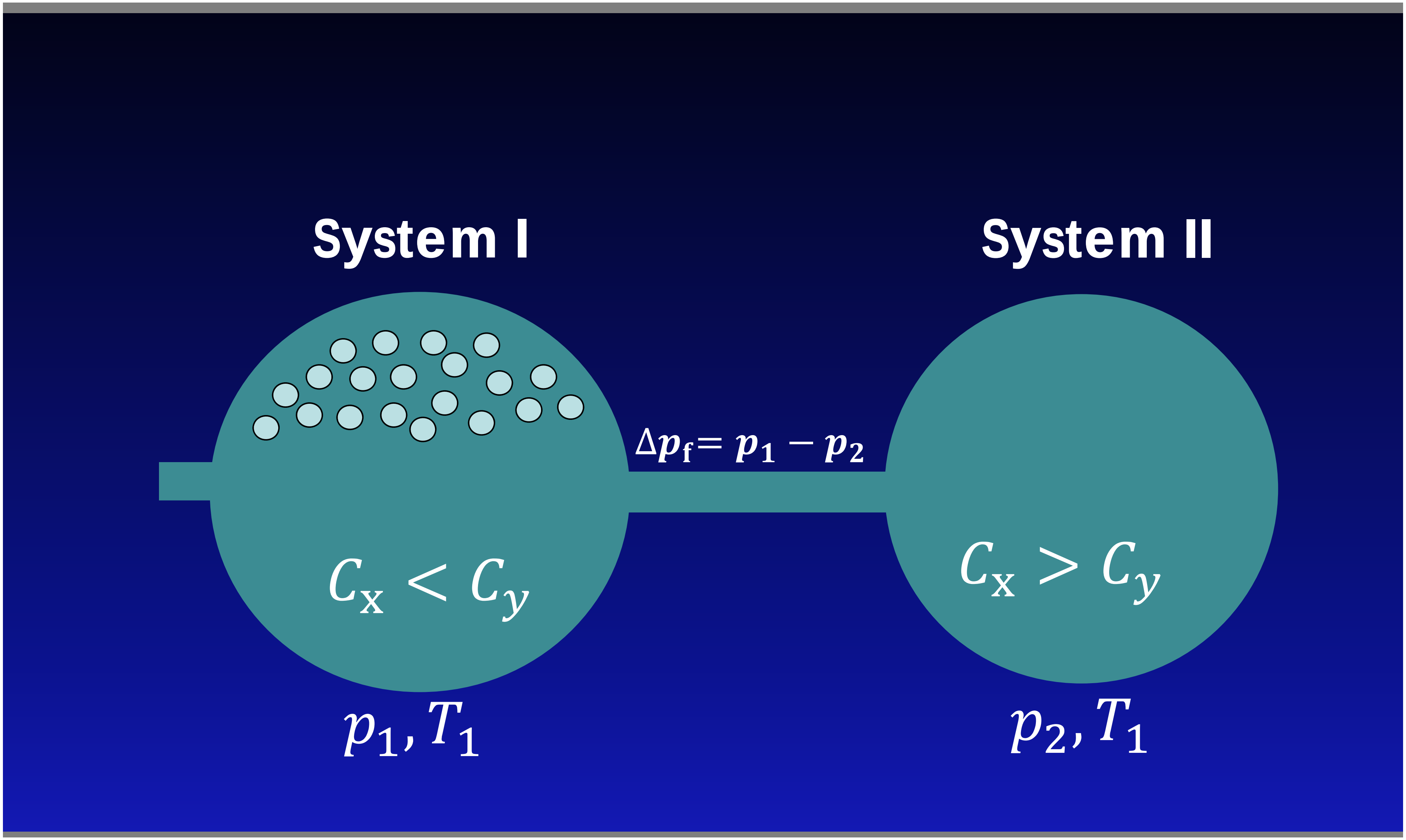

Methodology

- Perform flash calculations
- Assume filtration pressure

$$p_F = p_1 - p_2$$

- Compute fugacities

$$f_{C_x}^{L_1} = \Phi_{C_x}^{L} x_{C_x} P_1 = f_{C_x}^{L_2} = \Phi_{C_x}^{L} x_{C_x} P_2$$

- Compute membrane efficiency

$$\omega_f = \left(\frac{f_{C_y}^{L_2}}{f_{C_y}^{L_1}} \right)$$

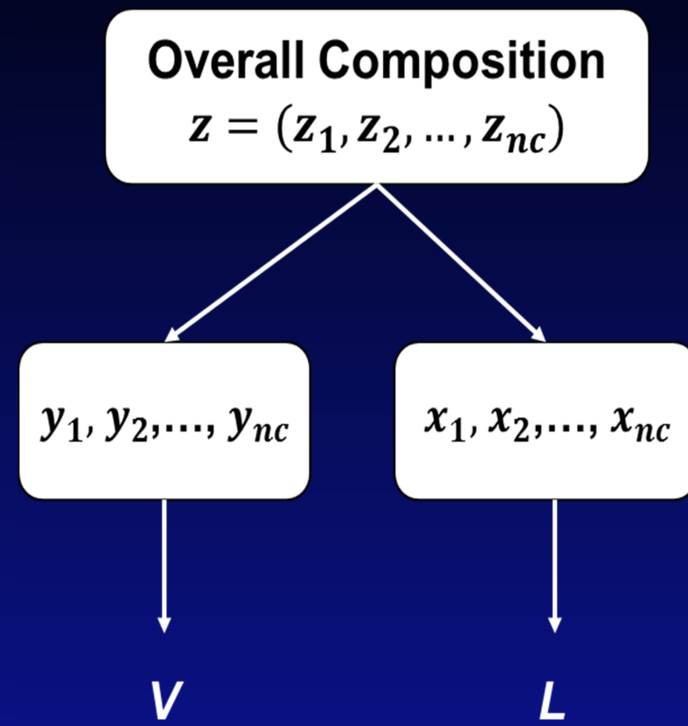

Preliminary Results

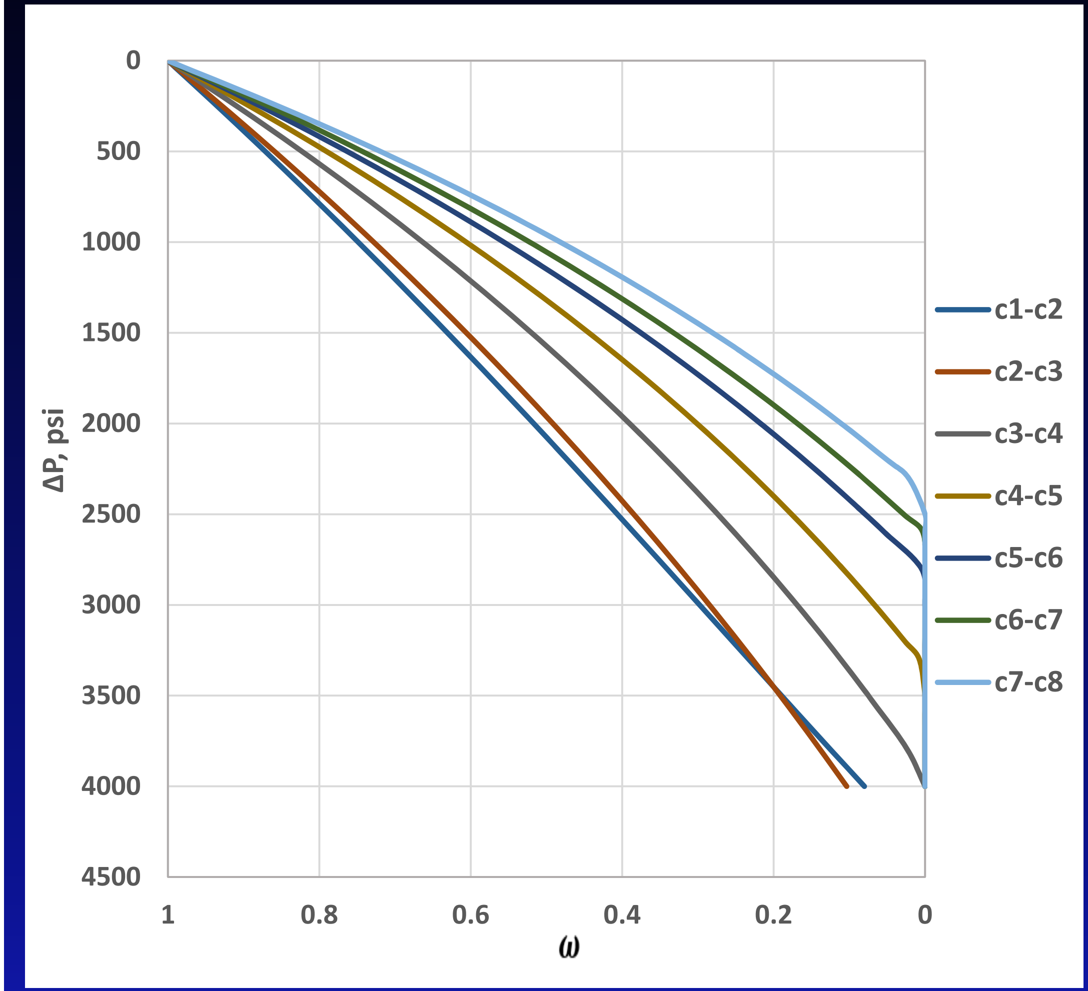

Case 1:

- 2 Components
- Mole fraction: 50% 50%
- Constant temperature: 660 °R= 220 °F=93 °C
- Pressure change: 500 psi-4000 psi

Preliminary Results

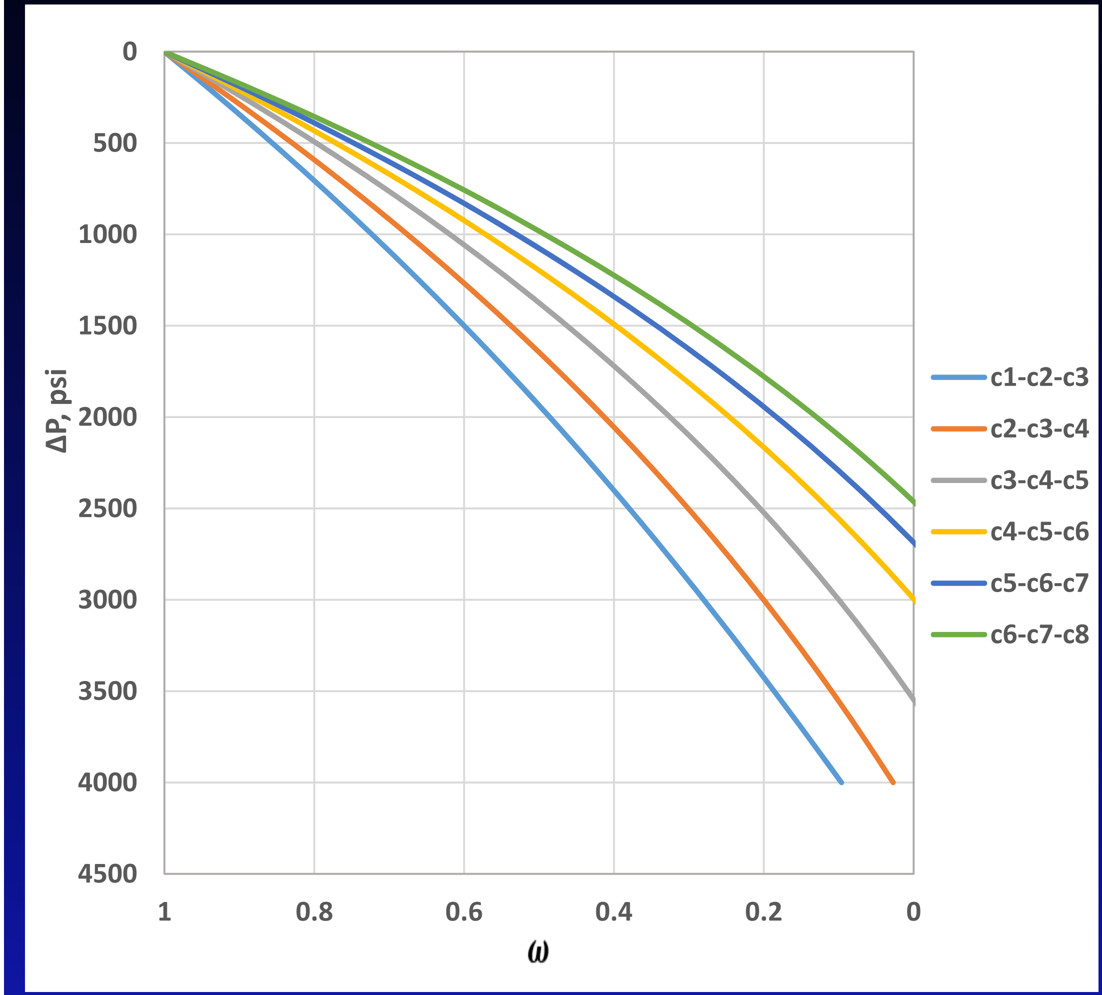

Case 2:

- 3 Components
- Mole Fraction:
  20% 30% 50%
- Constant temperature:
  660 °R= 220 °F=93 °C
- Pressure change:
  500 psi-4000 psi

Preliminary Results

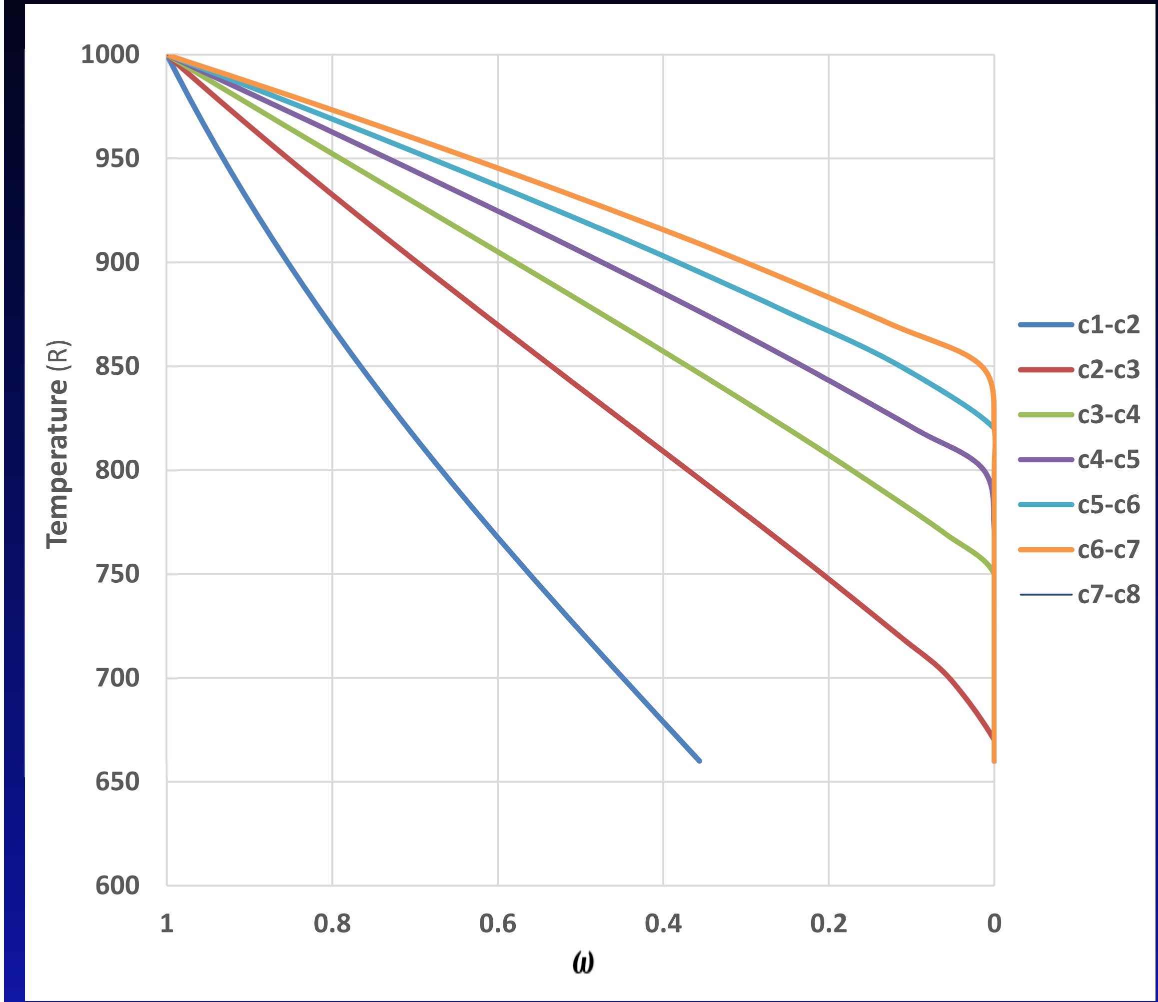

Case 3:

- 2 Components
- Mole fraction:
  50% 50%
- Constant pressure:
  10000 psi
- Temperature range:
  660 °R – 1200 °R

Preliminary Results

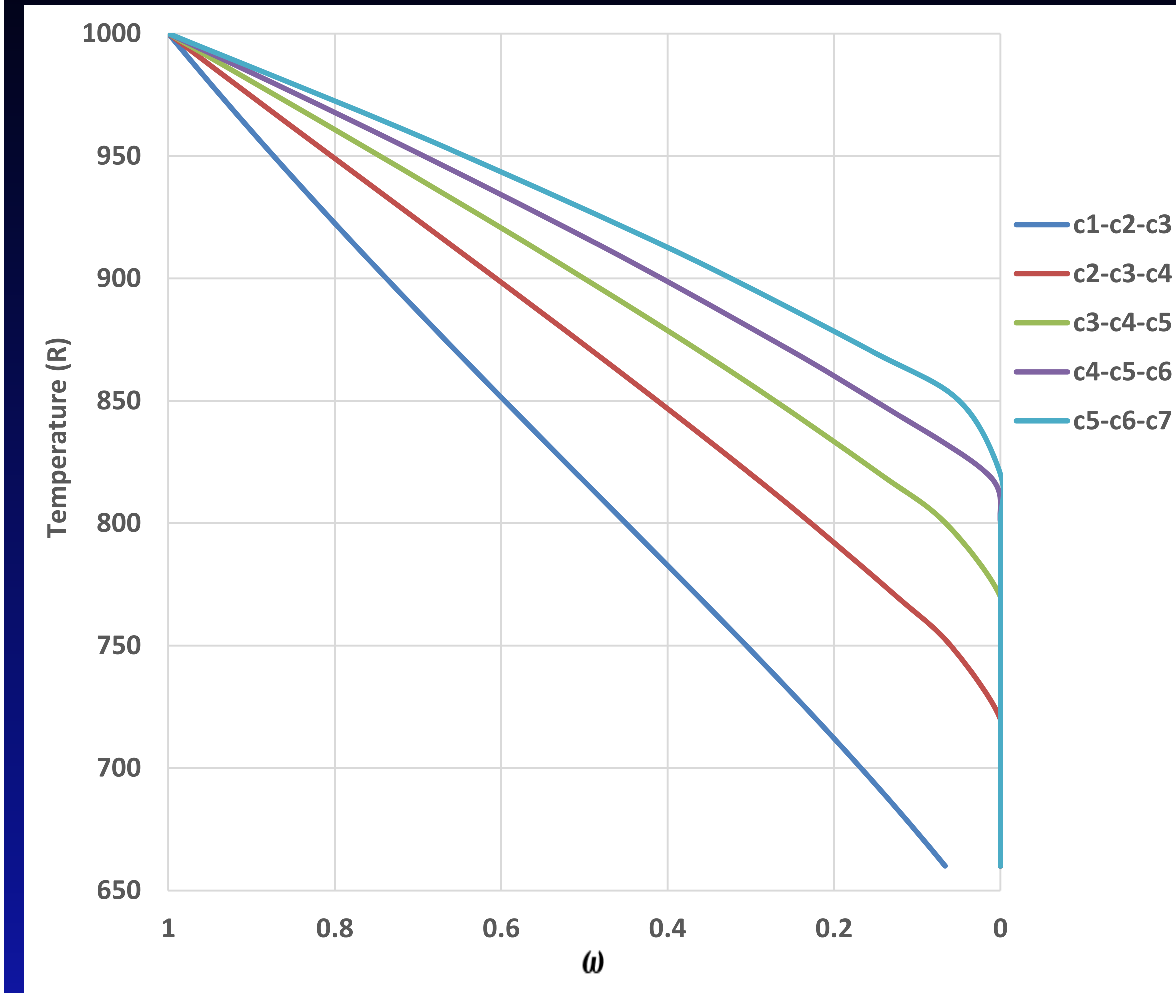

Case 4:

- 3 Components
- Mole fraction:
  20% 30% 50%
- Constant pressure:
  10000 psi
- Temperature range:
  $660\ °\mathrm{R} - 1200\ °\mathrm{R}$

Two Phase Compositional Flow Model

Molar balance equation

$$-\nabla\left(y_c\xi_g\bar{v}_g + x_c\xi_o\bar{v}_o\right) + \left(y_c\xi_g\bar{q}_g + x_c\xi_o\bar{q}_o\right) = \frac{\partial}{\partial t}\left[\emptyset z_c\left(\xi_g S_g + \xi_o S_o\right)\right]$$

Constraints:

$$\sum_{c=1}^{n_c} x_c = 1 \qquad \sum_{c=1}^{n_c} y_c = 1 \qquad \sum_{c=1}^{n_c} z_c = 1$$

$$S_o + S_g = 1$$

Two Phase Compositional Flow Model

LHS: Space derivative

$$-\nabla\left(y_c\xi_g\bar{v}_g + x_c\xi_o\bar{v}_o\right) + \left(y_c\xi_g\bar{q}_g + x_c\xi_o\bar{q}_o\right) = \frac{y^n_{c,i}\xi^n_{g,i}k^n_{i+\frac{1}{2}}\lambda^n_{g,i+\frac{1}{2}}}{\Delta x_i}\left(\frac{P^{n+1}_{o,i+1}-P^{n+1}_{o,i}}{\Delta x_{i+\frac{1}{2}}}\right) -$$

$$\frac{y^n_{c,i}\xi^n_{g,i}k^n_{i-\frac{1}{2}}\lambda^n_{g,i-\frac{1}{2}}}{\Delta x_i}\left(\frac{P^{n+1}_{o,i}-P^{n+1}_{o,i-1}}{\Delta x_{i-\frac{1}{2}}}\right) + \frac{y^n_{c,i}\xi^n_{g,i}k^n_{i+\frac{1}{2}}\lambda^n_{g,i+\frac{1}{2}}}{\Delta x_i}\left(\frac{P^n_{c,g,i+1}-P^n_{c,g,i}}{\Delta x_{i+\frac{1}{2}}}\right) -$$

$$\frac{y^n_{c,i}\xi^n_{g,i}k^n_{i-\frac{1}{2}}\lambda^n_{g,i-\frac{1}{2}}}{\Delta x_i}\left(\frac{P^n_{c,g,i}-P^n_{c,g,i-1}}{\Delta x_{i-\frac{1}{2}}}\right) + \frac{x^n_{c,i}\xi^n_{o,i}k^n_{i+\frac{1}{2}}\lambda^n_{o,i+\frac{1}{2}}}{\Delta x_i}\left(\frac{P^{n+1}_{o,i+1}-P^{n+1}_{o,i}}{\Delta x_{i+\frac{1}{2}}}\right) -$$

$$\frac{x^n_{c,i}\xi^n_{o,i}k^n_{i-\frac{1}{2}}\lambda^n_{o,i-\frac{1}{2}}}{\Delta x_i}\left(\frac{P^{n+1}_{o,i}-P^{n+1}_{o,i-1}}{\Delta x_{i-\frac{1}{2}}}\right) + \left(y^n_{c,i}\xi^n_{g,i}\widehat{q_g} + x^n_{c,i}\xi^n_{o,i}\hat{q}_o\right)$$

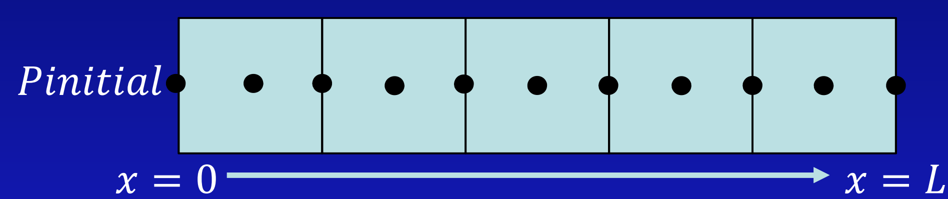

Two Phase Compositional Flow Model

RHS: Time derivative

$$\frac{\partial}{\partial t}\left[\emptyset z_c\left(\xi_o S_o + \xi_g S_g\right)\right]$$

$$v_t = \frac{1}{\left(\xi_o S_o + \xi_g S_g\right)} => \frac{\partial}{\partial t}\left[\emptyset\frac{z_c}{v_t}\right]$$

$$\frac{\partial}{\partial t}\left[\emptyset z_c\left(\xi_o S_o + \xi_g S_g\right)\right] = \frac{\partial}{\partial t}\left[\frac{\emptyset z_c}{v\ \ _t}\right]$$

$$\frac{\partial}{\partial t}\left[\frac{\emptyset z_c}{v\ \ _t}\right] = \frac{Vi}{\Delta t}\left(\frac{z_c^n}{v_t^n}\emptyset^n\right)\left\{\left(C_\emptyset + C_{vt}\right)^n\left(p_{oi}^{n+1} - p_{oi}^n\right) - \left[\sum_{d=1}^{nc}\left\{\left[\frac{1}{v_t^n}\overrightarrow{v^n}_{td}\right]\left(z_{d,i}^{n+1} - z_{d,i}^n\right)\right\}\right]\right\}$$

Two Phase Compositional Flow Model

The coupled fluxes concept may be applied for filtration in nanoporous media by considering a single-solute system (*M* = 1 and for dilute solutions $V_w \approx 1$).

$$q = -\frac{k}{\mu}\frac{\partial p}{\partial x} + \frac{\omega_f k}{\mu} RT \frac{\partial C_s}{\partial x}$$

$$J_s^d = \frac{\omega_f C_s k}{\mu}\frac{\partial p}{\partial x} - \left(\frac{\phi D_s^*}{RT} + \frac{\omega_f^2 C_s k}{\mu}\right) RT \frac{\partial C_s}{\partial x}$$

where

$$D_s^* = \tau_a D_s$$

s : solute, hydrocarbon component that is hindered by the pore-throat size

D_s^* : effective self-diffusion coefficient for hindered hydrocarbon component

T_a : Dimensionless apparent tortuosity

Conclusions

- Transportation through membrane causes produced mixture lighter.
- Pressure change increase and temperature decrease causes lower membrane efficiency.
- Compositional flow model will allow to observe mixture behavior with respect to time and distance.

UNCONVENTIONAL RESERVOIR ENGINEERING PROJECT

Colorado School of Mines

Experimental Study of the Membrane Properties of Shale Reservoirs

Ziming Zhu
Ph.D. Petroleum Engineering
Colorado School of Mines

Problem Statement

- Pore sizes of shale are in nano range

Pore/throat $\xleftrightarrow{\textit{Same order of magnitude}}$ Hydrocarbon molecule

- Shale can act as a semi-permeable membrane

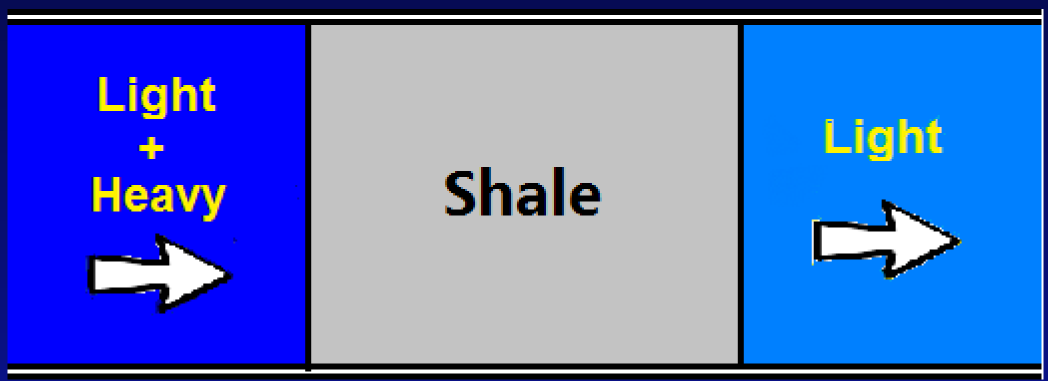

Light components can pass through

Heavy components will be completely or partially filtered

Objective

- Verify/Test the membrane property of shale
- Investigate factors controlling the membrane efficiency of shale
  - Membrane efficiency: $\omega = 1 - \frac{N_{i\_produced}}{N_{i\_reserved}}$
  - What factors have effects

    ΔP T component species …
  - How they affect the membrane efficiency
    - Qualitative
    - Quantitative

Experimental Setup

Complete setup

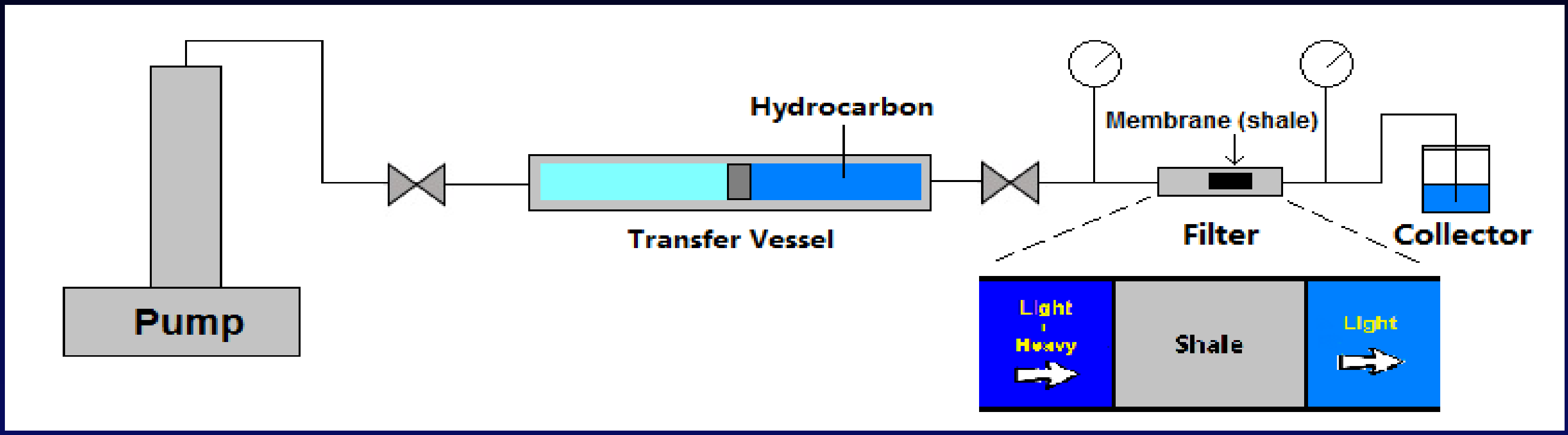

Current setup (leakage test)

Experimental Setup

- In-Line Filter

Pressure: 0-2500 psi

Temperature: -20 °F to 100 °F

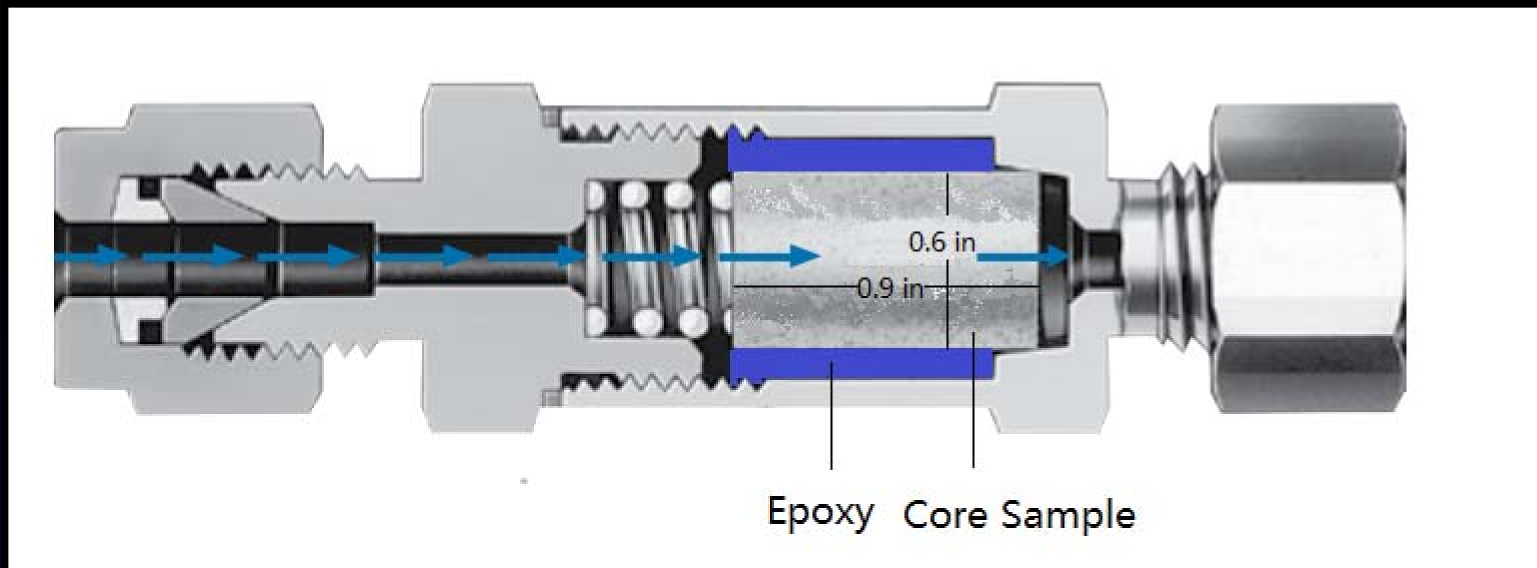

Composition Measurement

- Gas Chromatography (GC)

Injected fluid : n-C_7 (50%) + n-C_{12} (50%)

Filtered fluid:

Composition of Filter Fluid	Pore Volume (PV) injected				
	0.5	1	1.5	2	…
$Z_{(n\text{-}C_7)}$	-	-	-	-	-
$Z_{(n\text{-}C_{12})}$	-	-	-	-	-

Expected Results

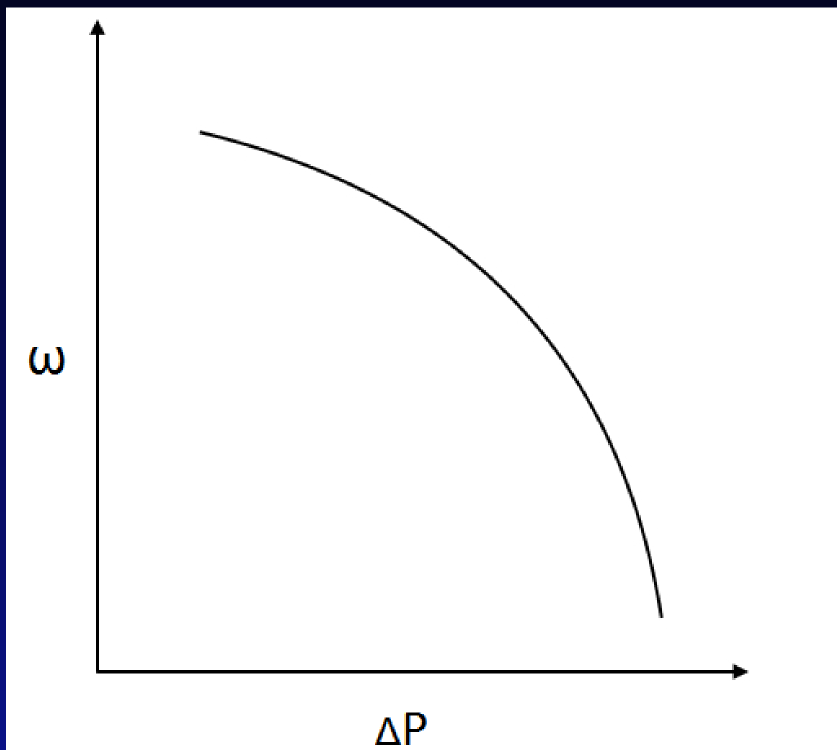

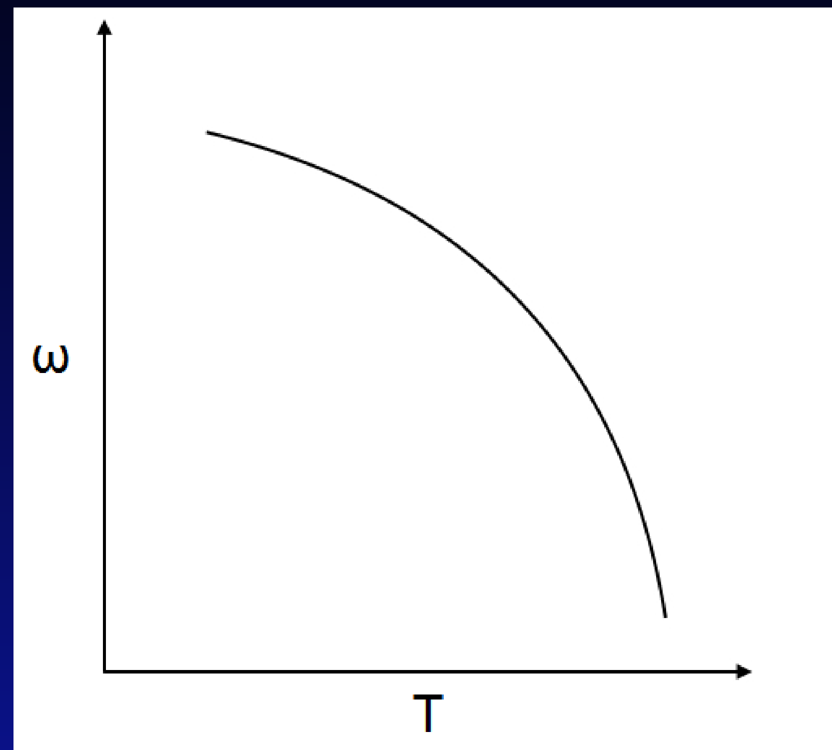

ΔP – Pressure difference across shale ω – Membrane efficiency
T - Temperature

Expected Results

- $\Delta P \uparrow \quad \omega \downarrow$
- $T \uparrow \quad \omega \downarrow$

By using this plot

- Determine the membrane efficiency (ω) of shale to the reservoir fluid at a certain T and ΔP
- Composition of reservoir fluid

$\updownarrow$ Membrane Efficiency

Composition of produced fluid

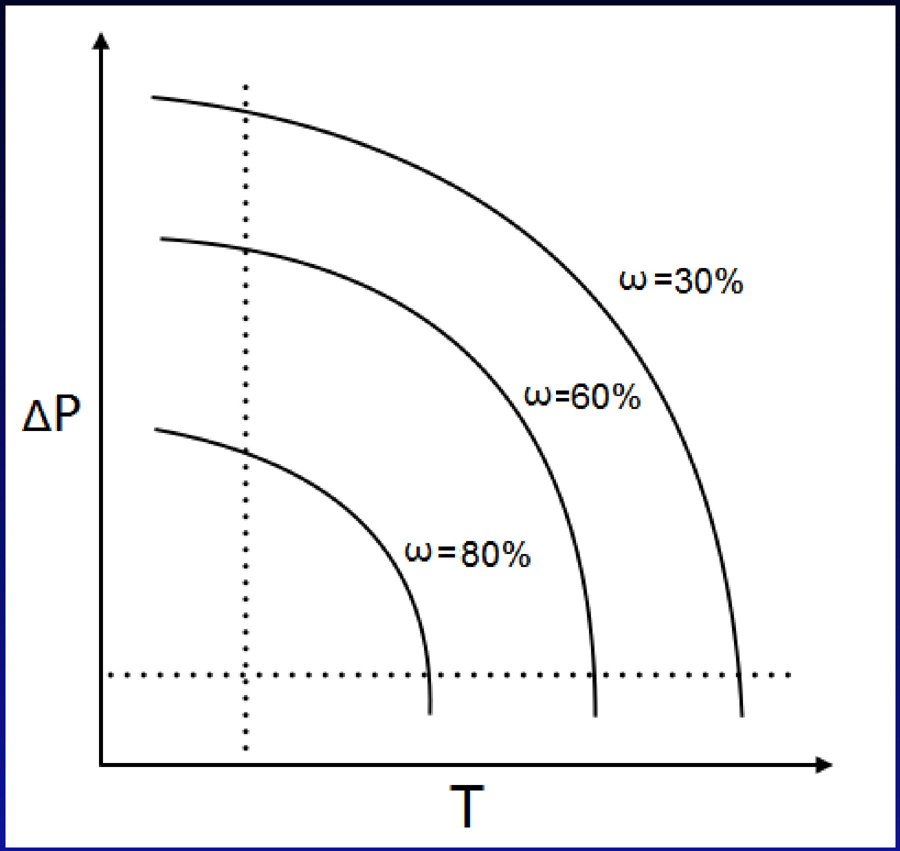

Thank You

Questions?

Slip Flow of Gas in Nanoporous Media using Lattice Boltzmann and DSMC Method

Ziming Zhu
Ph.D. Petroleum Engineering
Colorado School of Mines

LBM – Slip Flow

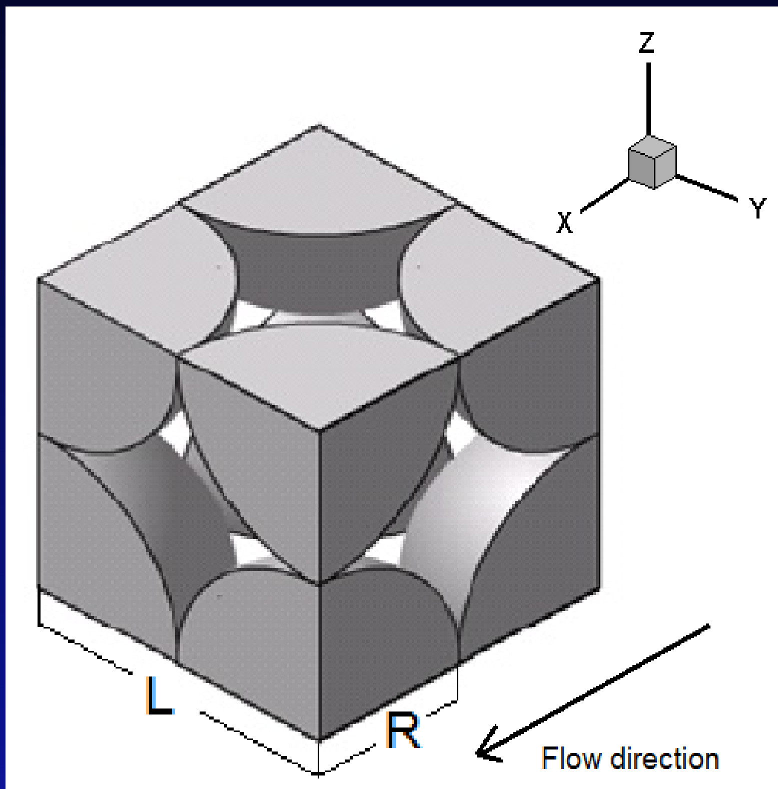

- Geometry/Parameter

  Gas: N_2 T=273.15 K

  R_{sp}=0.5L Porosity(ϕ)=0.4764

  Body force=1e-6

  TMAC=1.0 (diffuse wall accommodation coefficient)

- Simulation Case

  Slip flow (Kn=0.05)

- Result

  Vx=7.9373e-7 (lattice velocity)

  $V_{s\_x} = 0.07672$ m/s (converted)

DSMC – Slip Flow

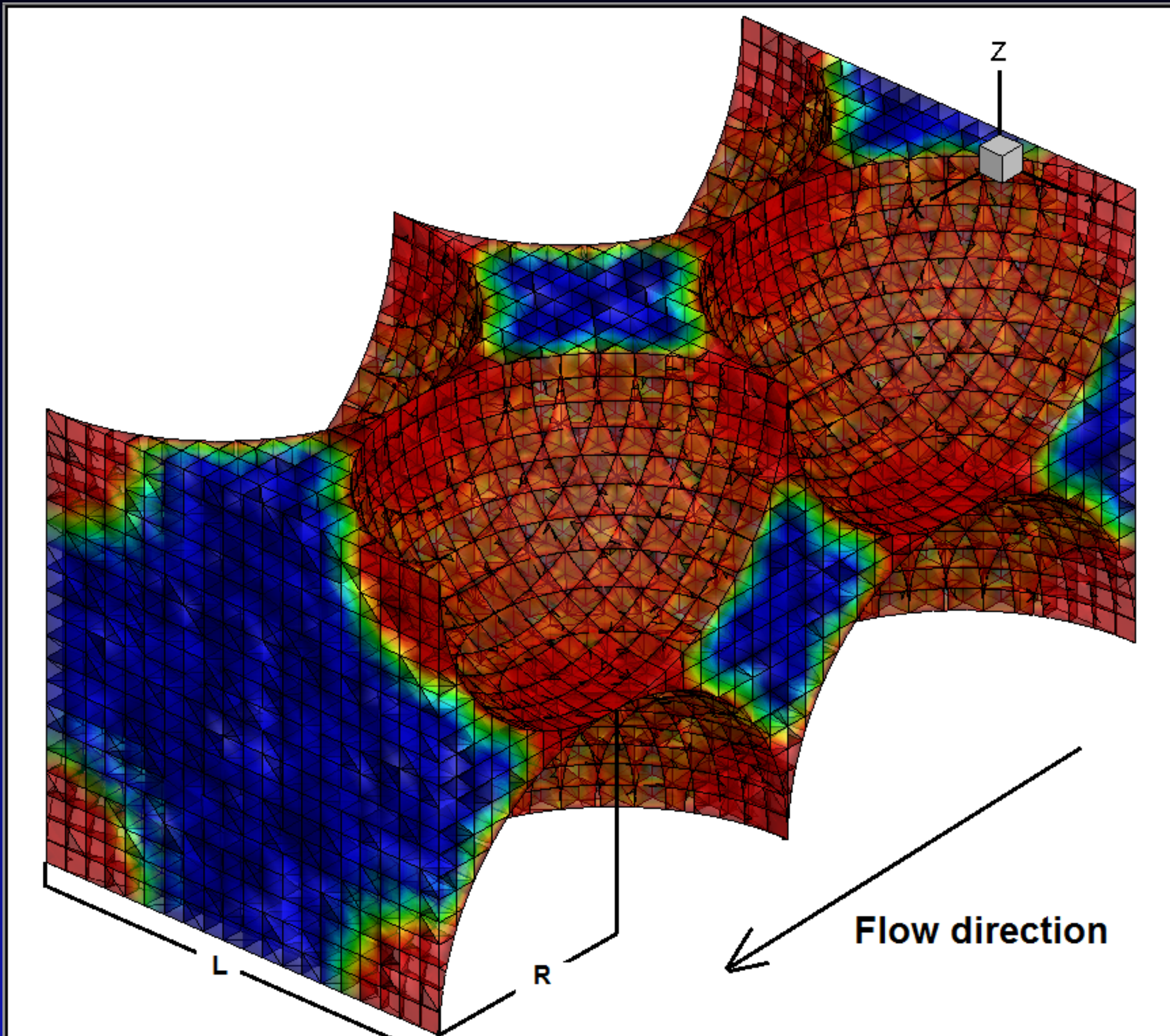

- **Parameter/Geometry**

  Gas: N_2 T=273.15 K

  R_{sp}=0.5L=1.497e-7 m

  Porosity(ϕ)=0.4764

  TMAC=1.0

  (Diffuse wall accommodation coefficient)

- **Simulation Case**

  Slip flow (Kn=0.05)

  ΔP=0.716 psia

- **Result**

  $V_{s\_x} = 0.0868$ m/s

  $$\frac{(V_{s\_x})_{DSMC}}{(V_{s\_x})_{LBM}} = \frac{0.0868}{0.0767} \approx 1.13$$

Thank You

Questions?

Research Summary

Pseudotransient Linear Flow in Unconventional Reservoirs

Wisam Assiri, CSM

Introduction

Interpretation of pseudotransient production data:

- Naturally fractured
- Hydraulically fractured

Such as, shale-gas and tight-oil plays

Assumption

- Single phase
- Constant bottomhole pressure

Motivation

- Most production comes from NF network within SRV.
- Hydraulic fracturing is expected to create or rejuvenate NF network.
- Boundary-dominated flow can be reached in the natural fractures.
- Transient flow continues in matrix blocks.

This will help us accurately interpret production data from tight, unconventional reservoirs

Background

- Pseudotransient flow has been observed in literature.
(Carlson and Mercer 1991; El-Banbi and Wattenbarger 1995; Mayerhofer et al. 2006; Medeiros et al. 2008)
- Ozkan et al. (1987) characterized the pseudotransient flow (referred to Flow regime 4).
- Ignoring pseudotransient flow leads to underestimating reserves.

Background cont'd

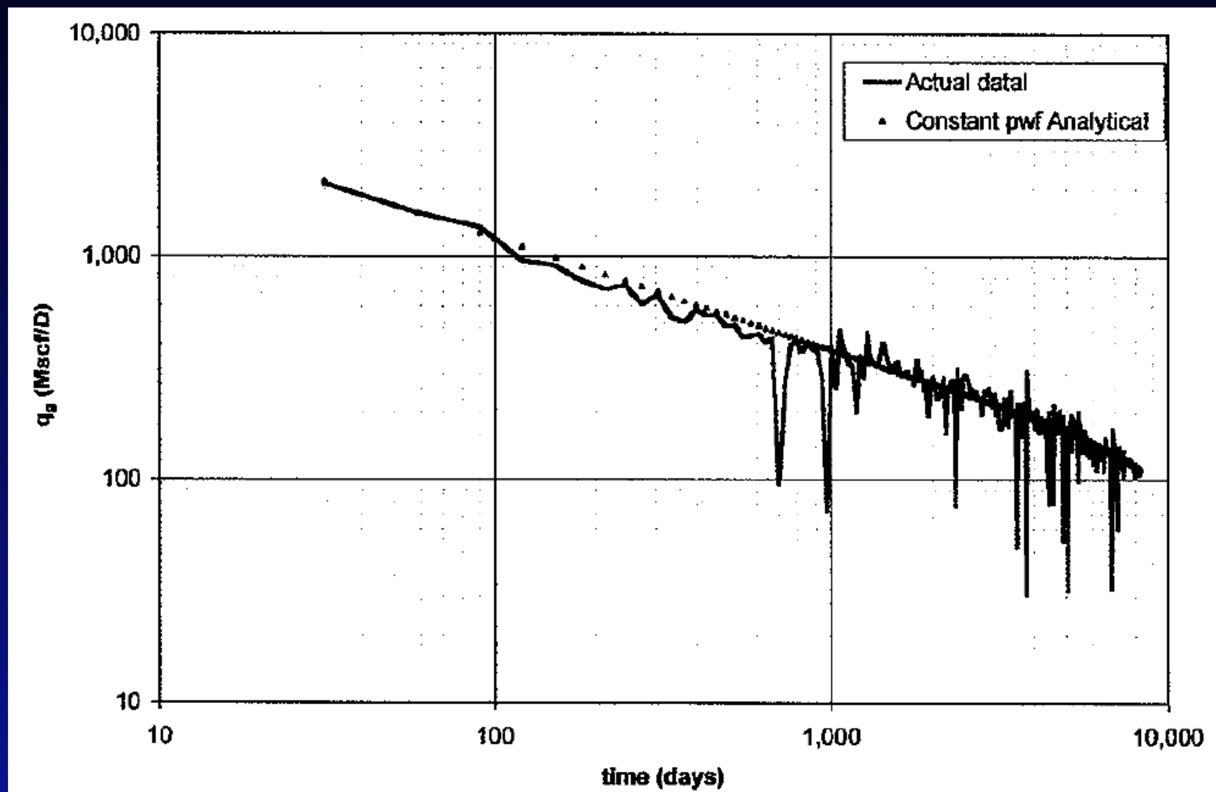

Production data from a shale-gas well displaying linear flow behavior for a period of over 20 years (Arévalo-Villagrán et al. 2001).

Scope of Research

- Define pseudotransient linear flow for fractured horizontal wells in dual-porosity unconventional reservoirs.
    - Analytical model to describe pseudotransient linear flow
    - Verifying the model
    - Analysis of production data
    - Compare it with existing analysis approaches

Approach

- Continue on previous work of Ozkan et al. (1987) and Brown et al. (2009)
- Derive the asymptotic solutions for each flow regime
- Compare the asymptotic approximations to the full solution and their start and end time to revert the reservoir properties
- Compare the model with other theoretical and field data

Approach cont'd

- Brown et al. (2009)

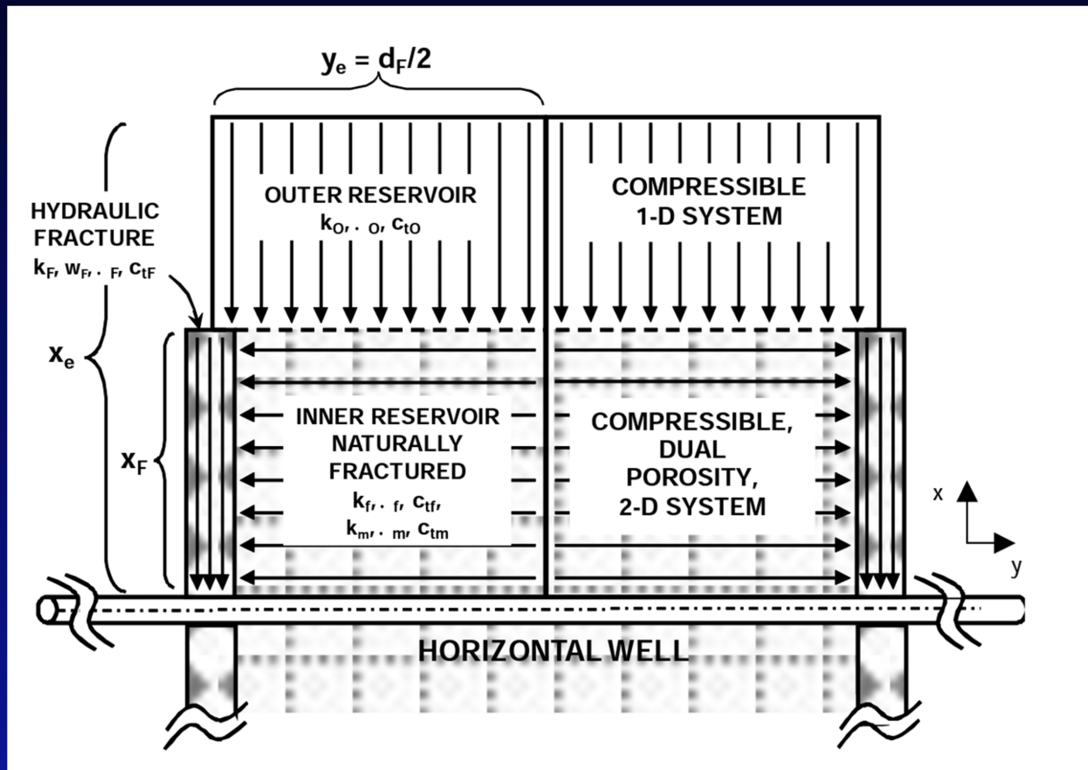

The setup for trilinear model, a top view.

Approach cont'd

- Possible Flow Regimes

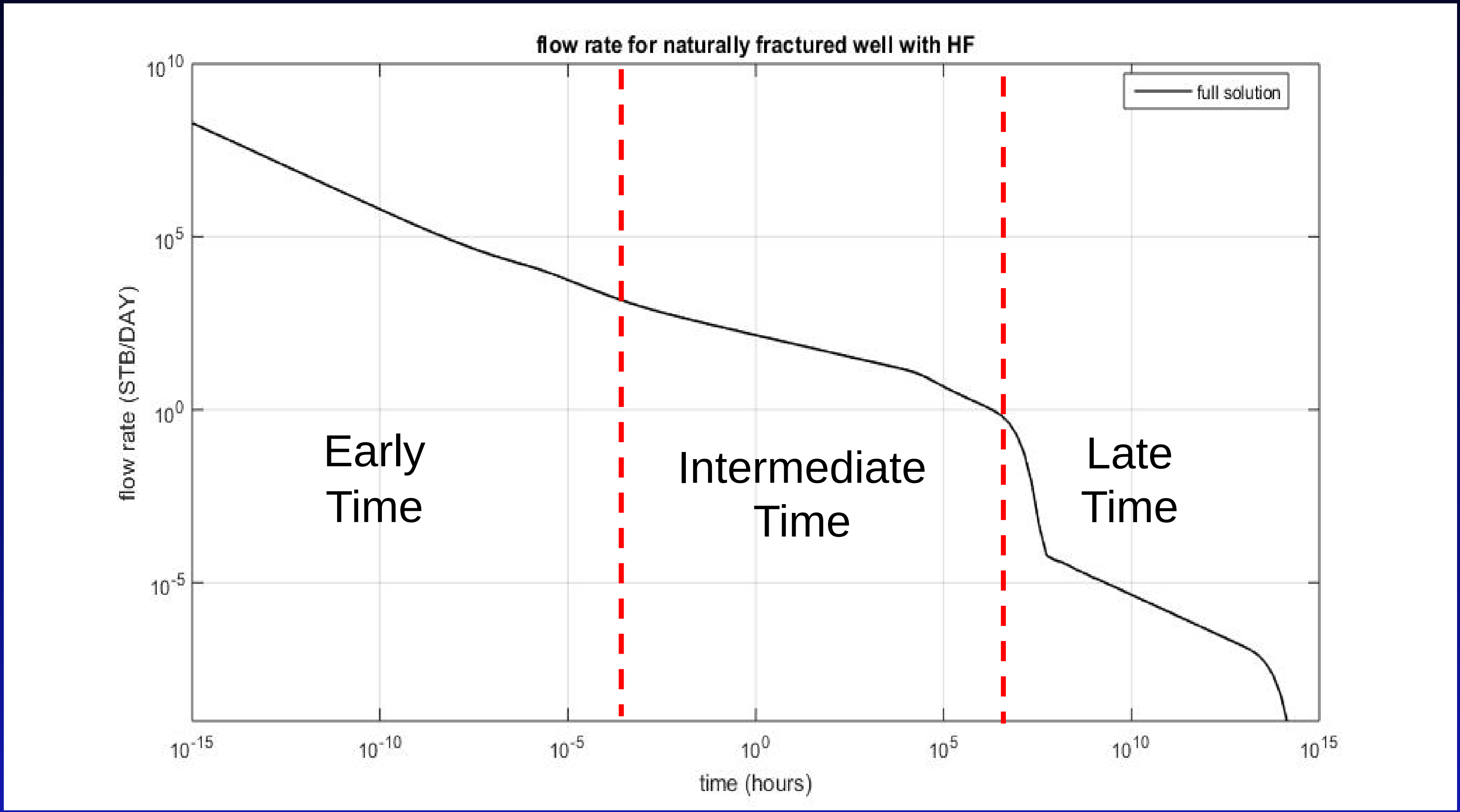

Approach cont'd

- Flow regime 1: Linear flow in HF only (no contribution from NF)

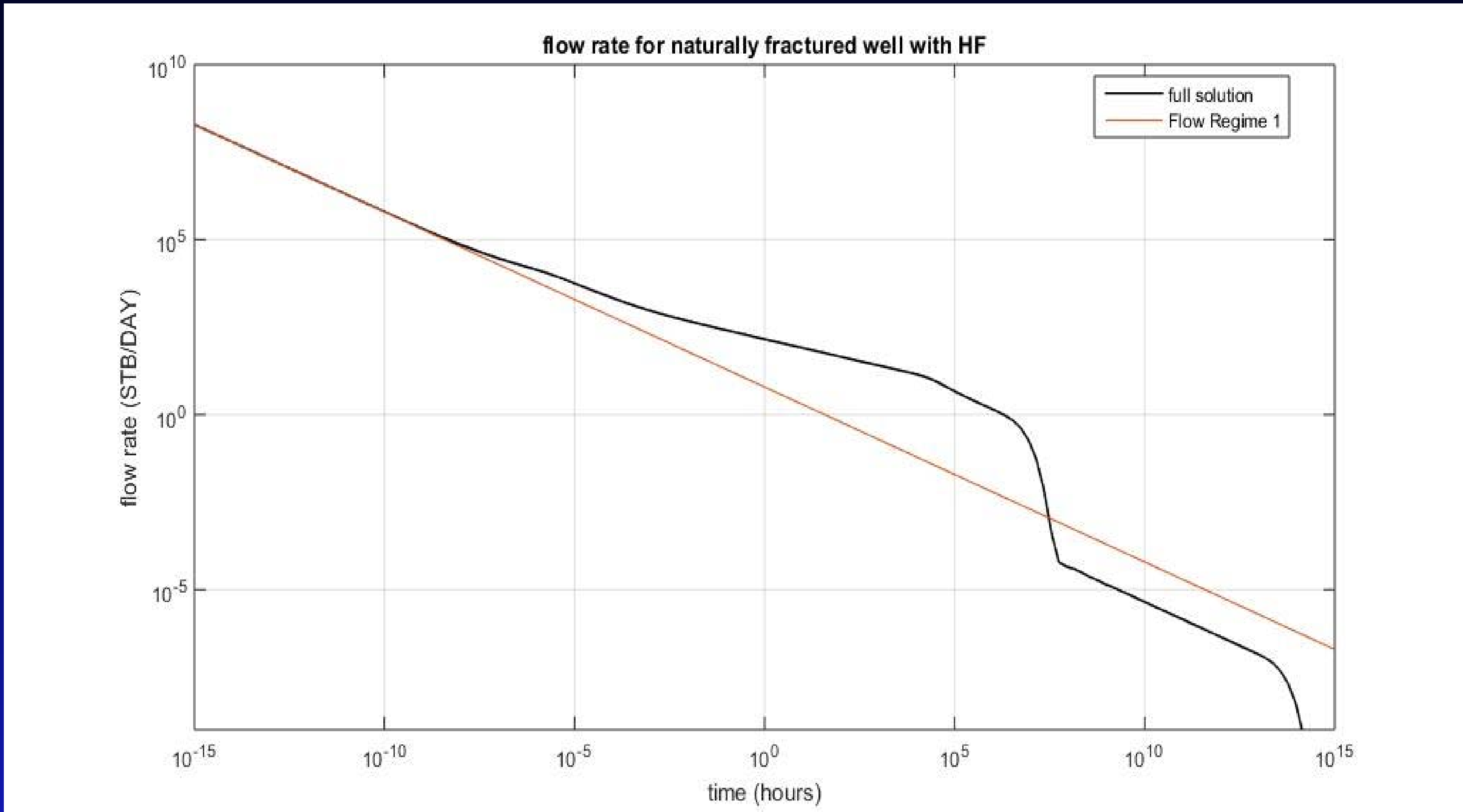

Approach cont'd

- Flow regime 2: Bilinear flow as a result of linear flows in HF and NF

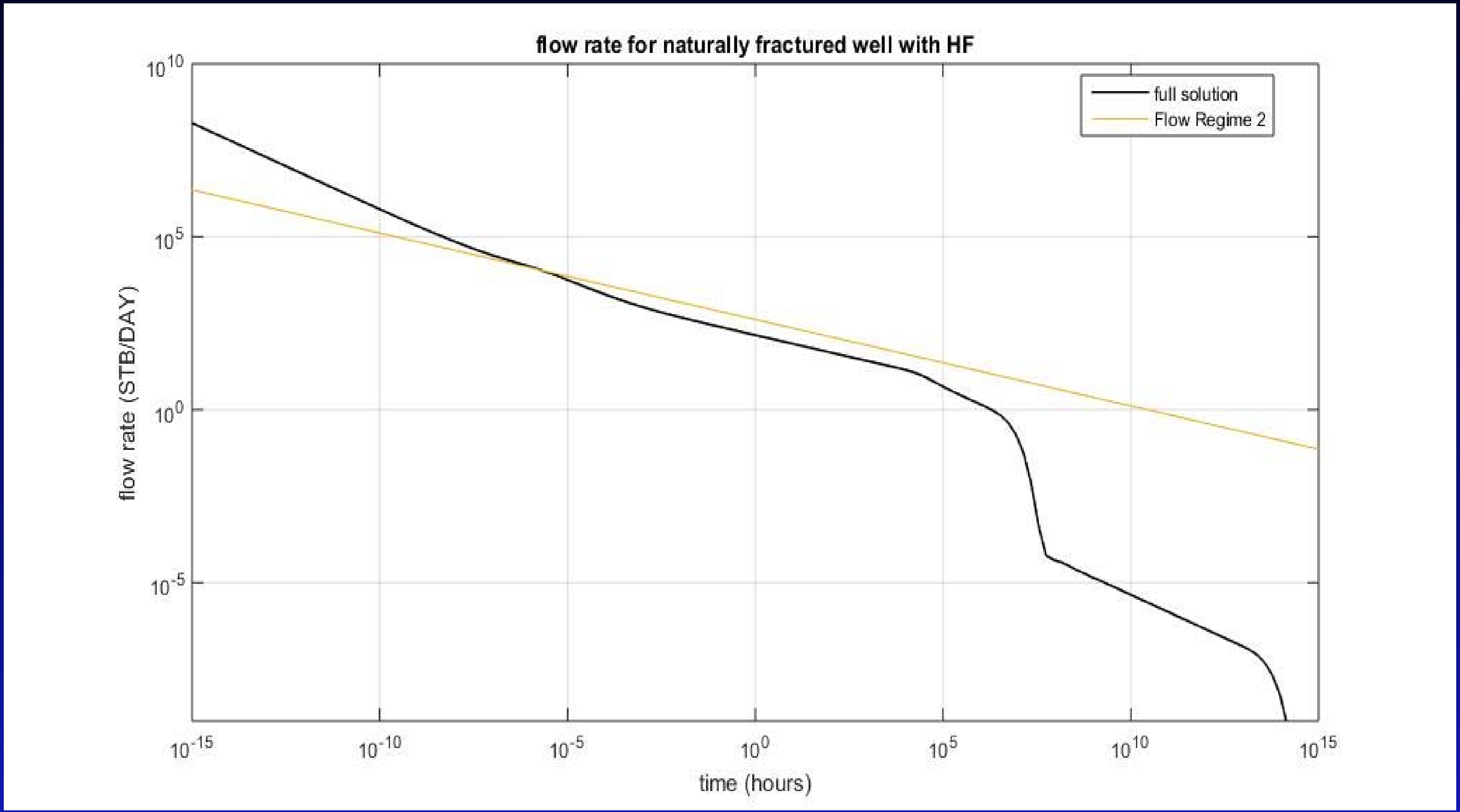

Approach cont'd

- Flow regime 3: Linear flow in NF only (no contribution from HF)

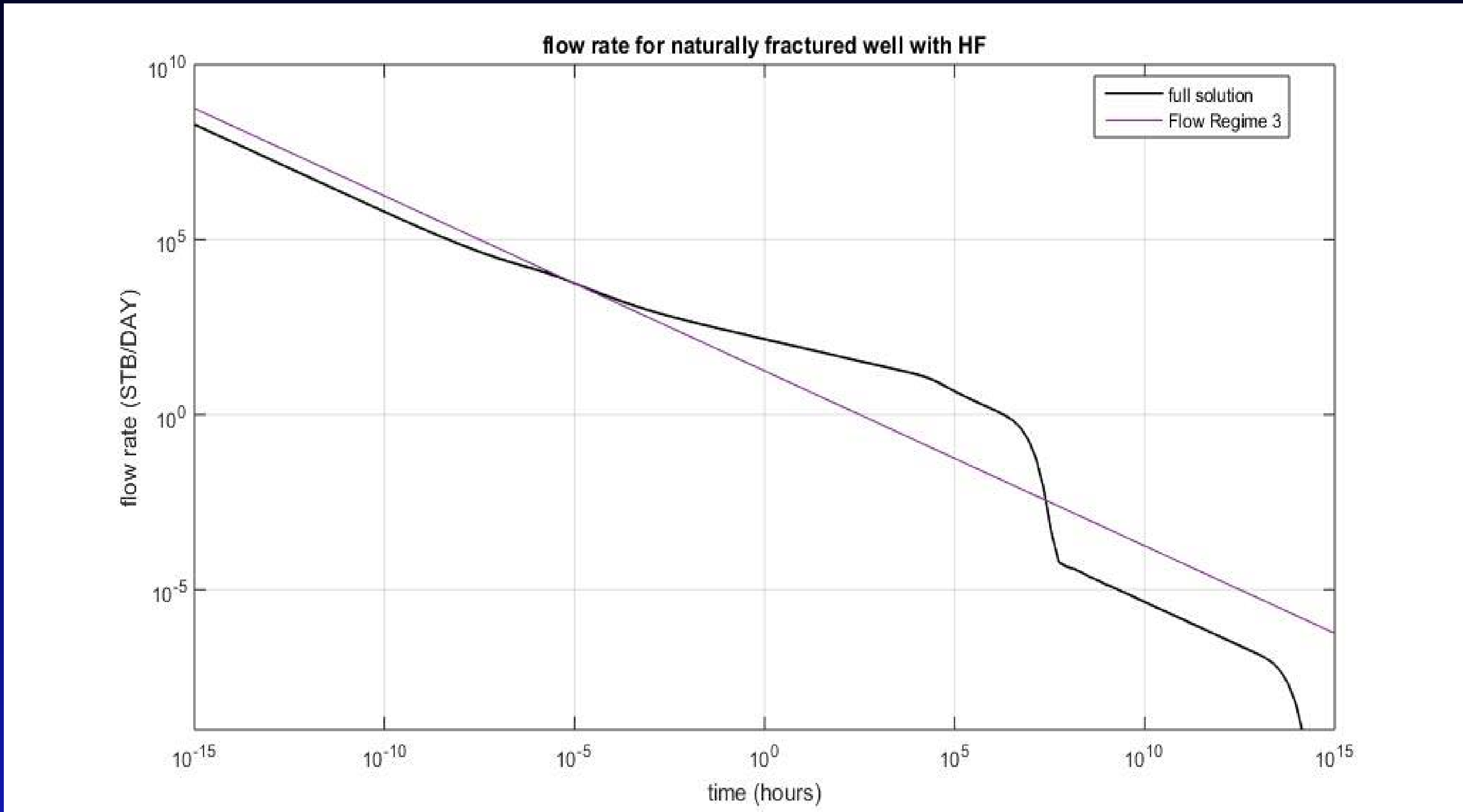

Approach cont'd

- Flow regime 5: Bilinear flow in the NF and IM (no contribution from HF)

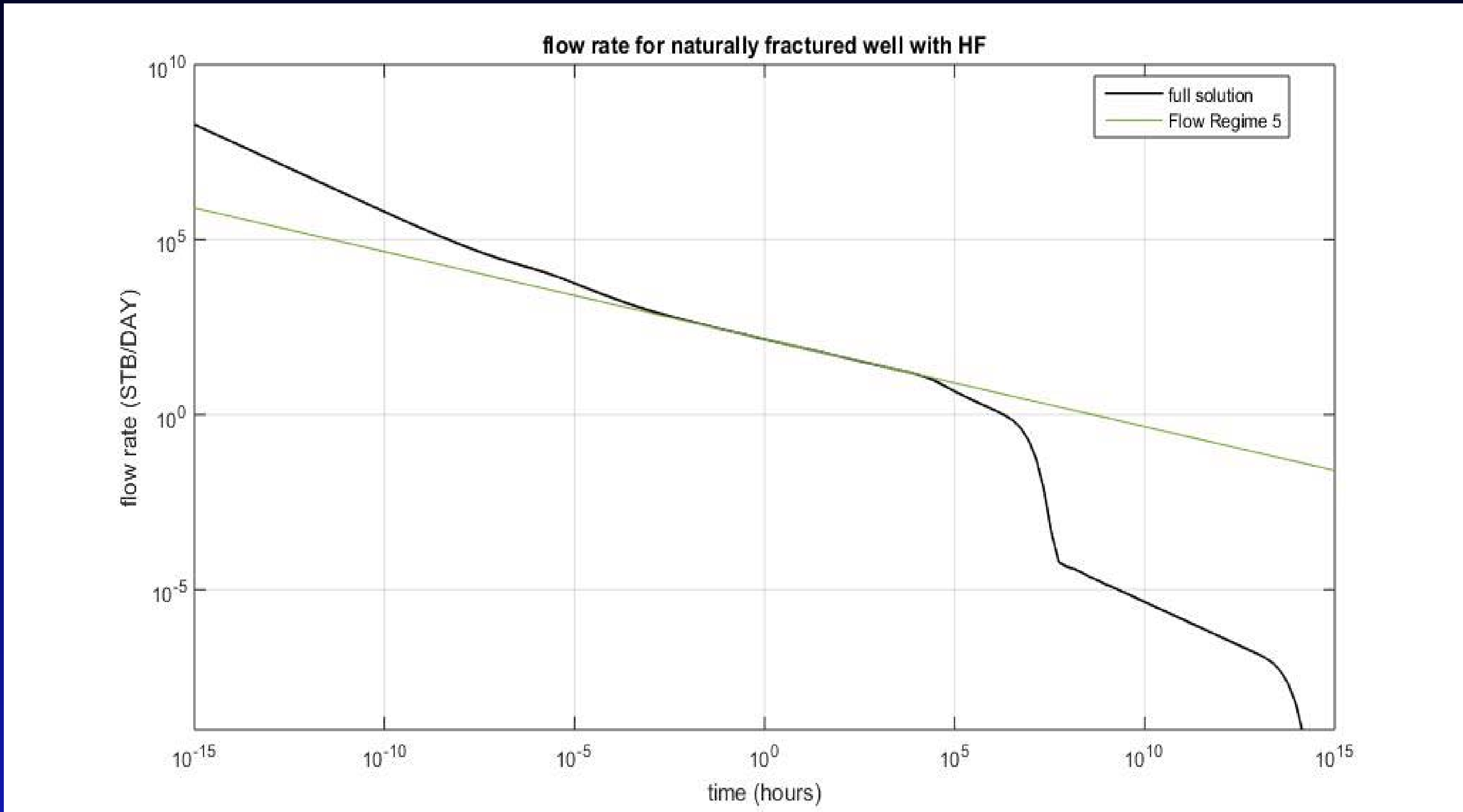

Approach cont'd

- Flow regime 6: Linear flow in the IM (no contribution from HF or NF)

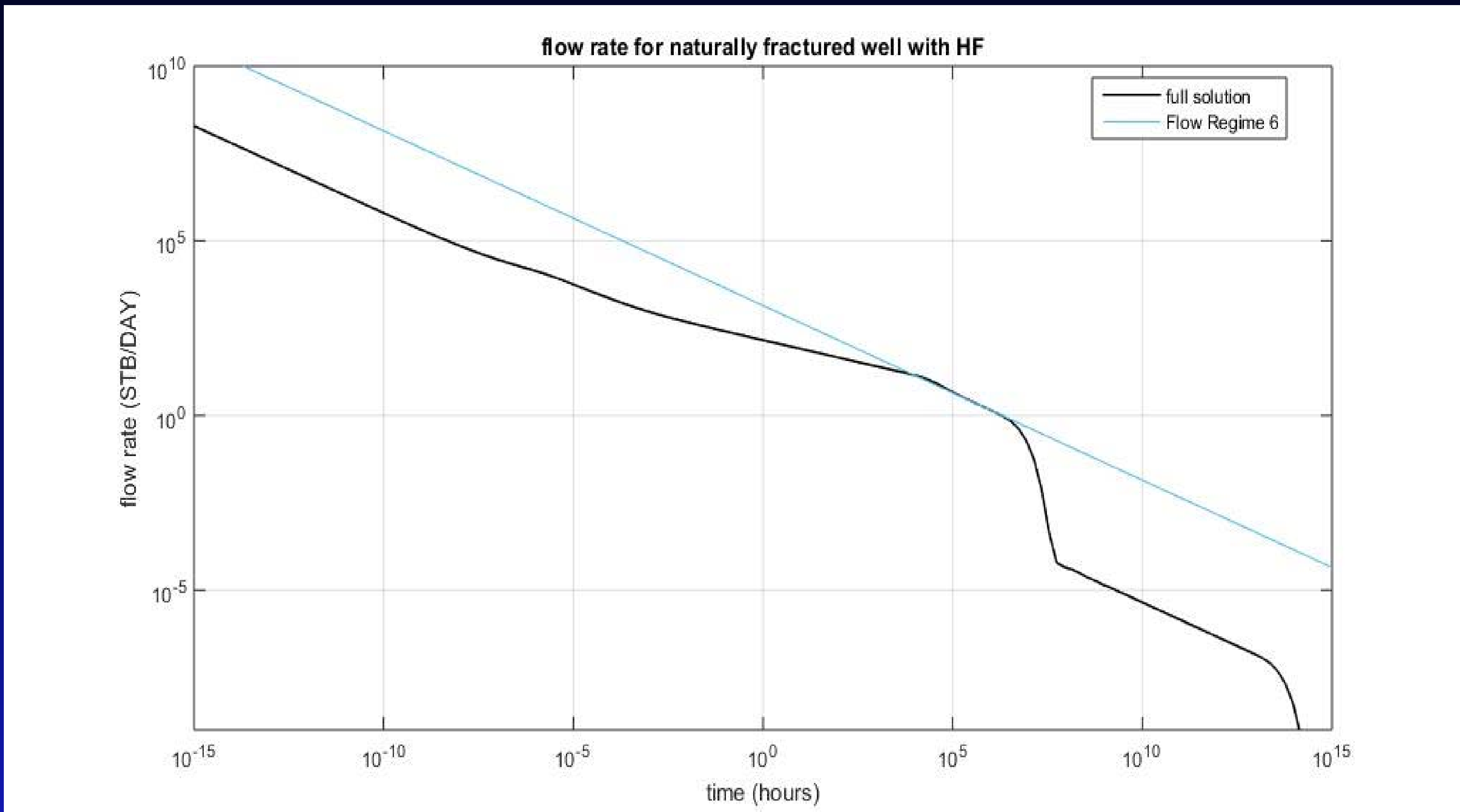

Approach cont'd

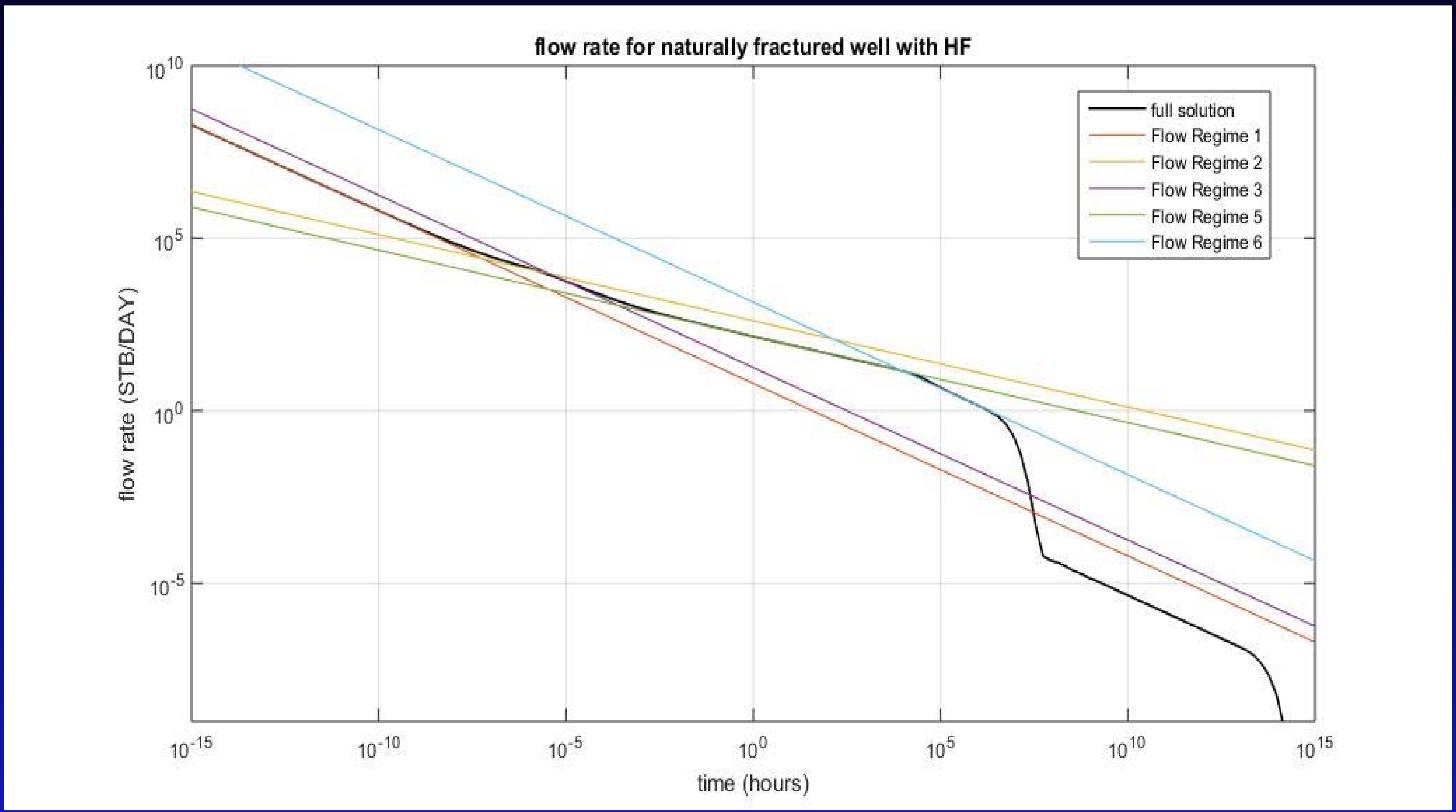

Approach cont'd

- Flow regime 1: Linear flow in the HF (no contribution from NF)

$$q_D = \frac{C_{FD}}{\sqrt{\pi^3}\sqrt{\eta_{FD}}}\frac{1}{\sqrt{t}}$$

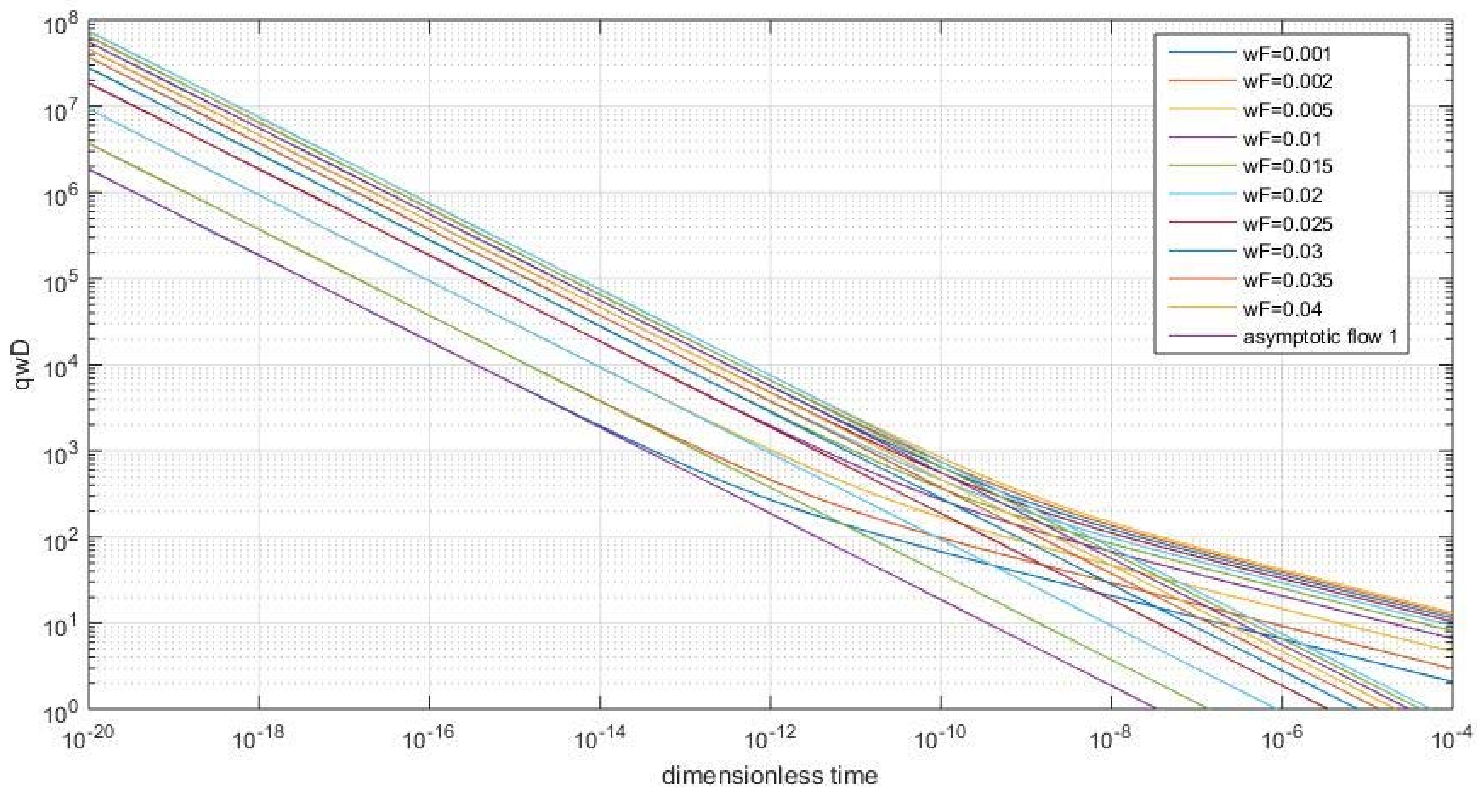

Approach cont'd

- Flow regime 2: Bilinear flow in HF and NF

$$q_D = \frac{\sqrt{2C_{FD}}}{\Gamma(^3/_4)\pi} t^{-1/4}$$

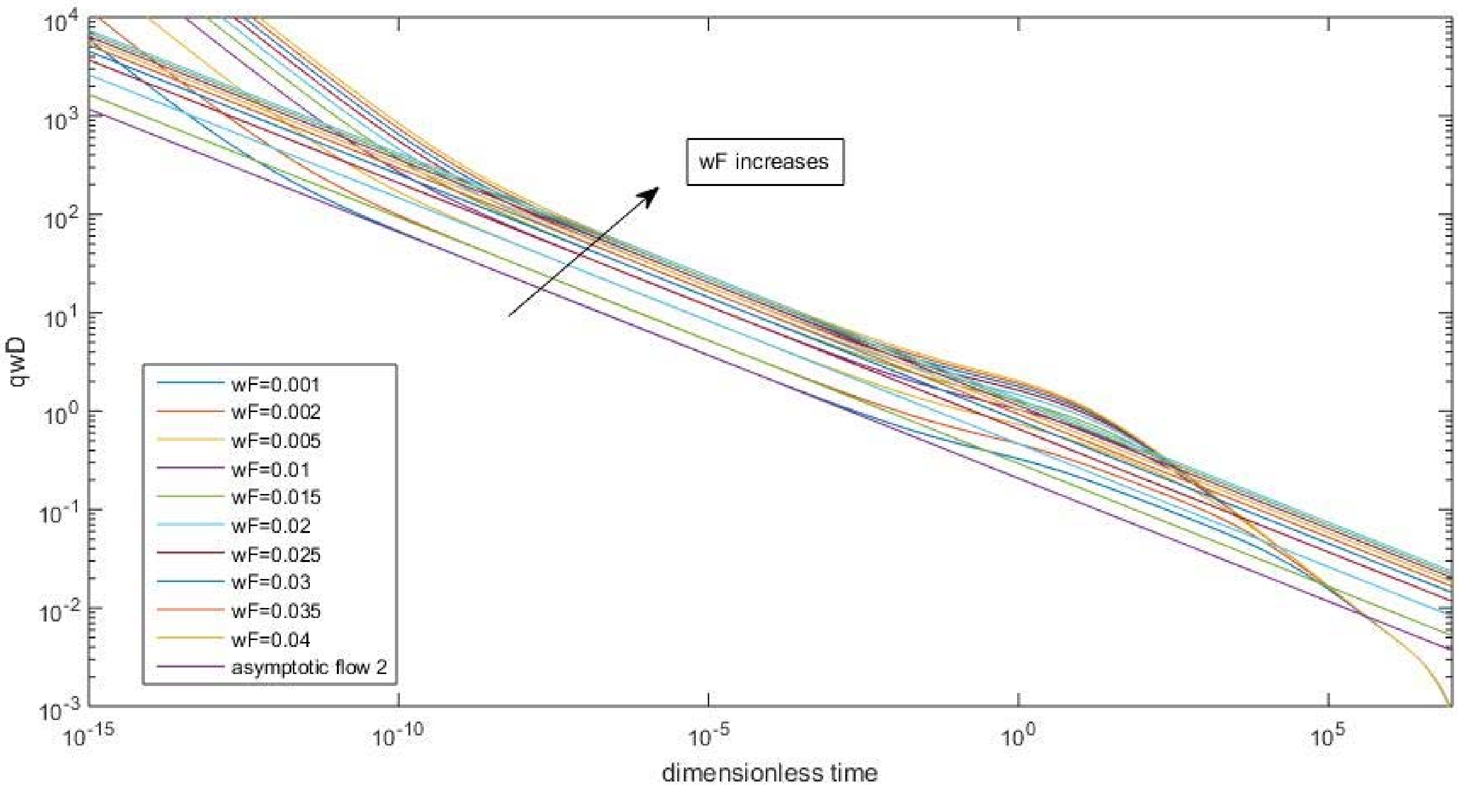

Approach cont'd

- Flow regime 3: Linear flow in NF only

$$q_D = \frac{2}{\sqrt{\pi^3 t_D}}$$

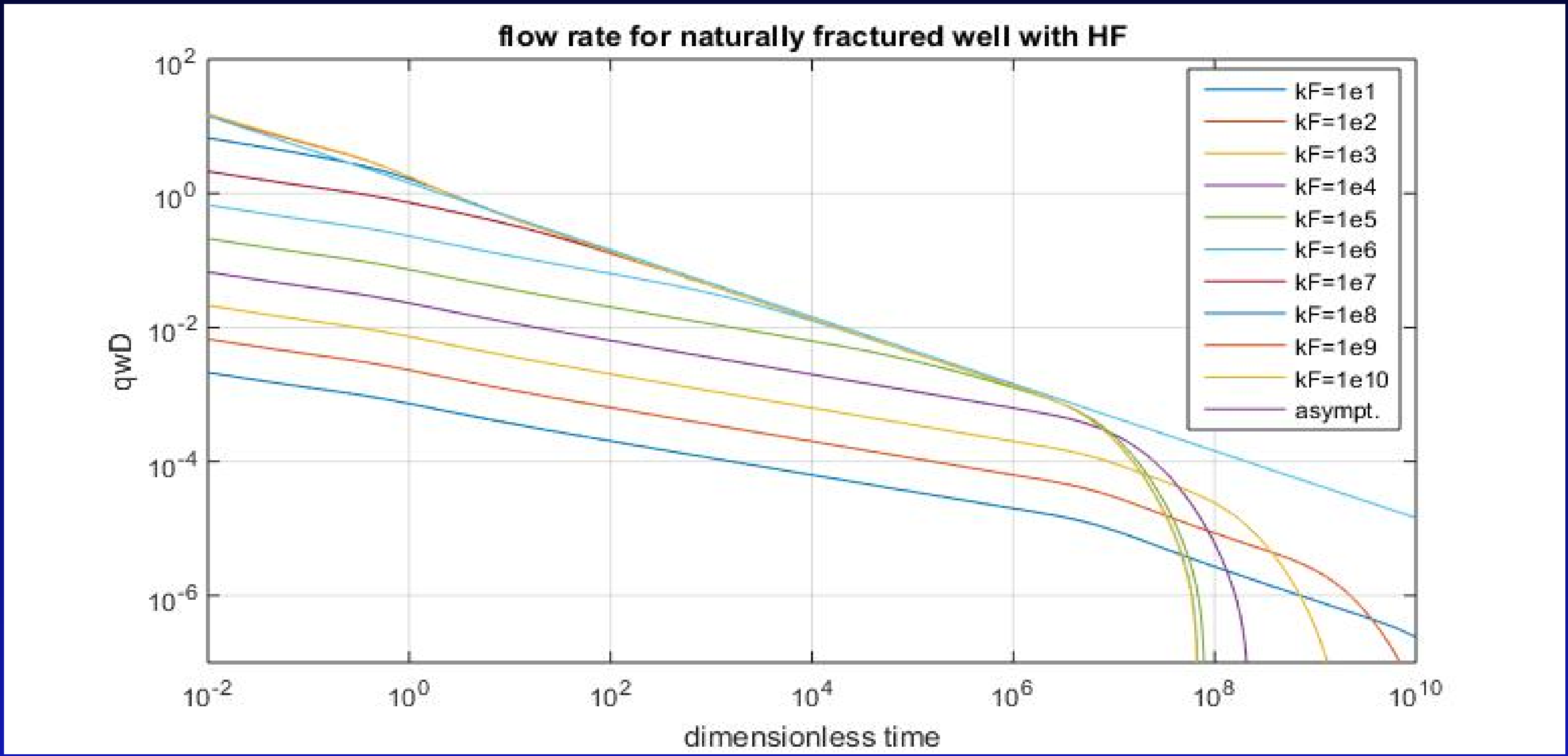

Approach cont'd

- Flow regime 5: Bilinear flow due to linear flows in the NF and IM

$$q_D = \left(\frac{\tilde{\lambda}\tilde{\omega}}{3}\right)^{1/4} \frac{2}{\pi\,\Gamma(3/4)\,(t_D)^{1/4}}$$

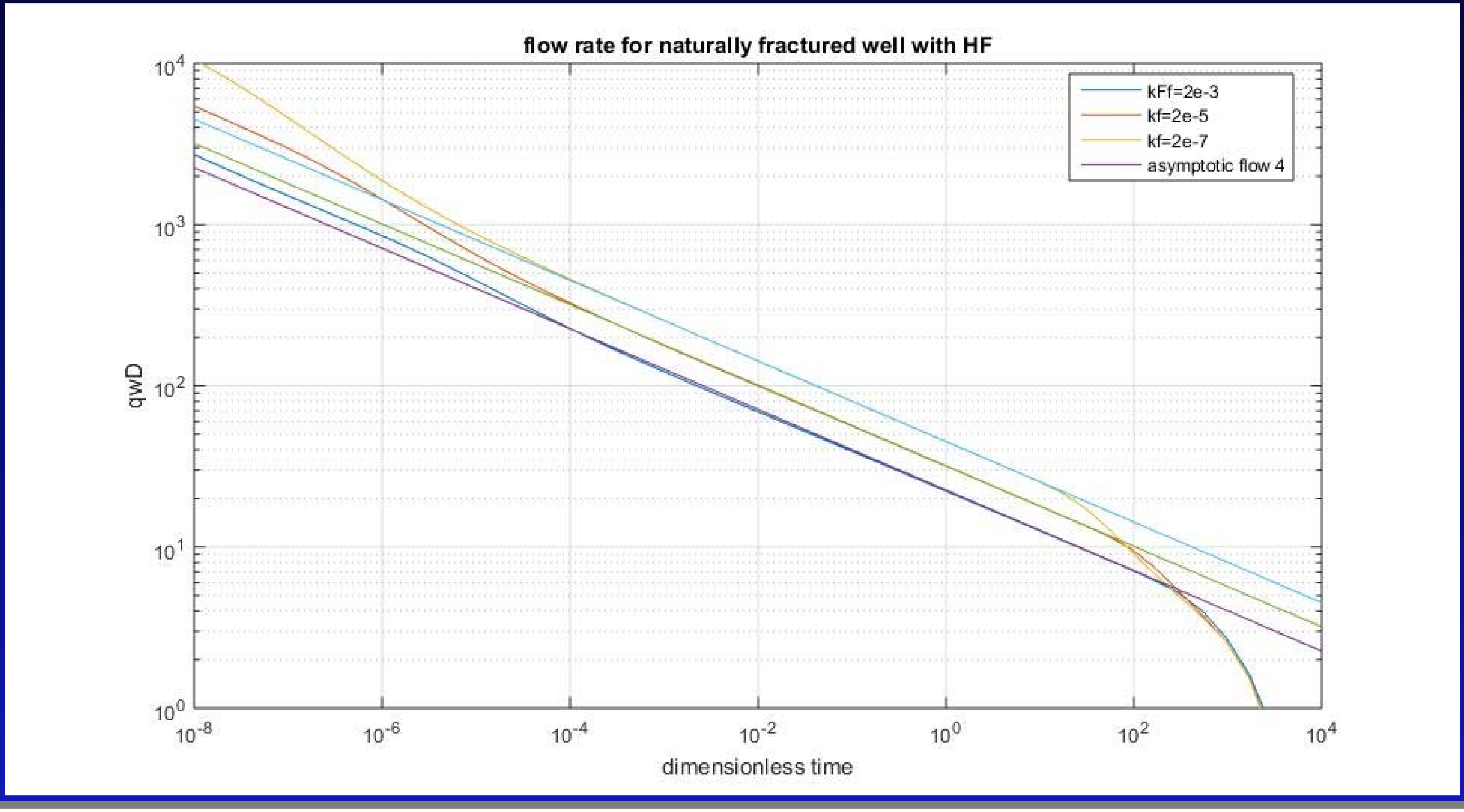

Approach cont'd

- Flow regime 6: Lilinear flow due to linear flows in the IM

$$q_D = 2\sqrt{\frac{(1+\omega')}{\pi^3 t_D}}$$

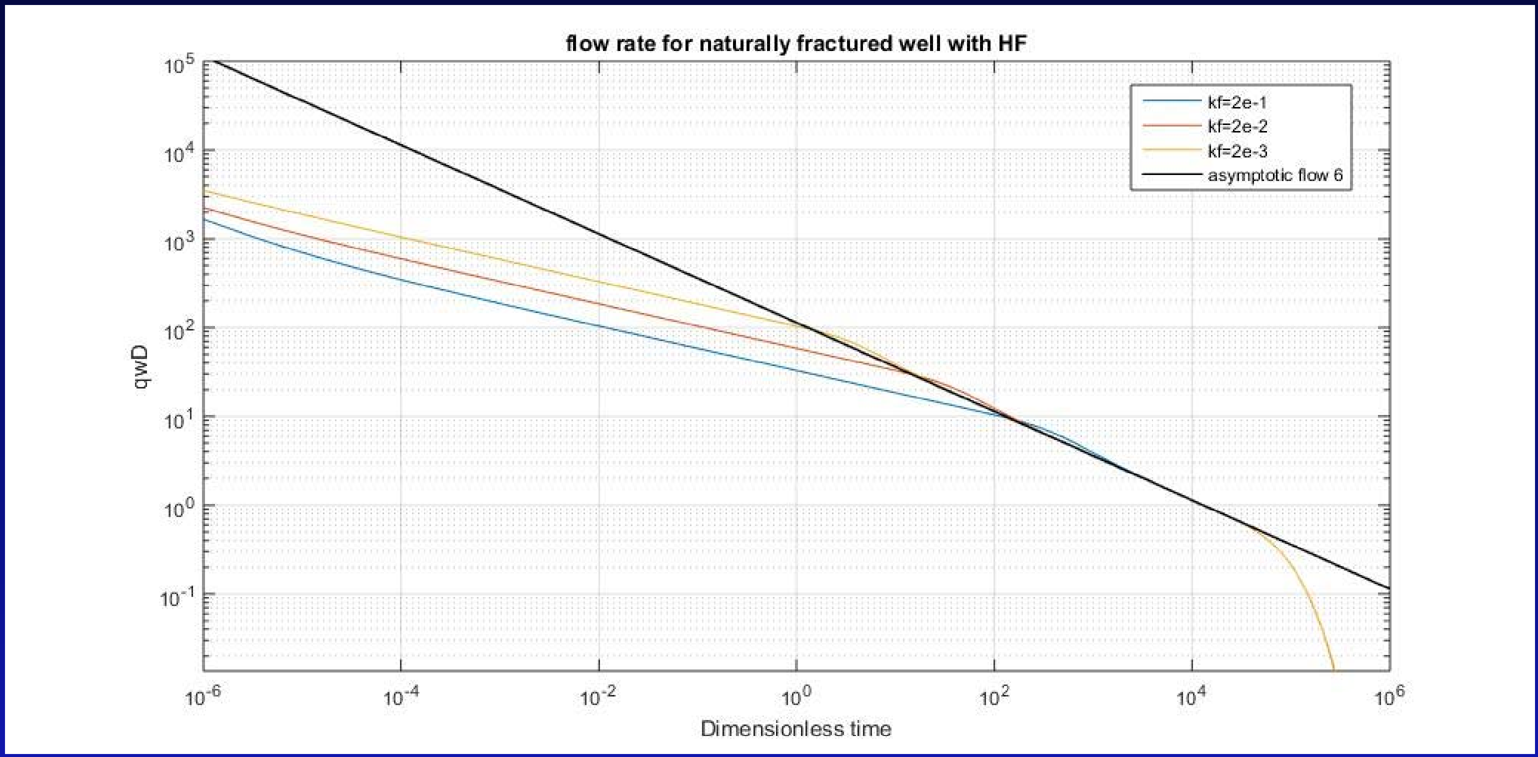

Approach cont'd

Table 2: The Pressure Response for the remaining flow regimes		
Flow regime	Equation	Remark
4	$P_{wD} = \left(\dfrac{3}{\tilde{\lambda}^9\, \tilde{\omega}^9}\right)^{\frac{1}{8}} \dfrac{\pi}{\sqrt{2\, C_{FD}}} \dfrac{t_D^{1/8}}{\Gamma(9/8)}$	This flow regime is expected when all the system is in transient flow where the productivity of HF, NF and IM are close to each other
8	$P_{wD} = \dfrac{\pi t_D}{2\,(1+\tilde{\omega})(y_{eD} - w_D/2)} + \dfrac{\pi}{6}(y_{eD} - w_D/2) + \dfrac{\pi}{3C_{FD}}$	This flow regime is when the whole system goes to BDF and no flow is expected beyond SRV
9	$\boxed{P_{wD} = \sqrt{\dfrac{3}{\tilde{\lambda}\tilde{\omega}} \dfrac{\sqrt{\pi t_D}}{(y_{eD} - w_D/2)}} + \dfrac{\pi}{6}(y_{eD} - w_D/2) + \dfrac{\pi}{3C_{FD}}}$	This flow regime shows linear flow from OM after the SRV goes under BDF.
10	$P_{wD} = \dfrac{\pi t_D}{2\,(1+\tilde{\omega})(y_{eD} - w_D/2)\left(1 + \dfrac{x_{eD} - 1}{(1+\tilde{\omega})\eta_{OD} C_{RD} y_{eD}}\right)} + \dfrac{\pi}{6}(y_{eD} - w_D/2) + \dfrac{\pi}{3C_{FD}}$	This flow regime is akin to flow 8 but when OM goes into BDF

Way forward

- Identifying and verifying all possible flow regimes under the proposed model;
- Deriving and testing the complete suite of equations governing these flow regimes;
- Finding the start and end time of the flow regimes in terms of intrinsic properties;
- Verifying the model with actual field data;
- Analyzing actual field data to demonstrate and verify the proposed analysis technique; and,
- Identifying the limitations of the proposed solution and the analysis technique.